Validation, Vérification, Quantification des erreurs et des incertitudes

Pierre Sagaut

Laboratoire de Mécanique, Modélisation et Procédés Propres

Université Aix-Marseille

pierre.sagaut@univ-amu.fr

Ecole Thématique de Simulation Numérique
23-27 avril, 2018

Validation on full-scale vehicles

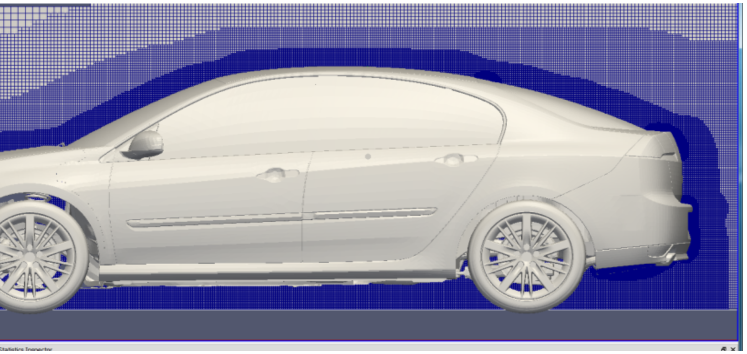

- ❑ Full scale vehicle simulation
- ❑ 186 surfaces (2,3 millions surface triangles)
- ❑ 10 levels of grid refinement, 88.6 millions cells
- ❑ dx_min=1.25mm
- ❑ 300 000 time steps → 0.96 sec
- ❑ U0 = 44.4 m/s
- ❑ Wall Model in first cell LES
- ❑ LBM-ADM model

Validation on full-scale vehicles

LaBS

Measurements

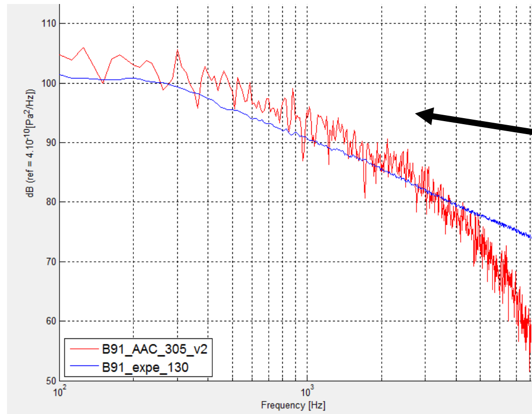

Laguna case : fine band spectra

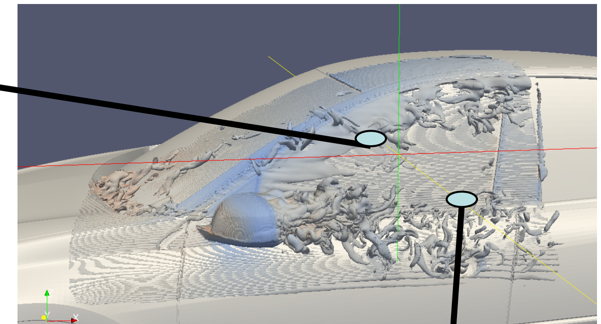

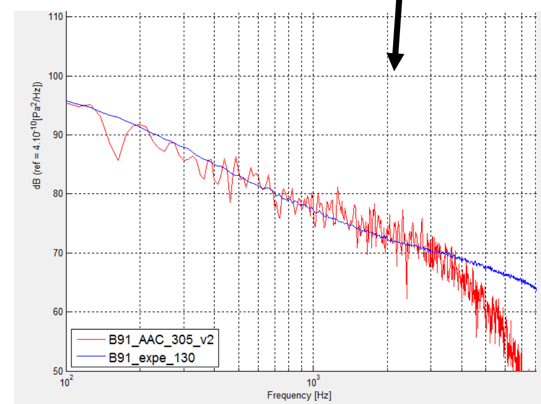

Clio case : third-octave band spectra, averaged on the whole surface of the side window

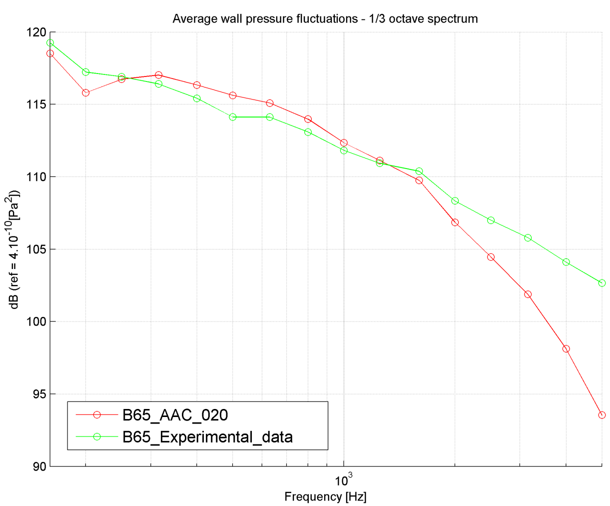

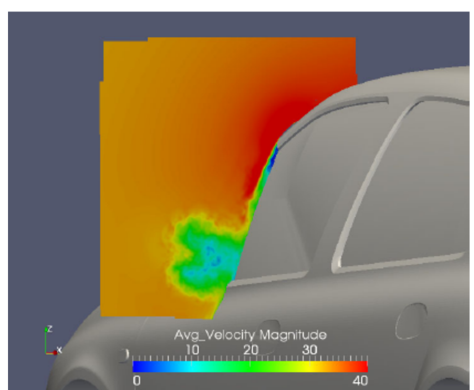

Motivation

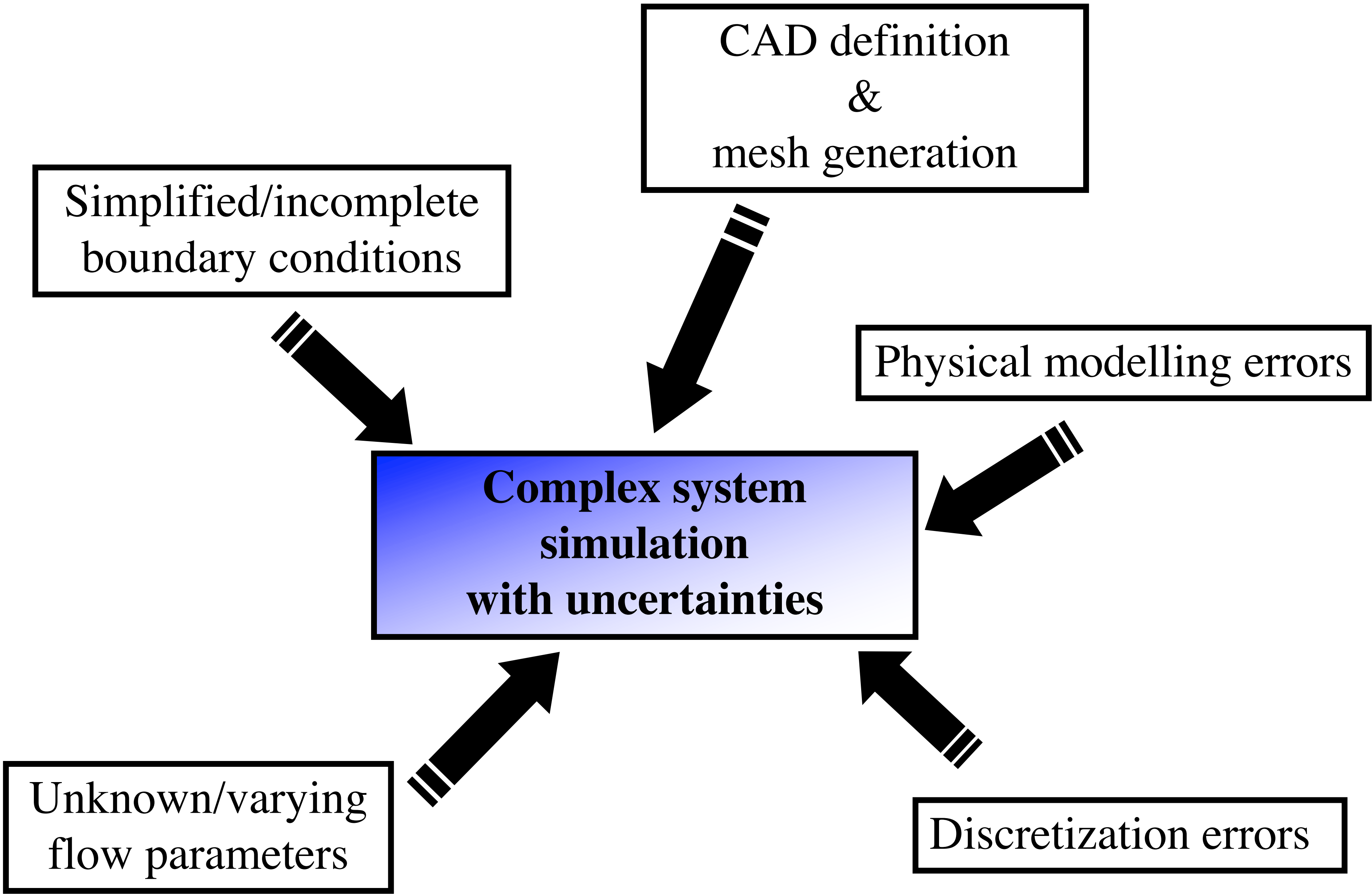
CAD definition
&
mesh generation
Simplified/incomplete
boundary conditions
Physical modelling errors
Complex system
simulation
with uncertainties
Unknown/varying
flow parameters
Discretization errors

Definitions

- **Aleatoric uncertainties** (or irreducible uncertainties):
  - describe physical variations caused by intrinsic randomness in the system and its environment
  - can be characterized in terms of probability distributions and covariance matrices
- **Epistemic uncertainty**:
  - caused by a certain lack of knowledge (structural uncertainty in the model form or insufficient measurement data to quantify the value of an input parameter)
  - not probabilistic in nature
  - can be better described using intervals
  - can be reduced either by increasing model fidelity or by performing additional experiments
- **Numerical errors**

Example: Green Roof Models

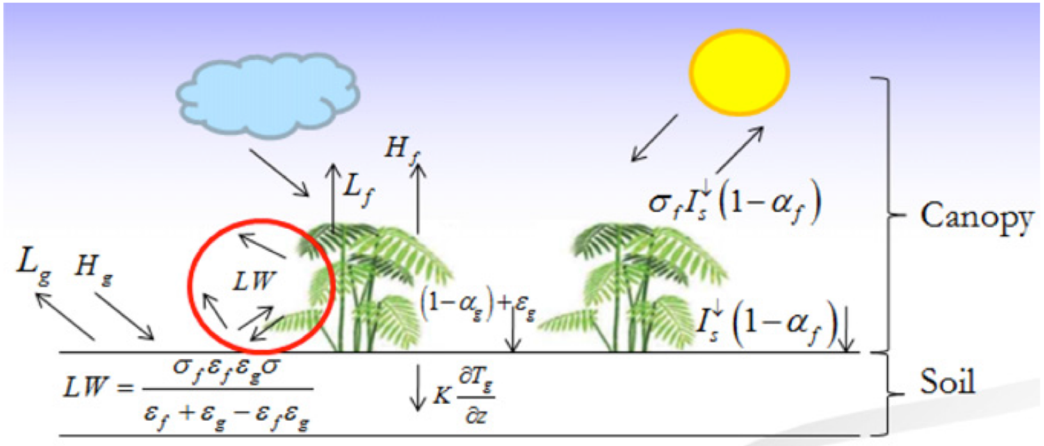

16 physical/free parameters

Fig. 1. Main heat flow on a green roof. (For interpretation of the references to color in this figure legend, the reader is referred to the web version of this article.)

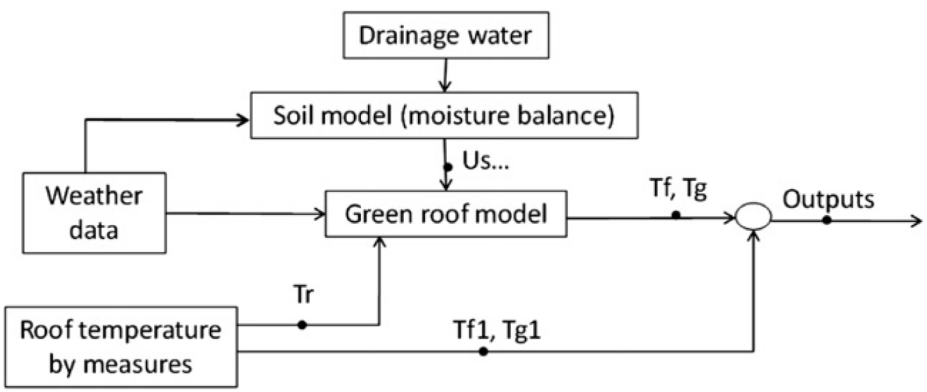

Fig. 5. The principle of the model validation.

Table 1
Different inputs data for the numerical model.

LAI	Leaf area index (m^2/m^2)
ϵ_f	Foliage emissivity
ϵ_g	Soil emissivity
α_f	Albedo for foliage
α_g	Albedo for soil
ρ_f	air density in the foliage (kg/m^3)
σ_f	Foliage density of (%)
Ta	Air temperature
RH	Air temperature
I_{ir}	Long-wave radiation (W/m^2)
I_s	Short-wave radiation (W/m^2)
W	Wind speed (m/s)
K	Thermal conductivity of the dry growing media ($W/m^{-1}.K^{-1}$)
Δ	Soil thickness (m)
Pa	Atmospheric pressure(Pa)
P	Precipitation (mm)
D	Drained water (mm)

[Ouldboukhitine et al., Building & Environment, 46, 2011]

How to increase fidelity ?

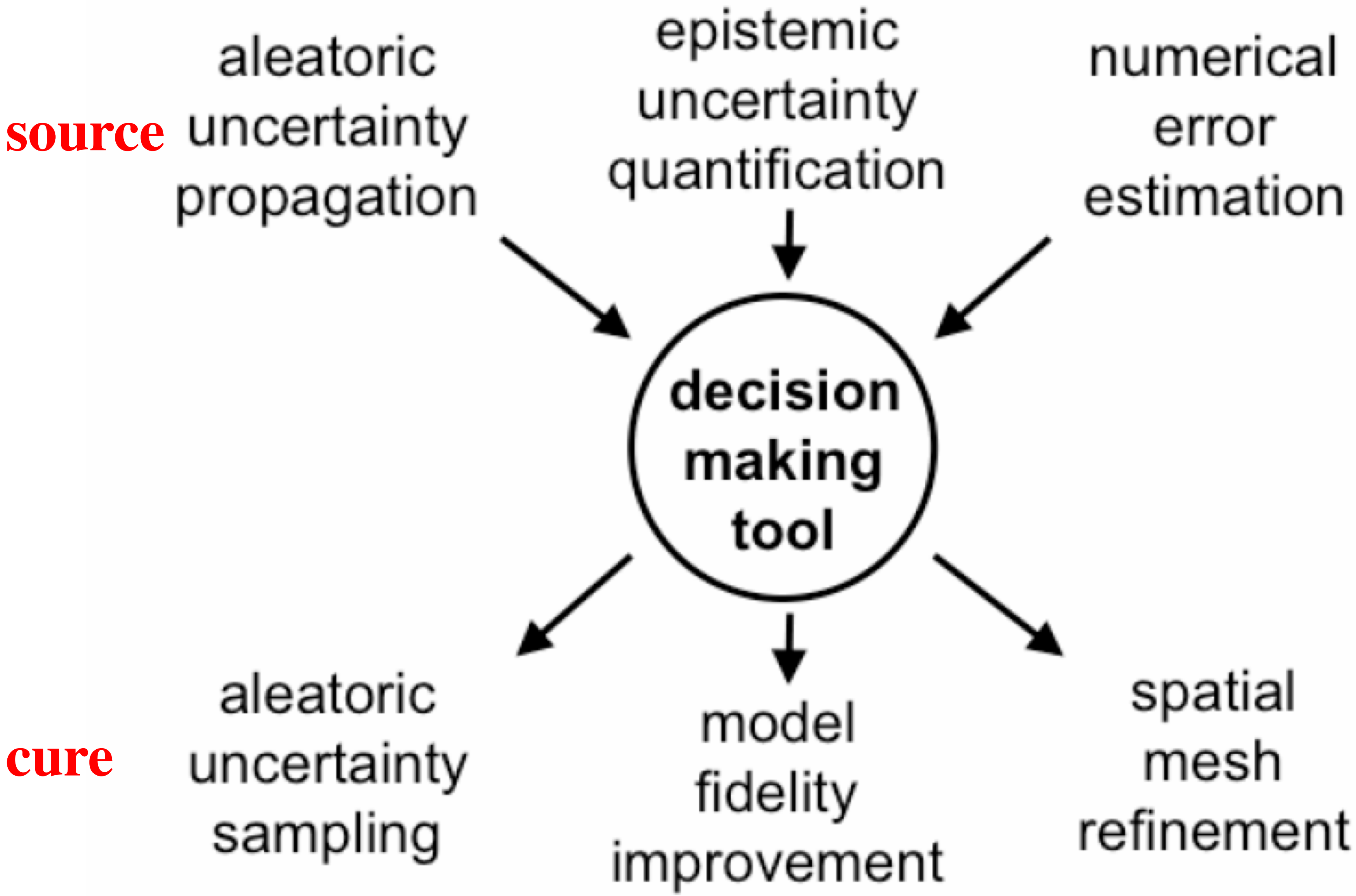

How to describe errors/uncertainties?

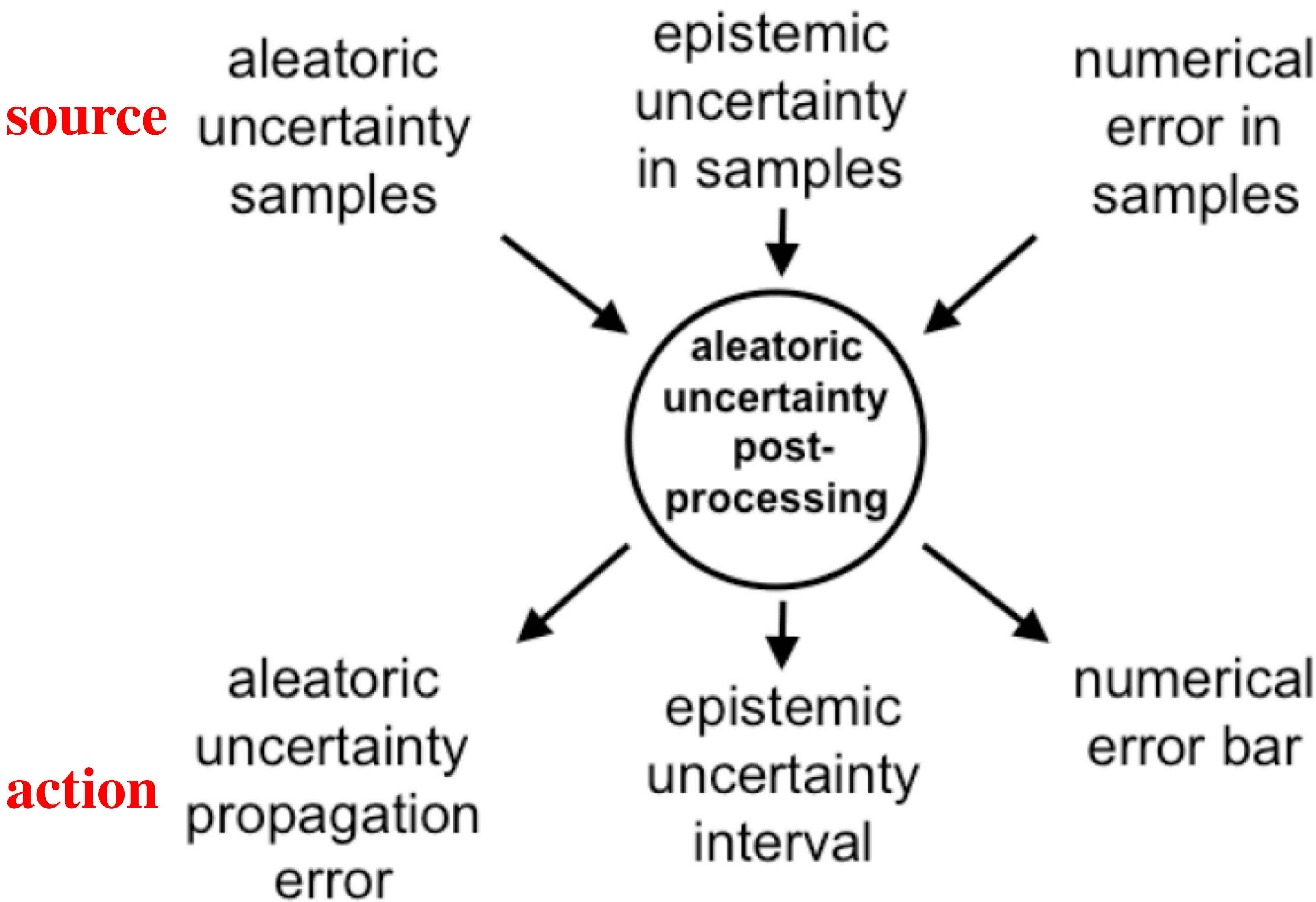

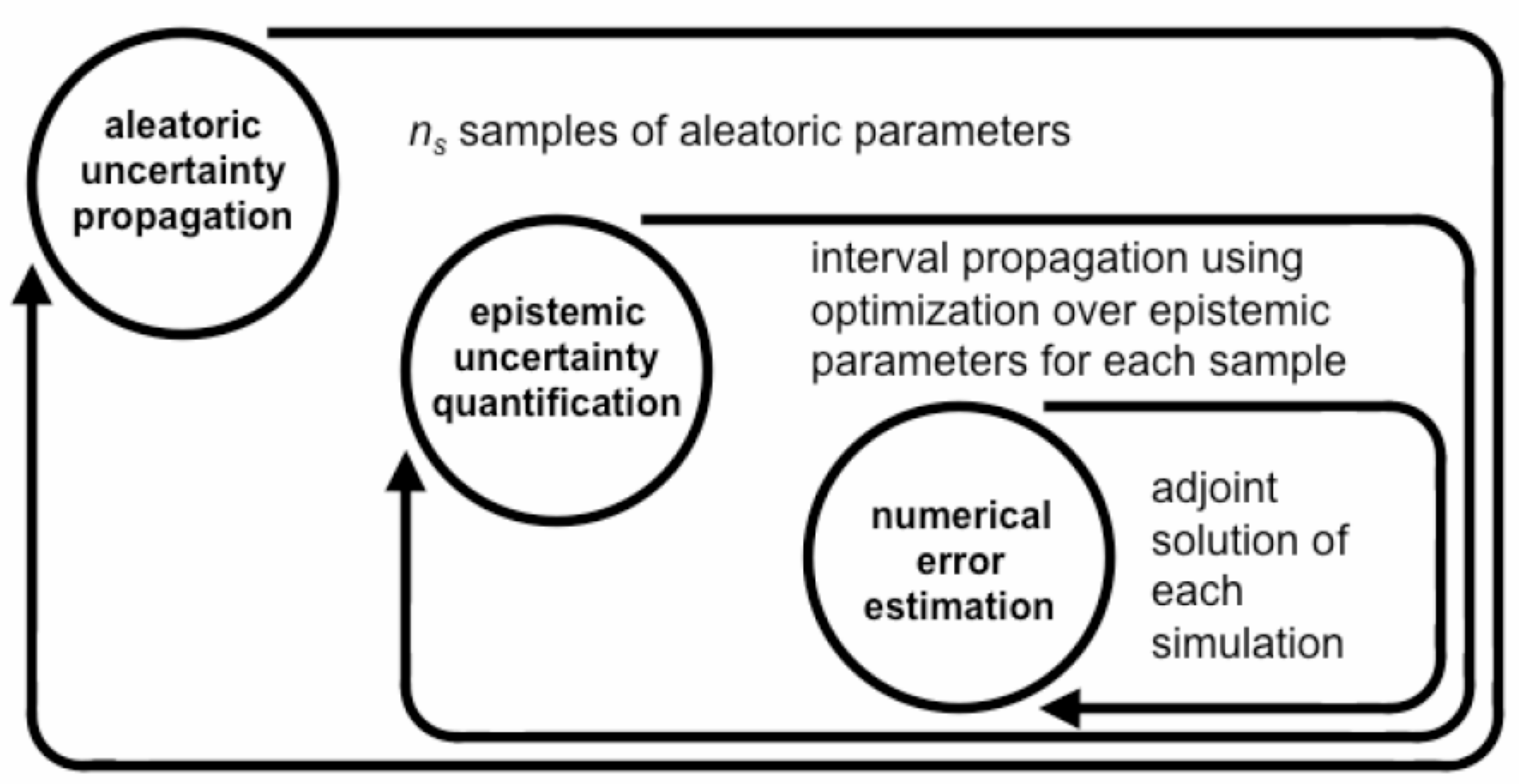

Figure 3. Nested uncertainty quantification and error estimation loop.

Numerical model building

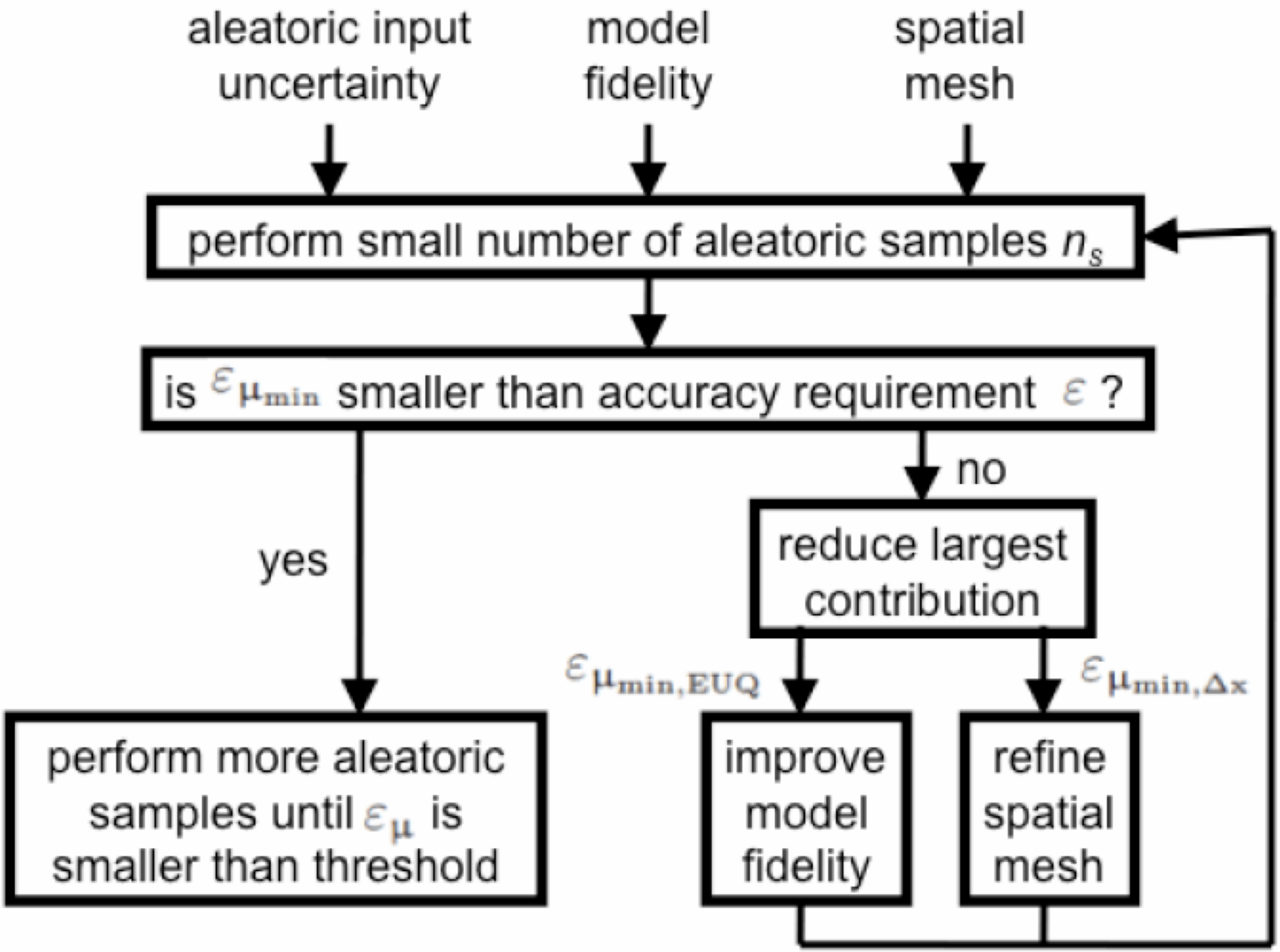

Outline

1. Validation using experimental data
2. Couplings between numerics and SGS models
3. LES numerics: beyond order of accuracy
4. Uncertainty quantification tools

First issue: validation using experimental data ?

Spectral analysis & sampling effect

Buffeting on OAT15A airfoil (DES)
(case with well-defined spectral peaks)

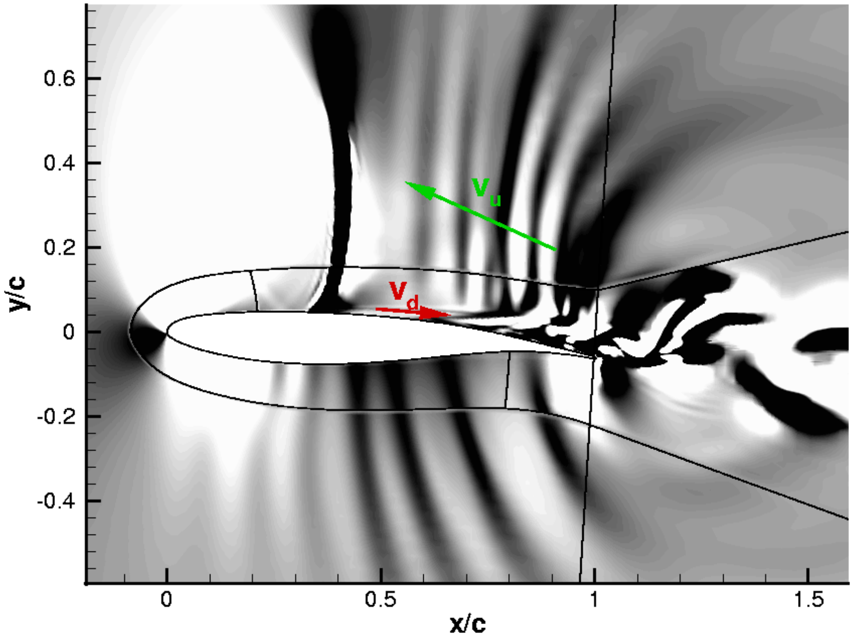

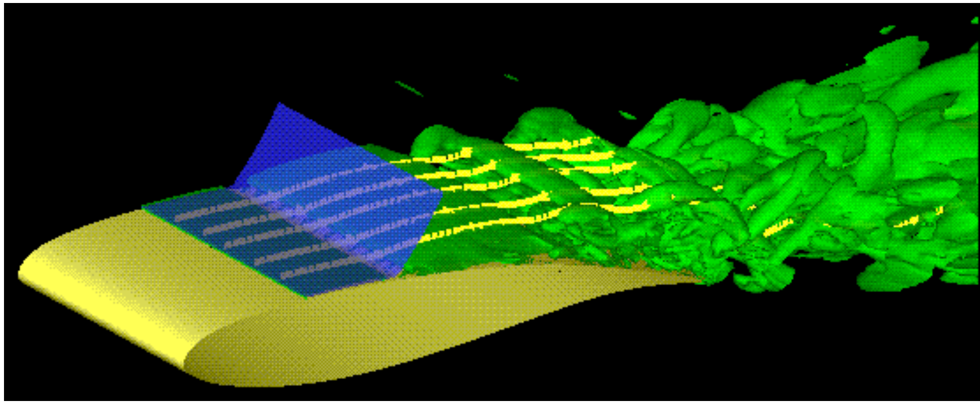

- Buffeting: large-amplitude pseudo-periodic shock oscillation
- Instability due to shock/boundary layer interaction
- High lift & Mach number

Instantaneous flow (grid C)

- 2D/3D interface (reflective) => numerically forced transition on the pressure side
- Periodic movement of the shock

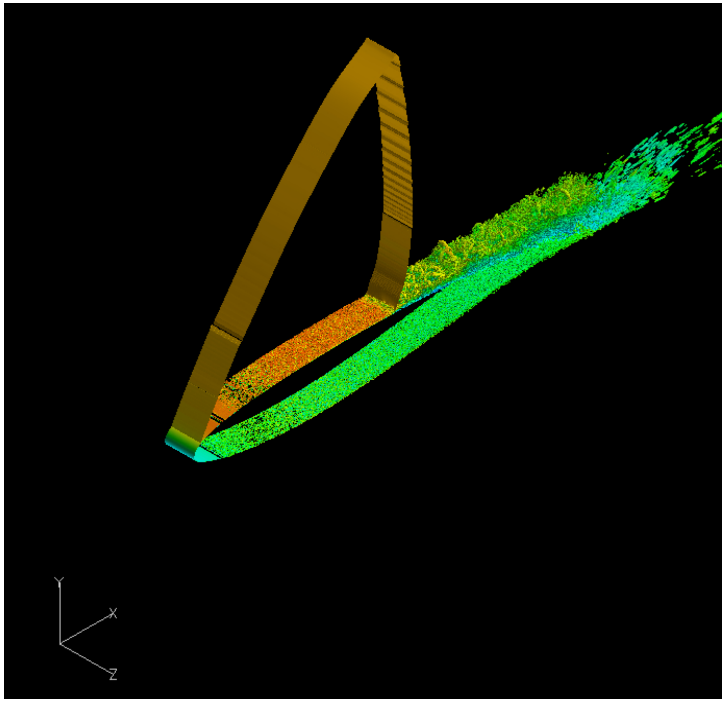

Q criterion colored by the longitudinal velocity (grid C)

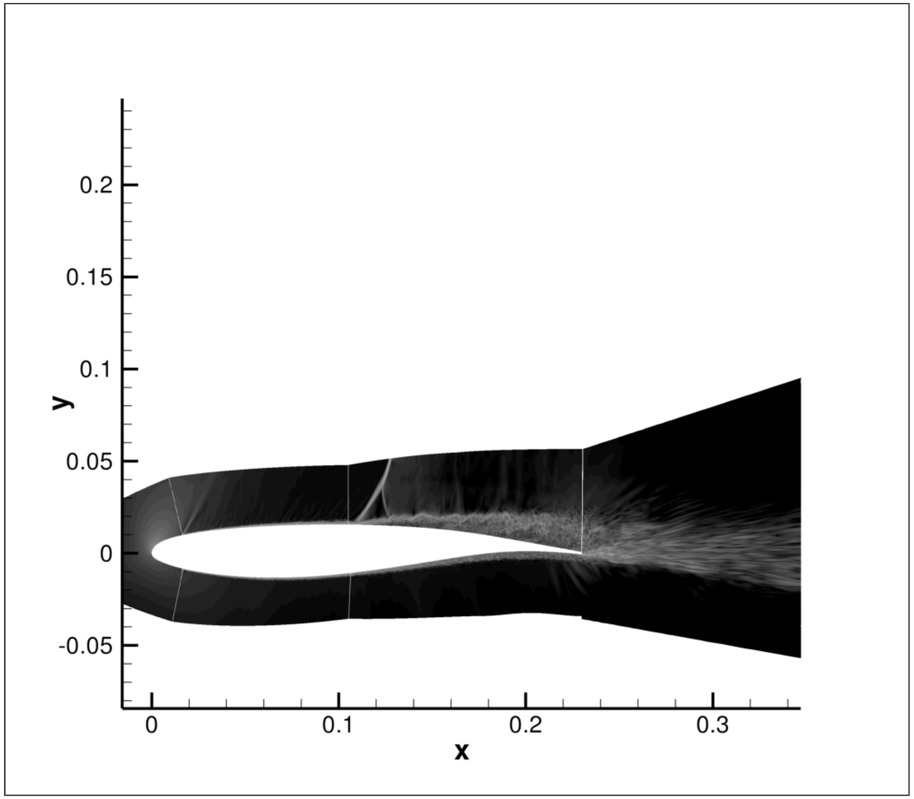

Sampling effect & spectral analysis (cont'd)

QUIZZ: which is the best CFD solution ?

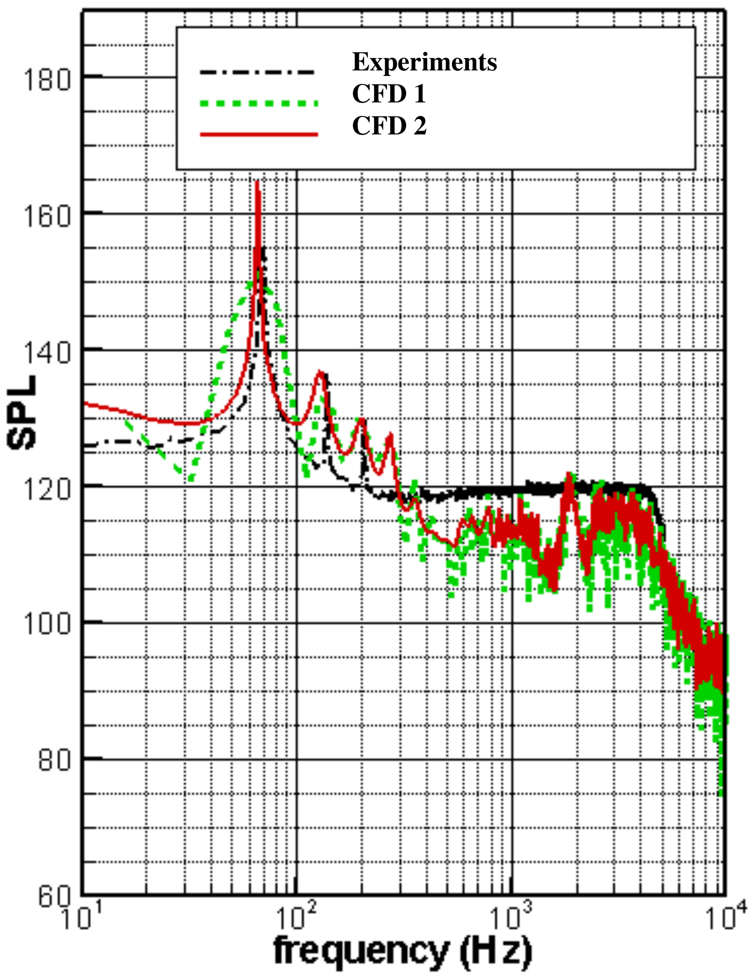

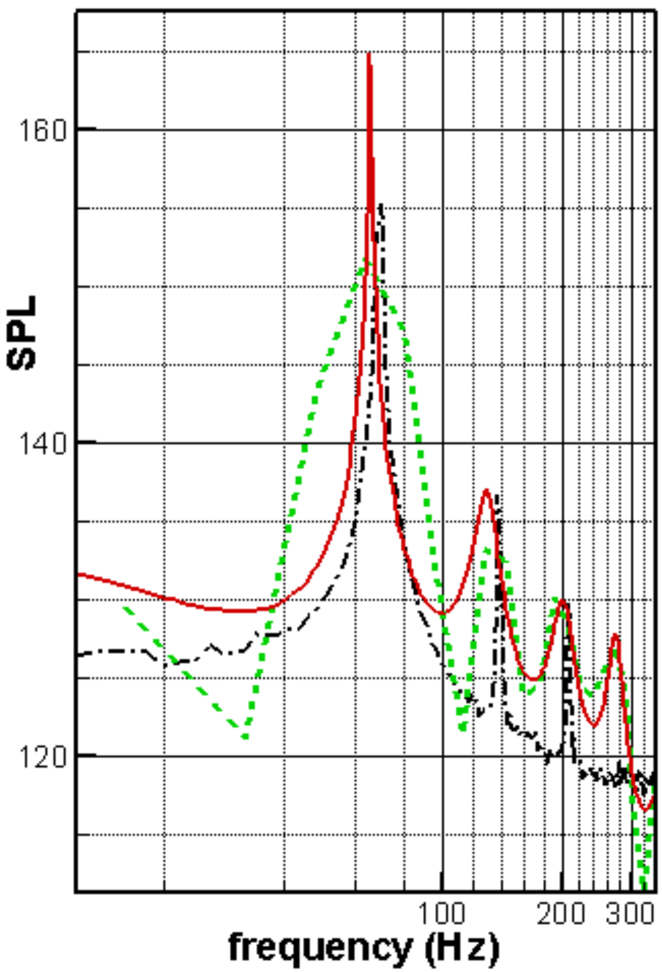

Spectral analysis & sampling effects (cont’d)

Experimental vs. Numerical data

Buffeting on a 2D OAT15A airfoil

	Sampling time	Sampling frequency	Time step
Wind tunnel experiment	50 s	10 kHz	-
CFD (ZDES)	0.08s	100 kHz	$5.\ 10^{-7}$ s

Sampling effects & spectral analysis (cont'd)

Exact definition of **Power Spectral Density**

$$S_{xx}(f) = \lim_{T \to +\infty} \frac{1}{T} E\left[|X(f,T)|^2\right]$$

Fourier transform

$$X(f,T) = \int_0^T x(t) e^{-2i\pi f t} dt$$

A first approximation: **periodogram**

$$S_{xx}^{per}(f) = \frac{1}{T} |X(f,T)|^2$$

Sampling effects & spectral analysis (cont'd)

- Periodogram is easy to compute, but not consistent: variance of the coefficient does not decrease when samling time is increased
  ➪ an averaged variant must be used

Initial sample set split into L non-overlapping blocks with length M

$$x_M^{[i]}[k] = x[iM + k] \quad 0 \le i \le L-1 \quad 0 \le k \le M-1$$

Averaged PSD estimate

Period of x(t)

$$S_{xx}^{aper}(f) = \frac{T_e}{L} \sum_{i=0}^{L-1} \frac{|X_M^{(i)}(f)|^2}{M}$$

Sampling effects & spectral analysis (cont'd)

Pressure PSD

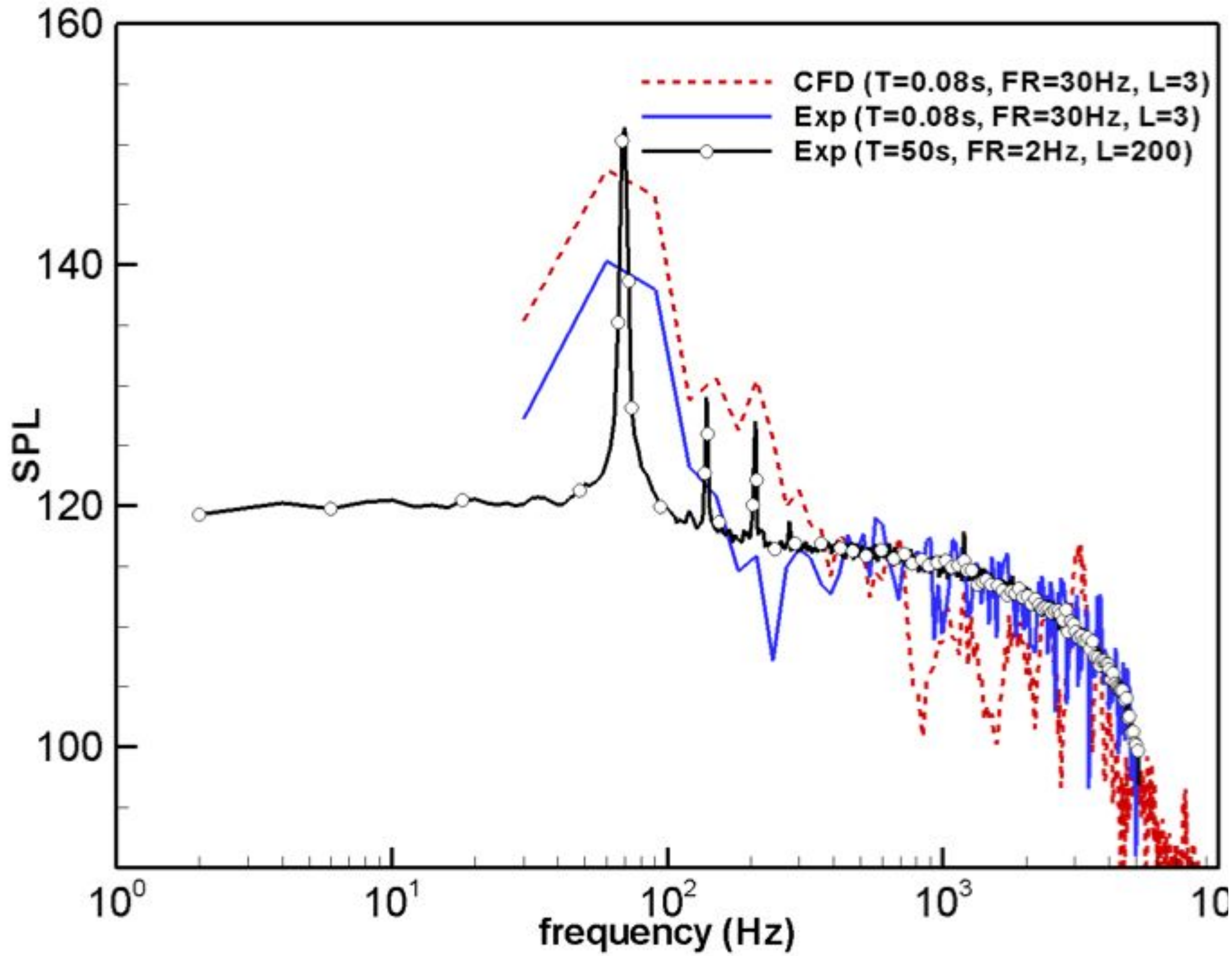

Is that a fair comparison ?

Sampling effects & spectral analysis (cont'd)

Kay's formula for confidence interval on PSD

- confidence interval $(1-\alpha)$ x 100%
- L non-overlapping sample sets
- $\chi_n^2 = \chi^2$ distribution with n degrees of freedom
- α = confidence level such that $\mathrm{Prob}\left[\chi_n^2 < \chi_{n;\alpha}^2\right] < \alpha$

$$\left[\frac{2L.S_{xx}^{aper}(f)}{\chi^2_{2L;1-\alpha/2}};\frac{2L.S_{xx}^{aper}(f)}{\chi^2_{2L;\ \alpha/2}}\right]$$

Sampling effects & spectral analysis (cont'd)

Pressure PSD - 95% confidence interval

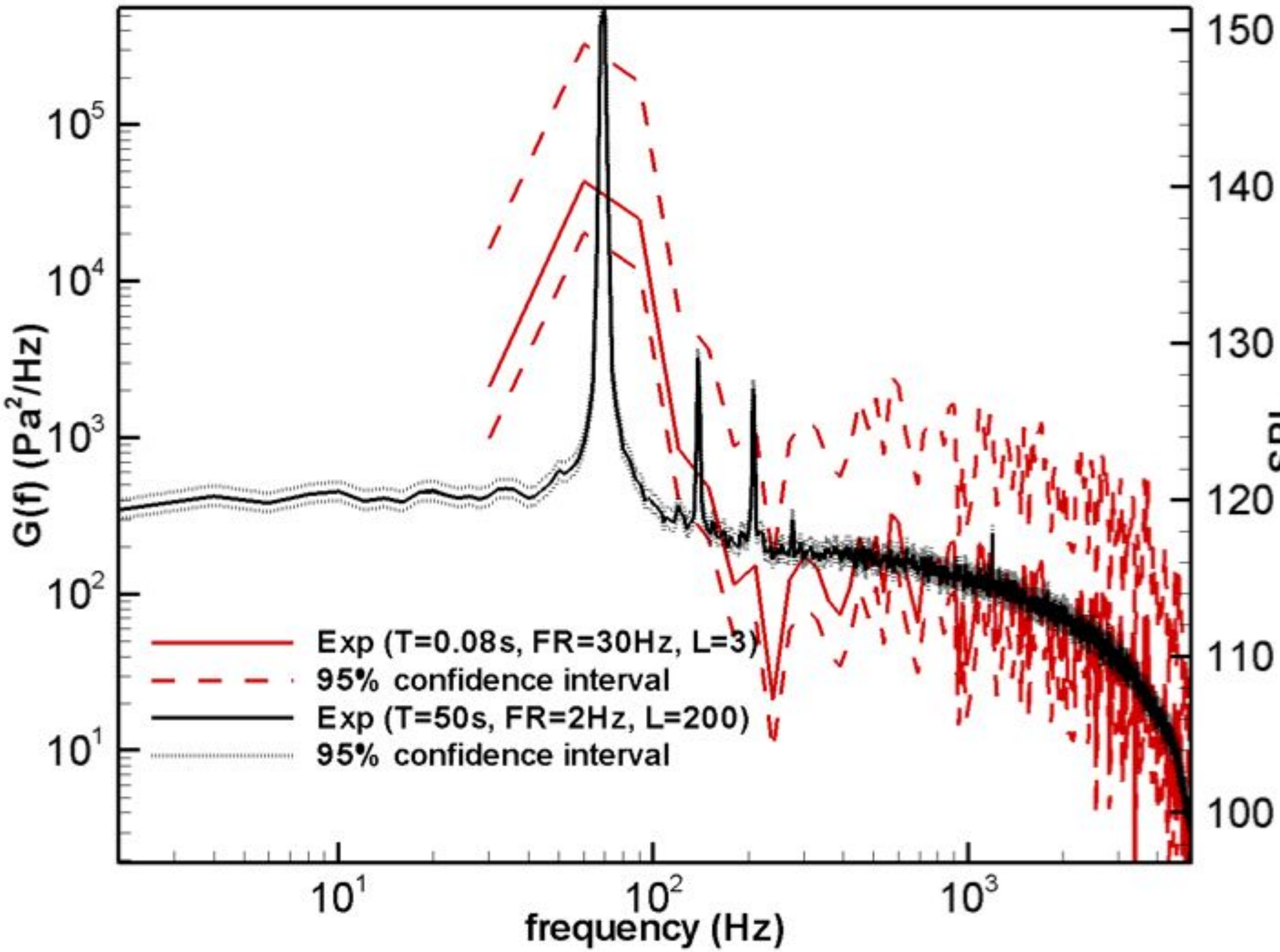

⇨ ***confidence intervals should be always plotted on PSD !***

Sampling effect & spectral analysis (cont'd)

Pressure PSD

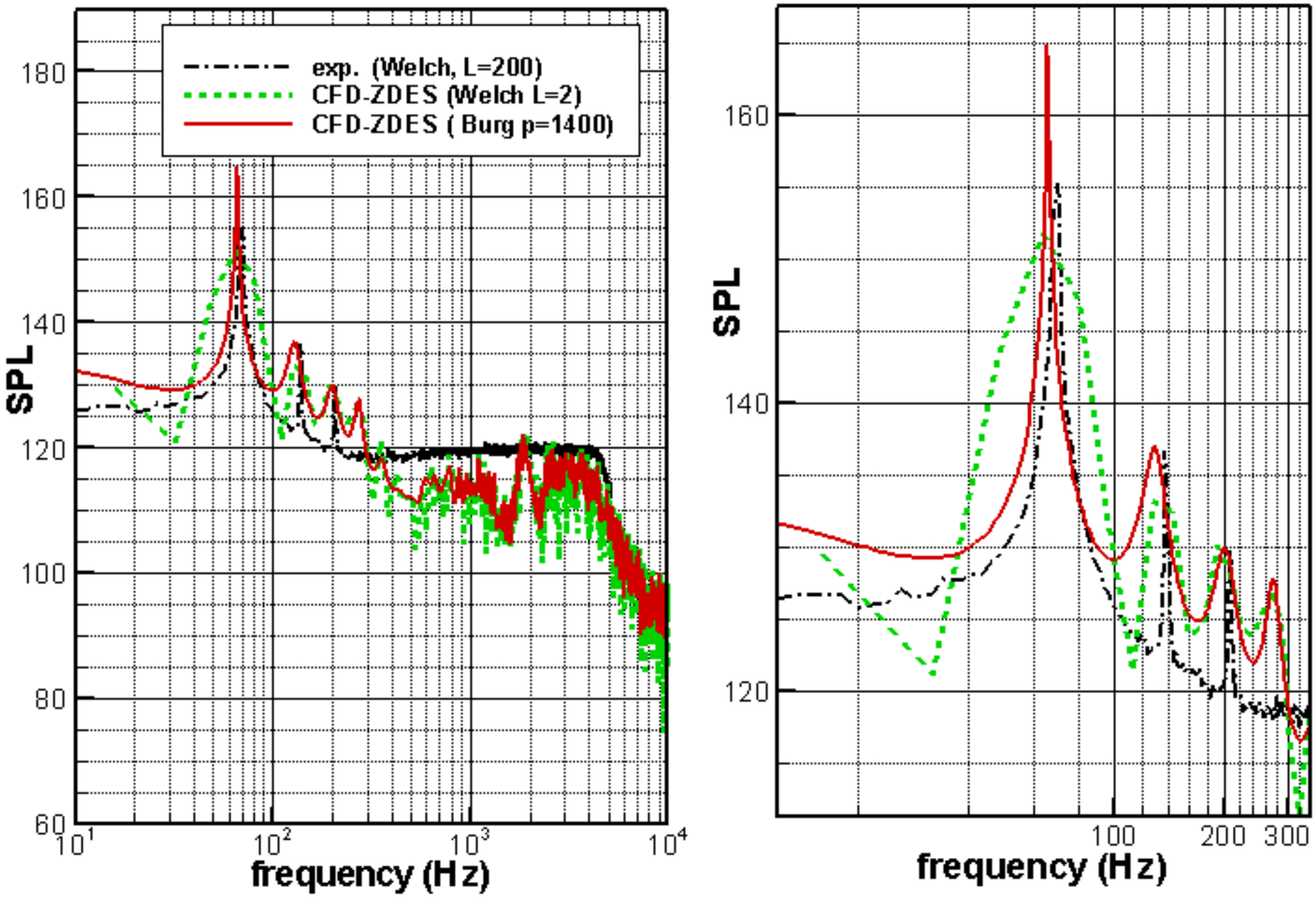

QUIZZ solution: there was only 1 CFD data set !

Refined Spectral analysis

Pressure PSD - AR-Burg vs. Welch
Sensitivity to details of Welch's method

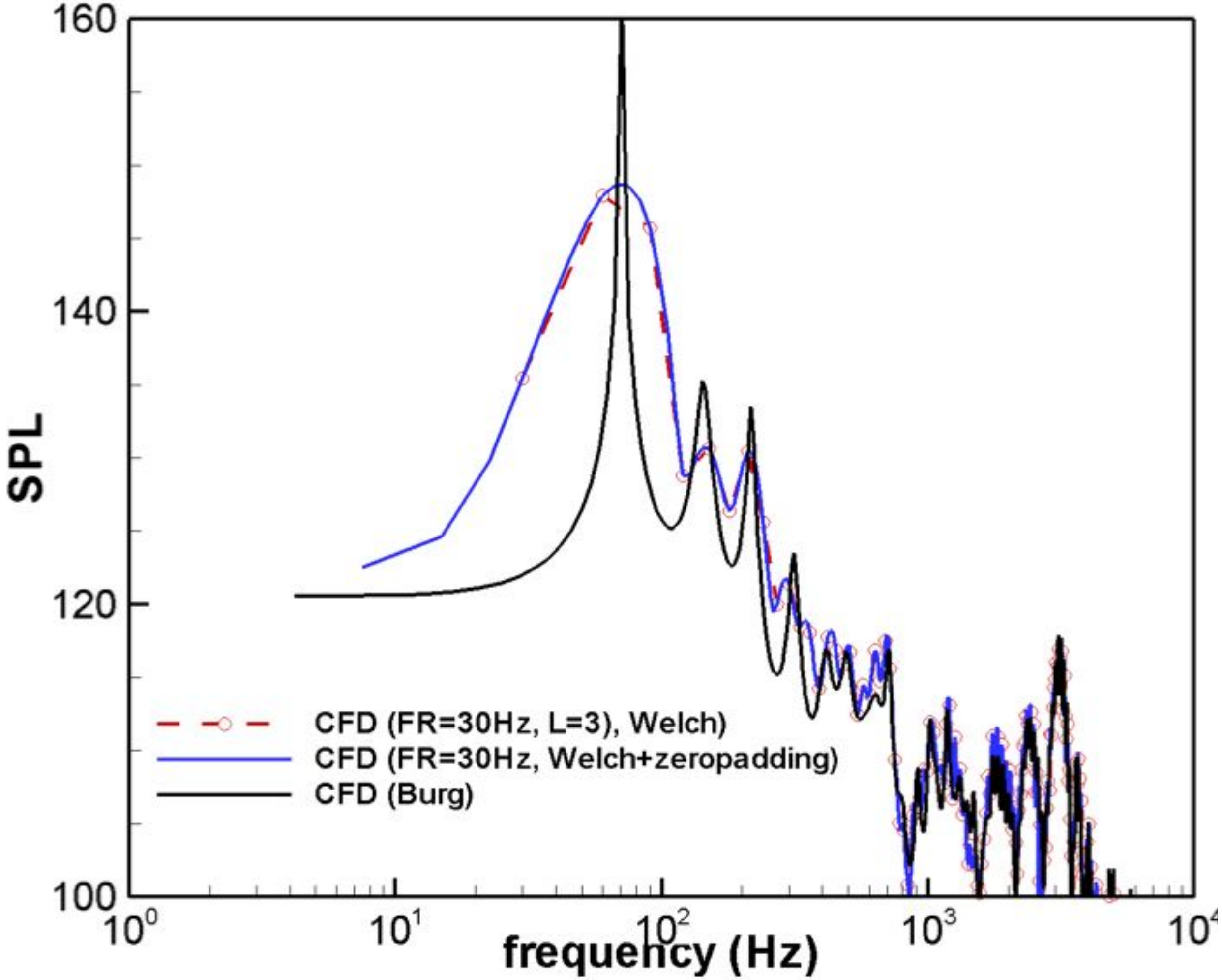

Aix*Marseille université

Pressure PSD - AR-Burg

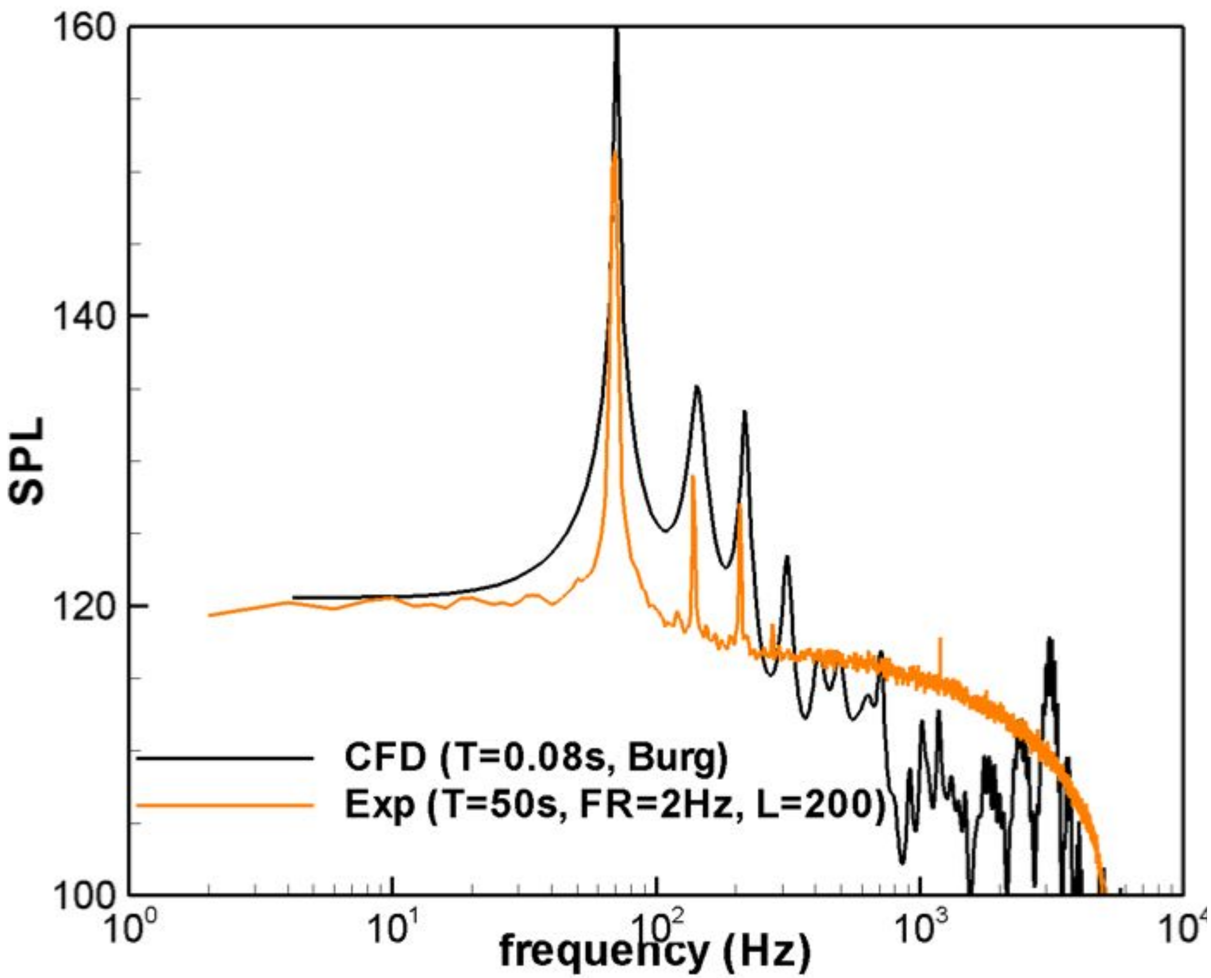

- Existence of peaks is accurately predited
- not very efficient for spectral plateau capturing

Flow past a supersonic truncated contoured nozzle (case with broadband spectrum)

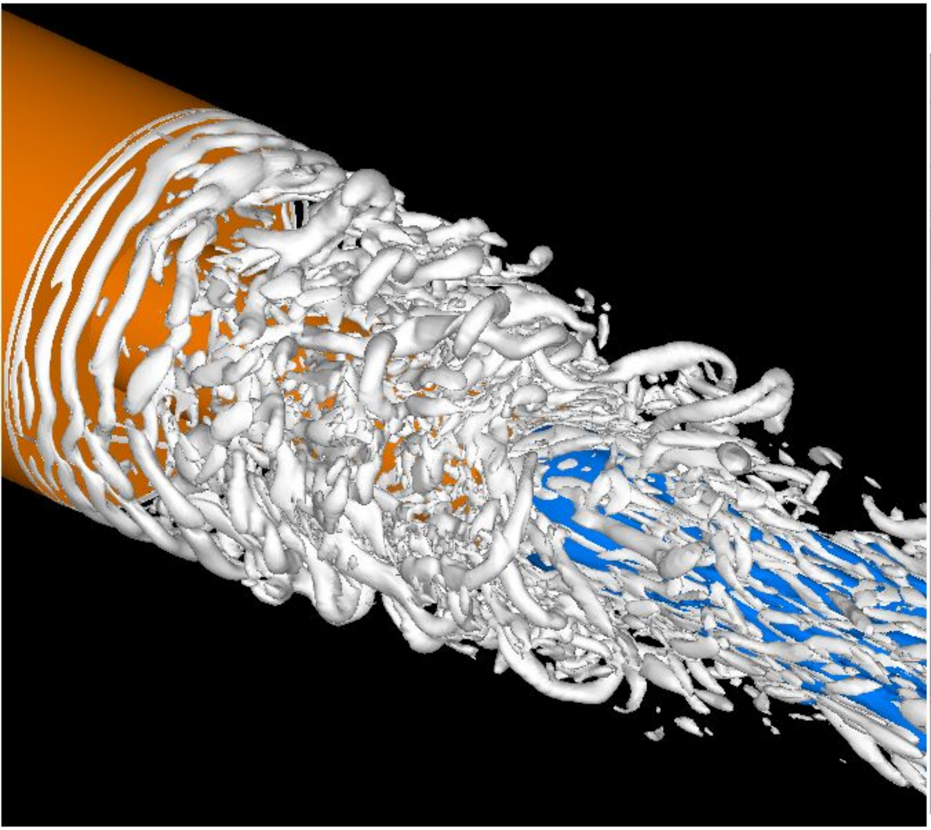

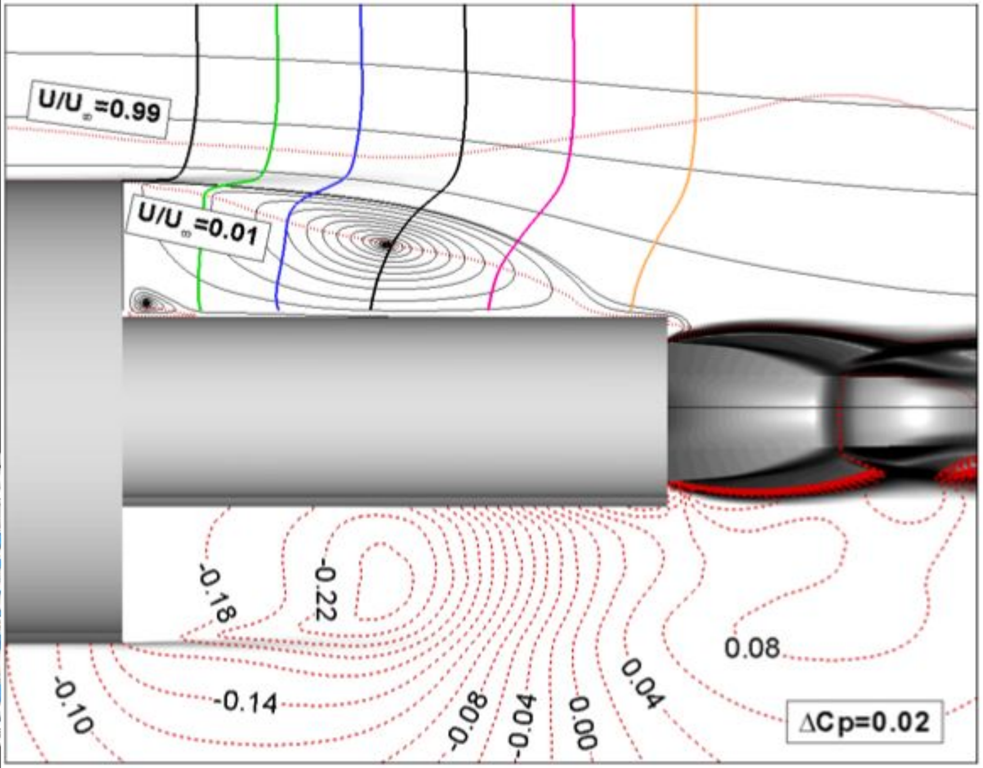

- **experiments: sampling time = 1.6 s, sampling frequency = 10 kHz**
- **CFD (DES): sampling time = 0.2 s, sampling frequency = 100 kHz**

Pressure PSD - Welch

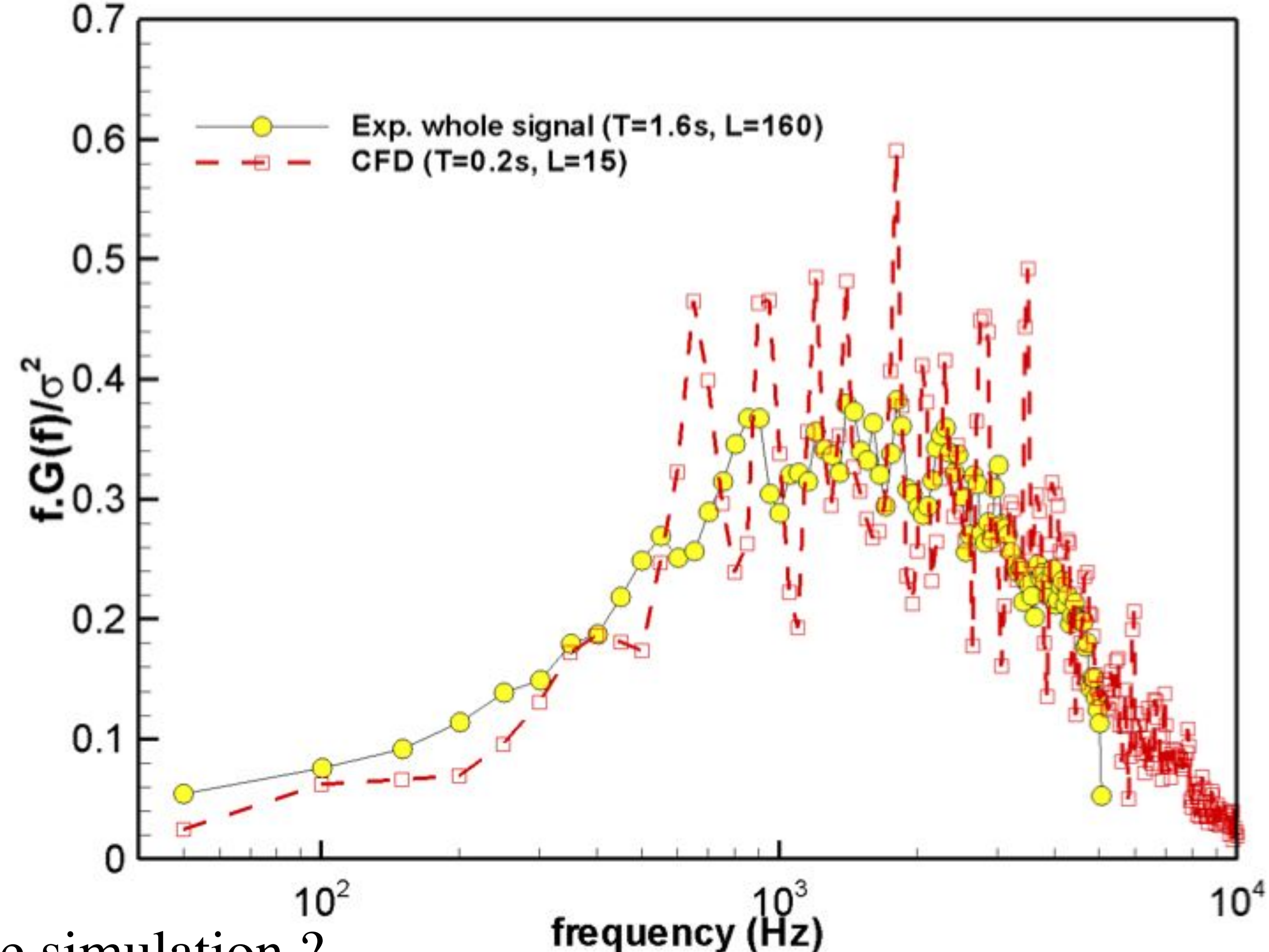

Inaccurate simulation ?

Pressure PSD - Welch

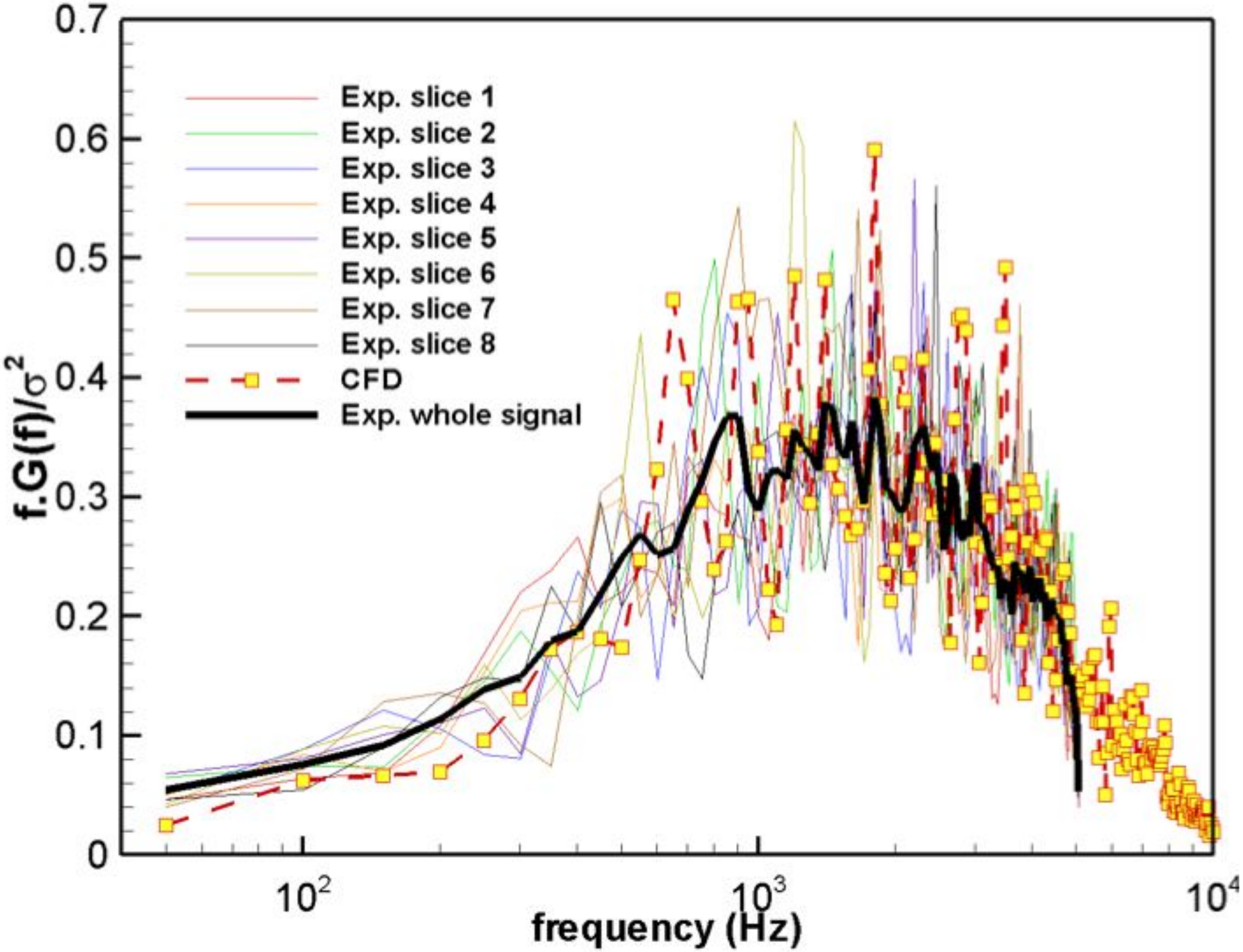

Introduction to numerical errors

LES: the key observation

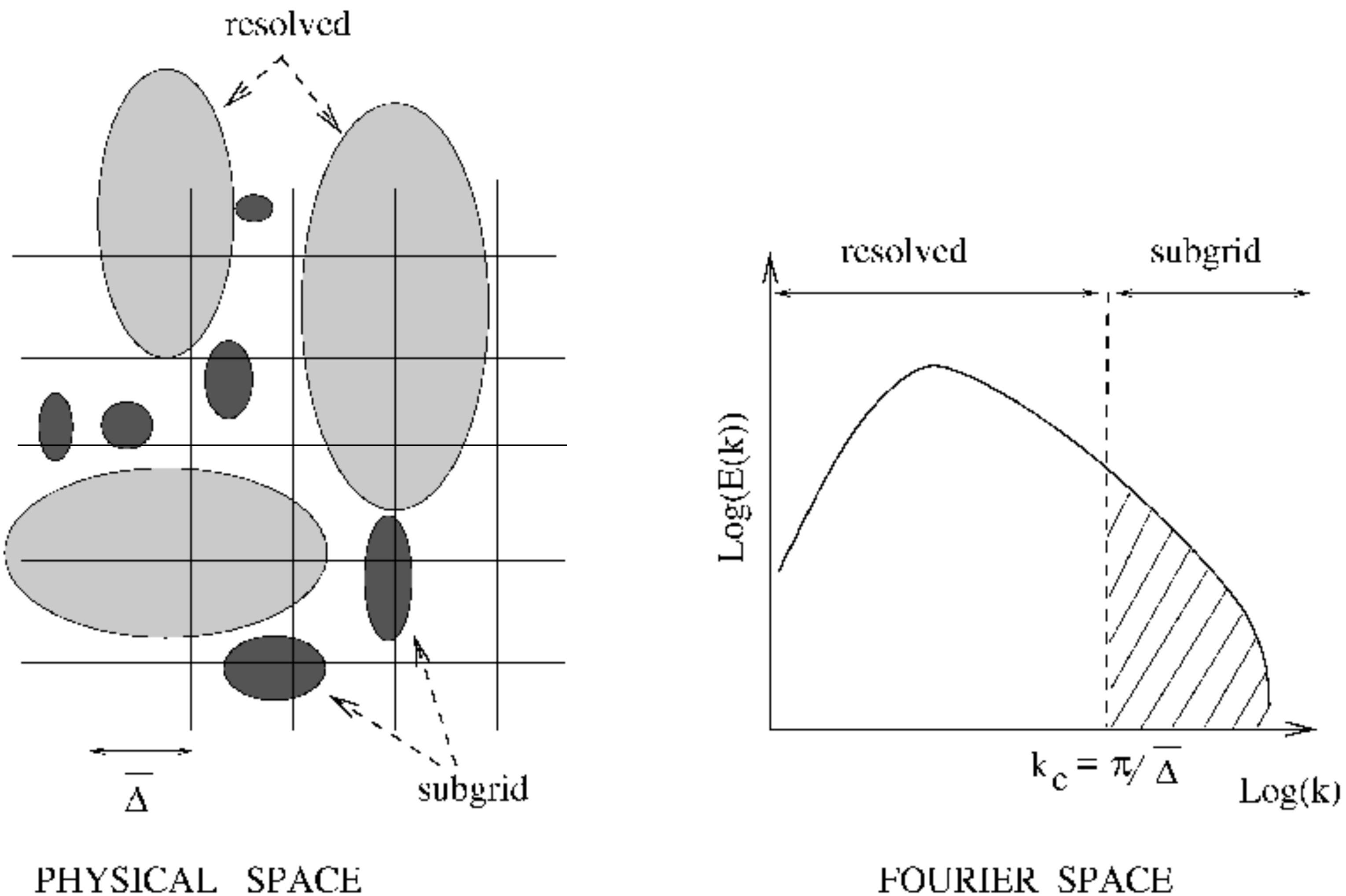

Hierarchy of CFD methods

***Multiscale & Multiresolution approaches for turbulence**, 2nd edition*

Sagaut, Deck & Terracol, Imperial College Press, 2013

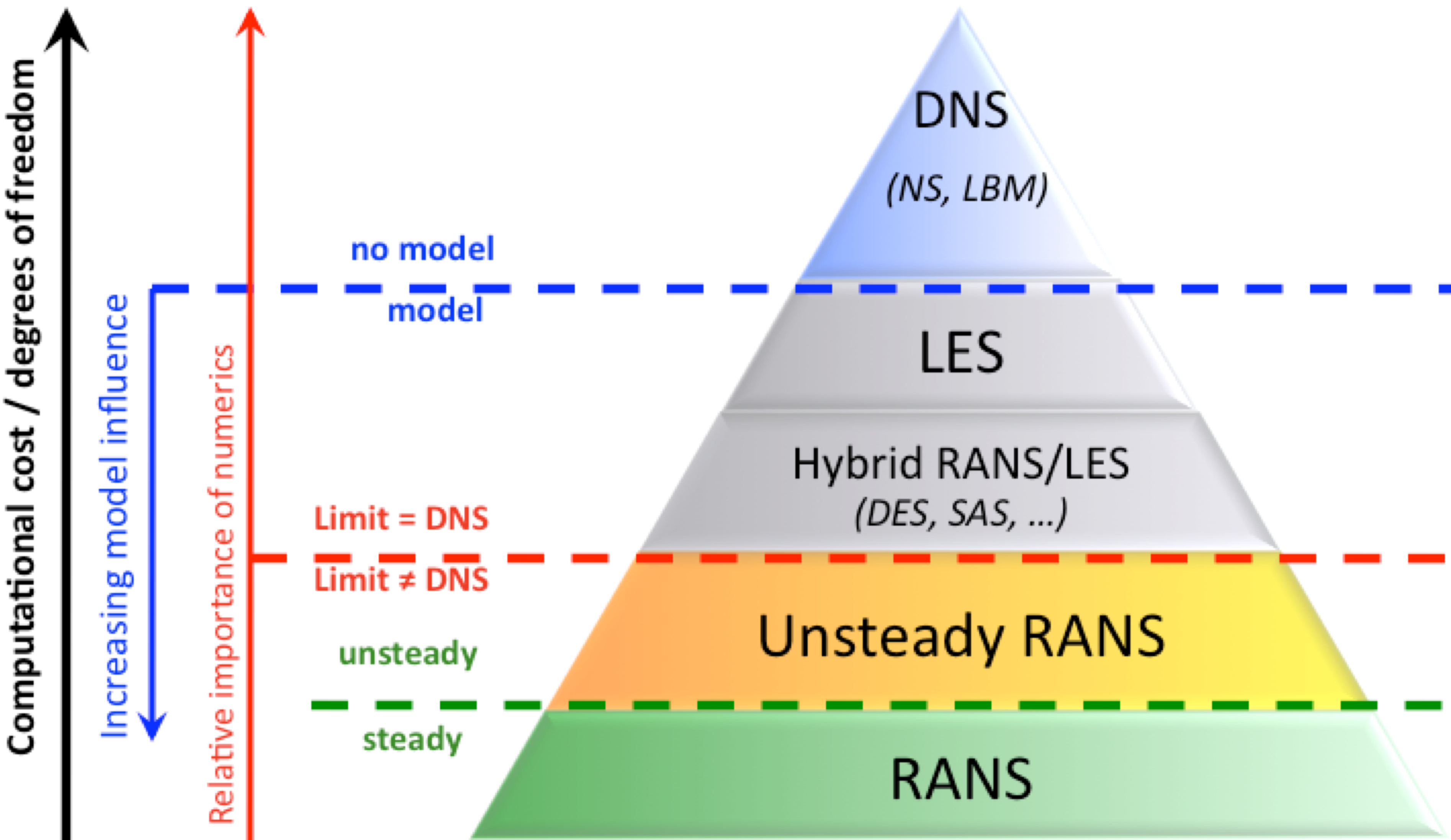

Do theories agree with experimental data ?

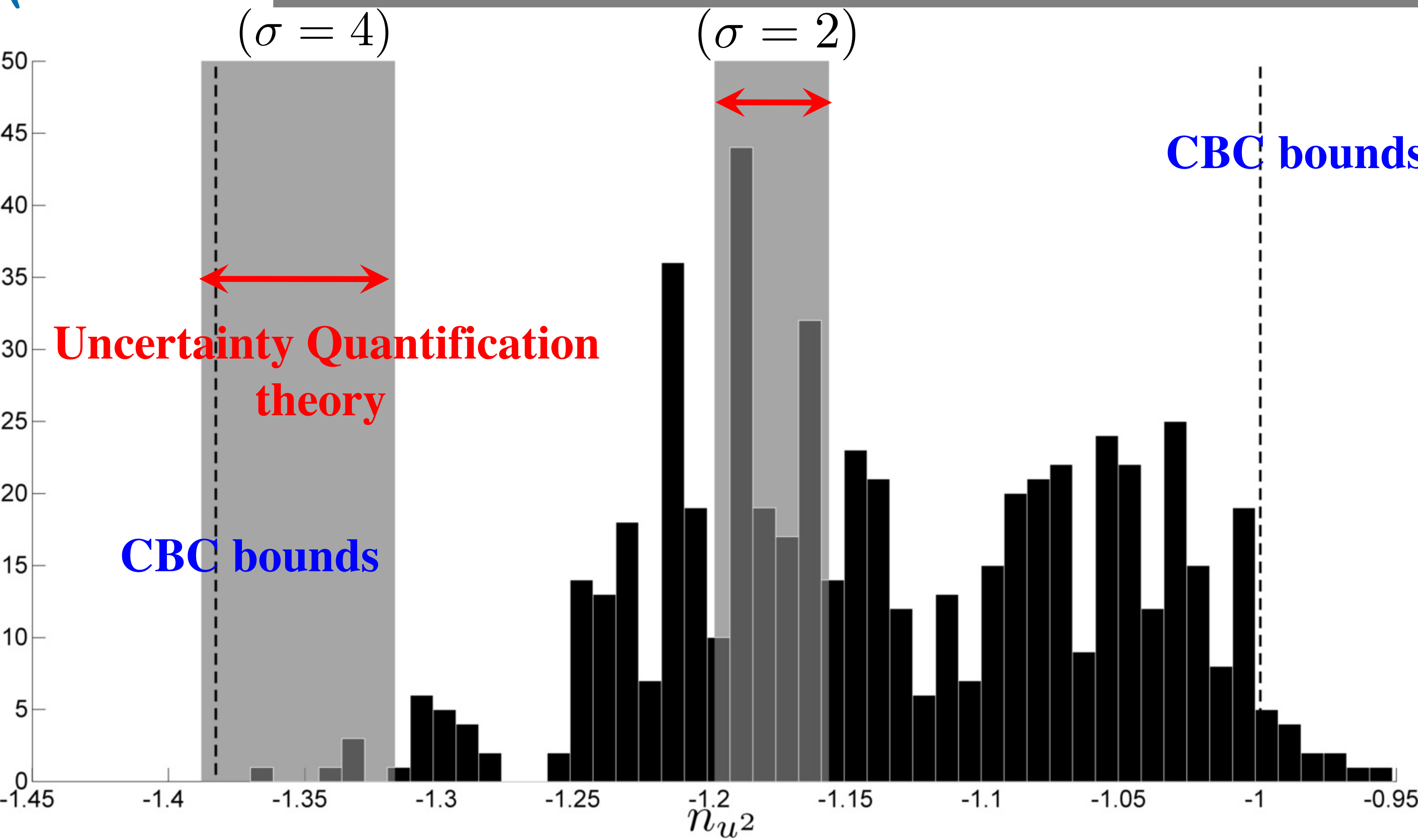

[Meldi et al., J. Fluid Mech. 668, 2011]
[Meldi & Sagaut, J. Fluid Mech. 711, 2012]

Need for theoretical analyis?

- ***Fundamental theorem of Blind CFD***
  1. Solving equations of crude physical model
  2. Using poorly accurate numerical methods
  3. Implemented in a bugged code

  → It is possible to fit experimental data in many cases

- ***Proof***: daily practice !

- But when it doesn't work, we need to understand what is going on!

Aix*Marseille université

LES: a deeper analysis

$$\frac{\partial u}{\partial t} + F\left(u, u\right) = 0$$

u: exact turbulent solution

$$\frac{\delta u_h}{\delta t} + F_h(u_h, u_h) = 0$$

u_h: discrete solution

LES:

- discrete solution ➪ **projection error**
- approximate integro-differential operators ➪ **discretization error**
- unresolved scales ➪ **resolution error**

LES : Modified PDE Model

Discrete numerical model

$$\frac{\delta u_h}{\delta t} + F_h(u_h, u_h) = 0$$

Equivalent continuous PDE

$$\frac{\partial u_h}{\partial t} + F(u_h, u_h) = M + \varepsilon_r + \varepsilon_h$$

Exact subgrid model

Subgrid modelling error

numerical error

Implicit non-linear couplings in LES

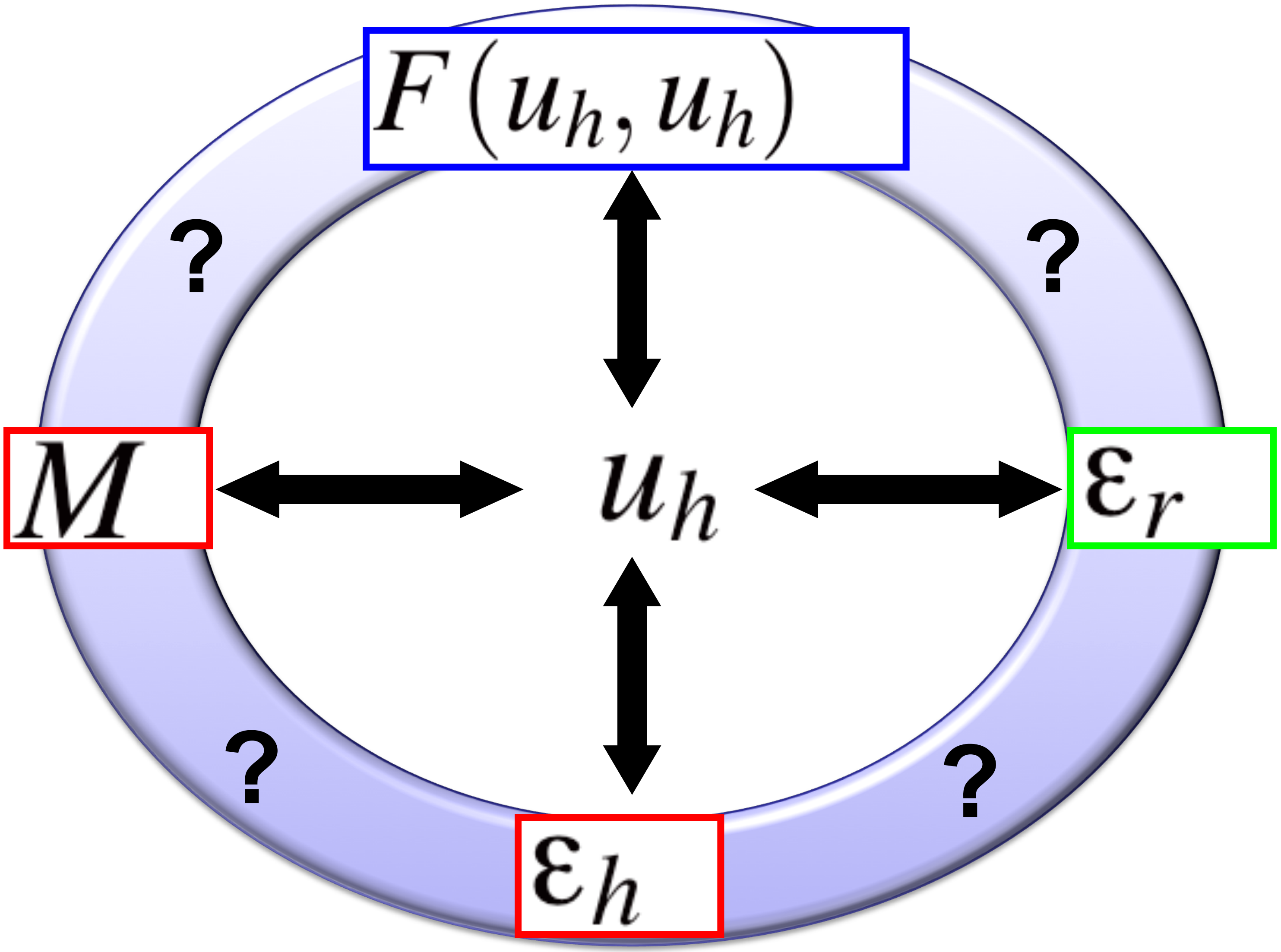

Aix*Marseille université

Error sources

$$e(h_r,\eta) = e_\Pi(h_r,\eta) + e_h(h_r,\eta) + e_r(h_r,\eta)$$

projection discretization resolution

Discretization/numerical error

$$\nabla_h(u) - \nabla(u) \neq 0 \Longrightarrow e_h(h_r,\eta)$$

Resolution/modelling error

$$F_h(u_h,u_h) \neq F_h(u,u) = F(u,u) \Longrightarrow e_r(h_r,\eta)$$

DNS as a limit (consistency)

$$\lim_{h_r \to \eta} e(h_r,\eta) = 0$$

E.g. Numerical and VMS viscosities

(Ciardi & al., JOT, 2006)

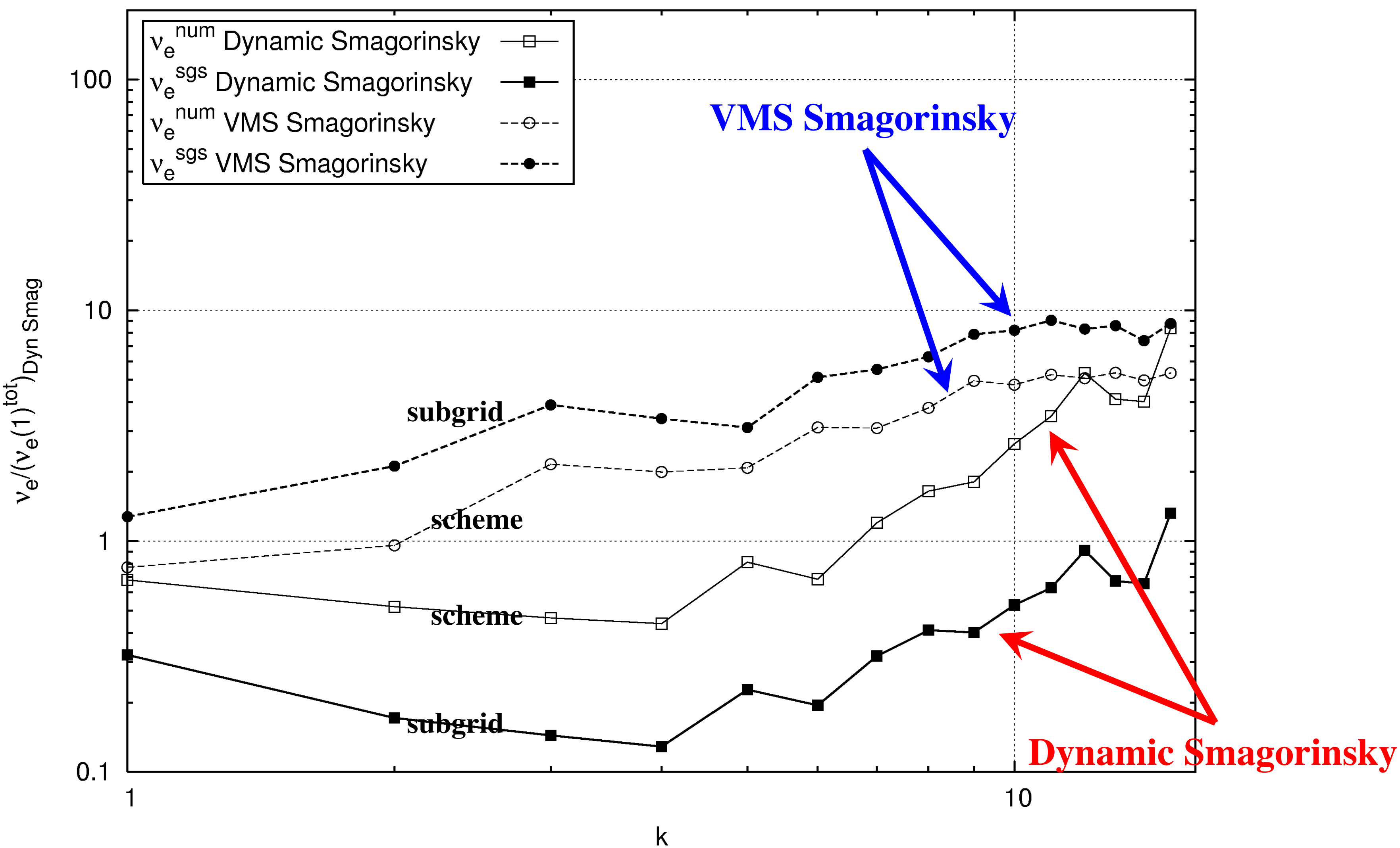

What is the optimal LES solution ?

Definition of an optimal LES solution

$$\min(e_\pi + e_h + e_r) = \min(e_\pi)$$

$$e_h + e_r = 0$$

Implicit LES:

- No physical subgrid model
- Ad hoc scheme

$$e_h = e_r = 0$$

Classical LES:

- Explicit subgrid model
- Neutral scheme

2. Couplings between numerics and SGS models

Static & Dynamic analysis

- **Linearized analysis**:
  - reminiscent of von Neuman analysis for numerical schemes
  - linearized terms
  - monochromatic plane wave solution
  - Drawbacks: linearization, turbulent spectrum ignored, no feedback
- **Static analysis**
  - nonlinear terms
  - turbulent spectrum prescribed
  - Drawback: no feedback
- **Dynamic analysis**
  - nonlinear terms
  - turbulent solution computed
  - feedback & couplings taken into account
  - Issue: simplified model

EDQNM-based analysis

Lin's equation for turbulent spectrum (1939)

$$\frac{\partial}{\partial t}E(k,t) + 2\nu k^2 E(k,t) = T(k,t)$$

EDQNM model (Orszag, 1971)

$$\frac{\partial}{\partial t}E(k,t) + 2\nu k^2 E(k,t) = T_{EDQNM}(k,t)$$

Exact/ideal EDQNM-LES

$$\frac{\partial}{\partial t}\bar{E}(k,t) + 2\nu k^2 \bar{E}(k,t) = T^{<}_{EDQNM}(k,t) + T^{>}_{EDQNM}(k,t)$$

EDQNM-LES with subgrid model

$$\frac{\partial}{\partial t}\bar{E}(k,t) + 2\nu {k'}^2 \bar{E}(k,t) = {T'}^{<}_{EDQNM}(k,t) + T'_{sg}(k,t)$$

EDQNM-LES tool flexibility

$$\frac{\partial}{\partial t}\bar{E}(k,t) + 2\nu k'^2\bar{E}(k,t) = T'^{<}_{EDQNM}(k,t) + T'_{sg}(k,t)$$

- Discretization errors in viscous terms

$$2\nu k^2\bar{E}(k,t) \longrightarrow 2\nu k'^2\bar{E}(k,t)$$

- Discretization errors in convection & pressure terms

$$T^{<}_{EDQNM}(k,t) \longrightarrow T'^{<}_{EDQNM}(k,t)$$

- Subgrid modelling errors

$$T^{>}_{EDQNM}(k,t) \longrightarrow T_{sg}(k,t)$$

- Discretization errors in subgrid model

$$T_{sg}(k,t) \longrightarrow T'_{sg}(k,t)$$

Ideal LES (EDQNM-based)

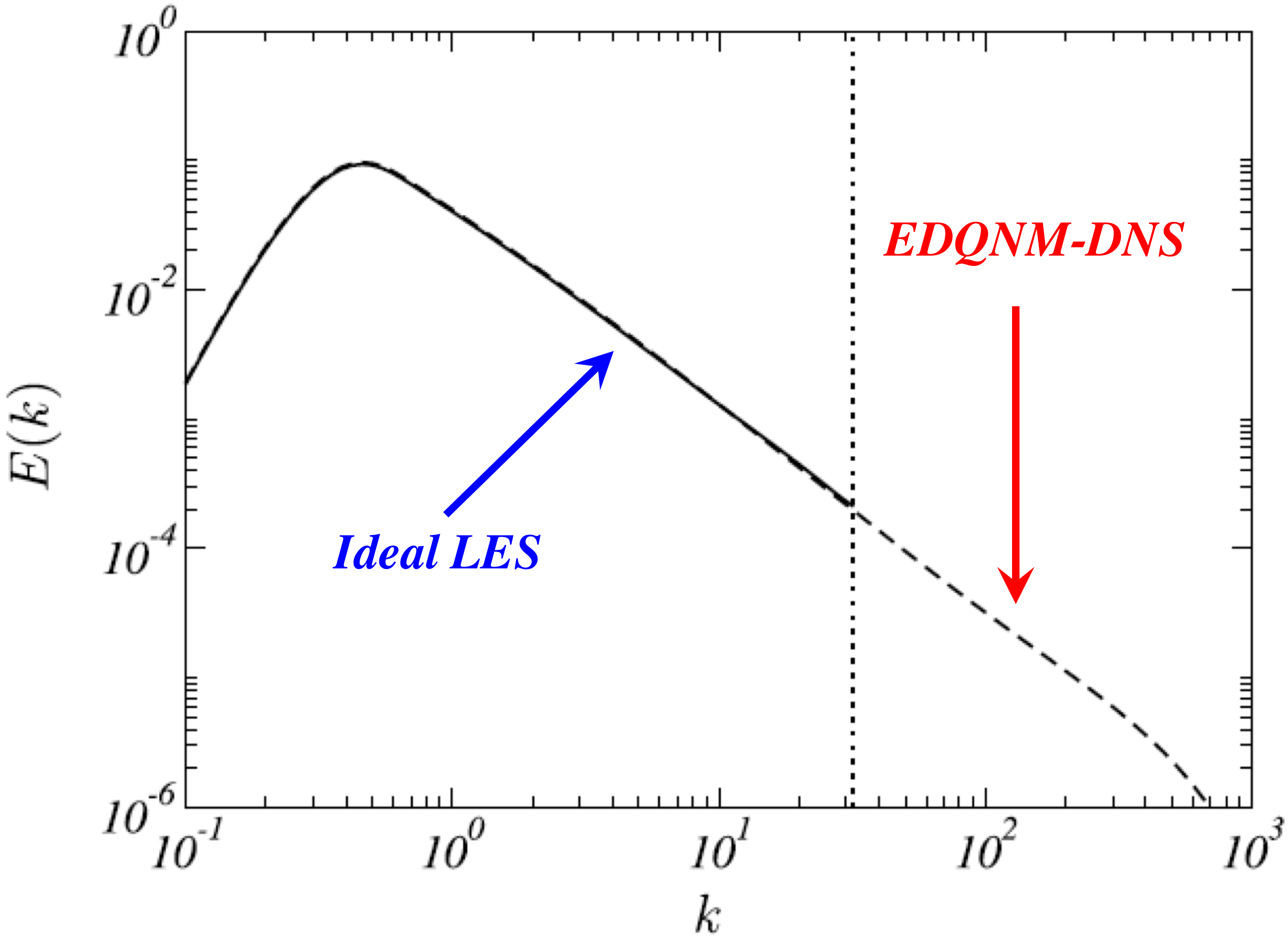

Sensitivity to convection discretization

Real physical-space LES | EDQNM-LES

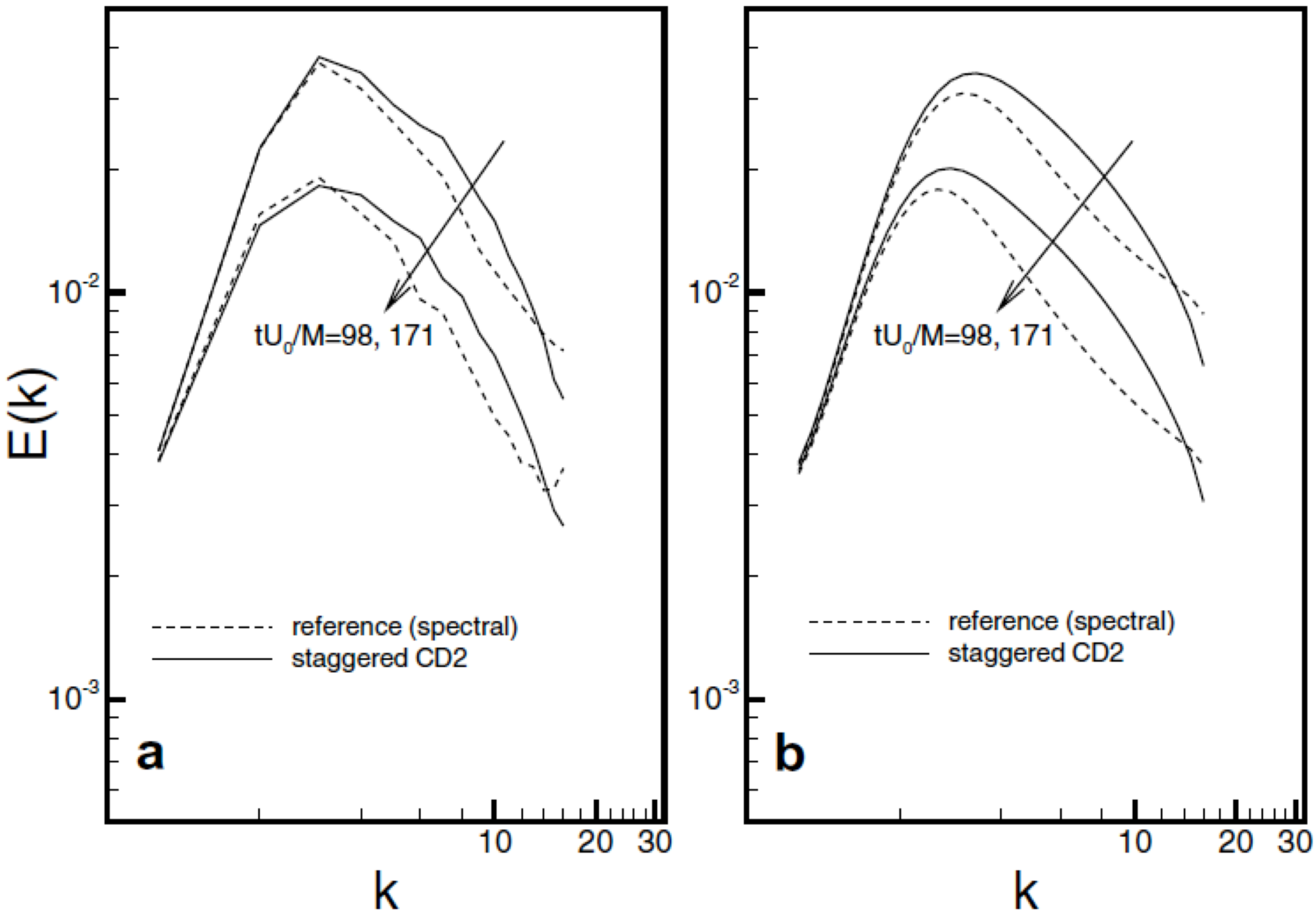

Sensitivity to convection discretization

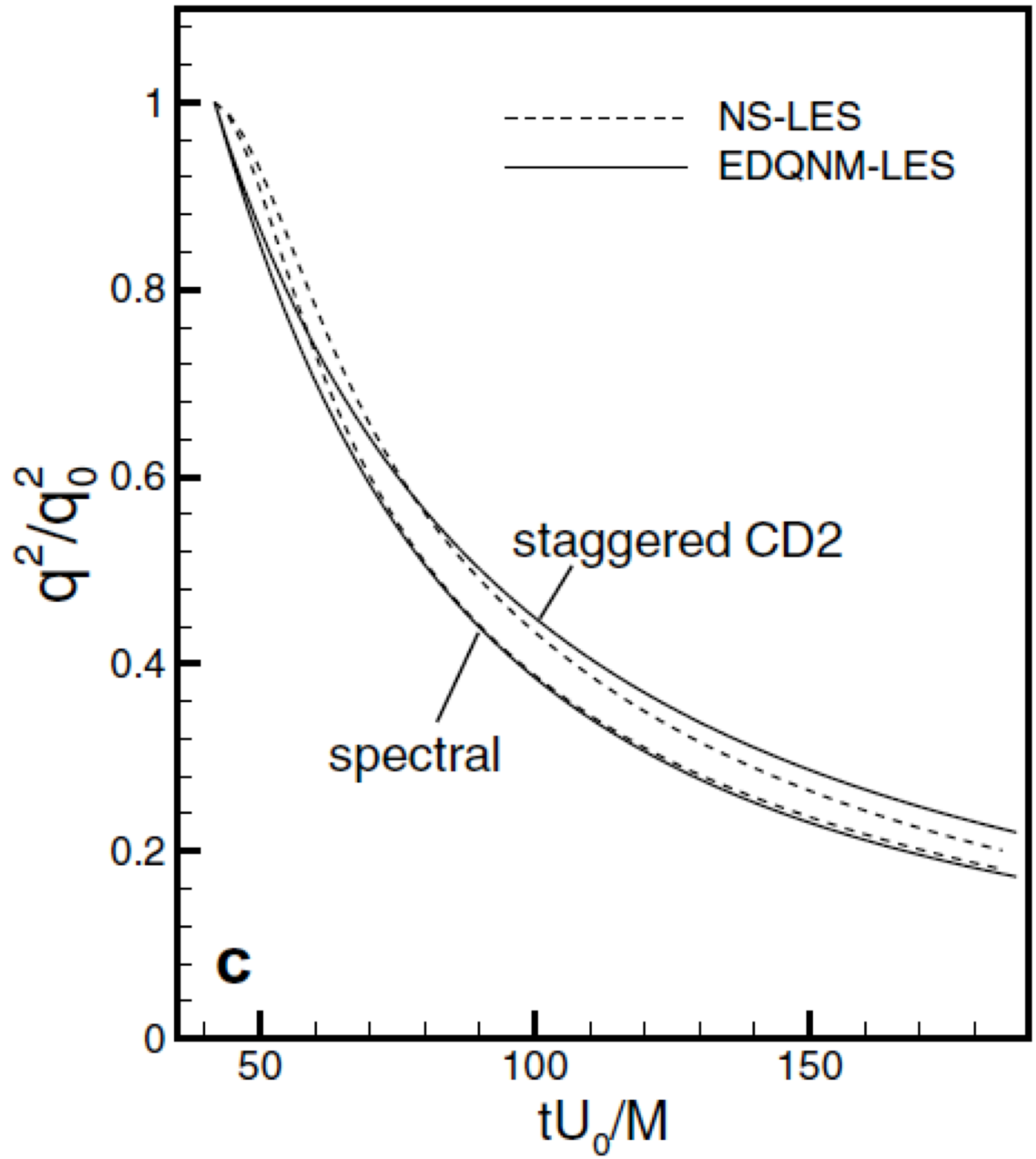

Sensitivity to viscous term discretization

3-pt 2nd order scheme

$$\left.\frac{\partial^2}{\partial x^2} u\right|_i \sim \frac{u_{i-1} - 2u_i + u_{i+1}}{h^2}$$

5-pt 2nd order scheme

$$\left.\frac{\partial^2}{\partial x^2} u\right|_i \sim \frac{u_{i-2} - 2u_i + u_{i+2}}{4h^2}$$

Ghost mode $\quad u = (..., 1, -1, 1, -1, ...)$

Sensitivity to viscous term discretization

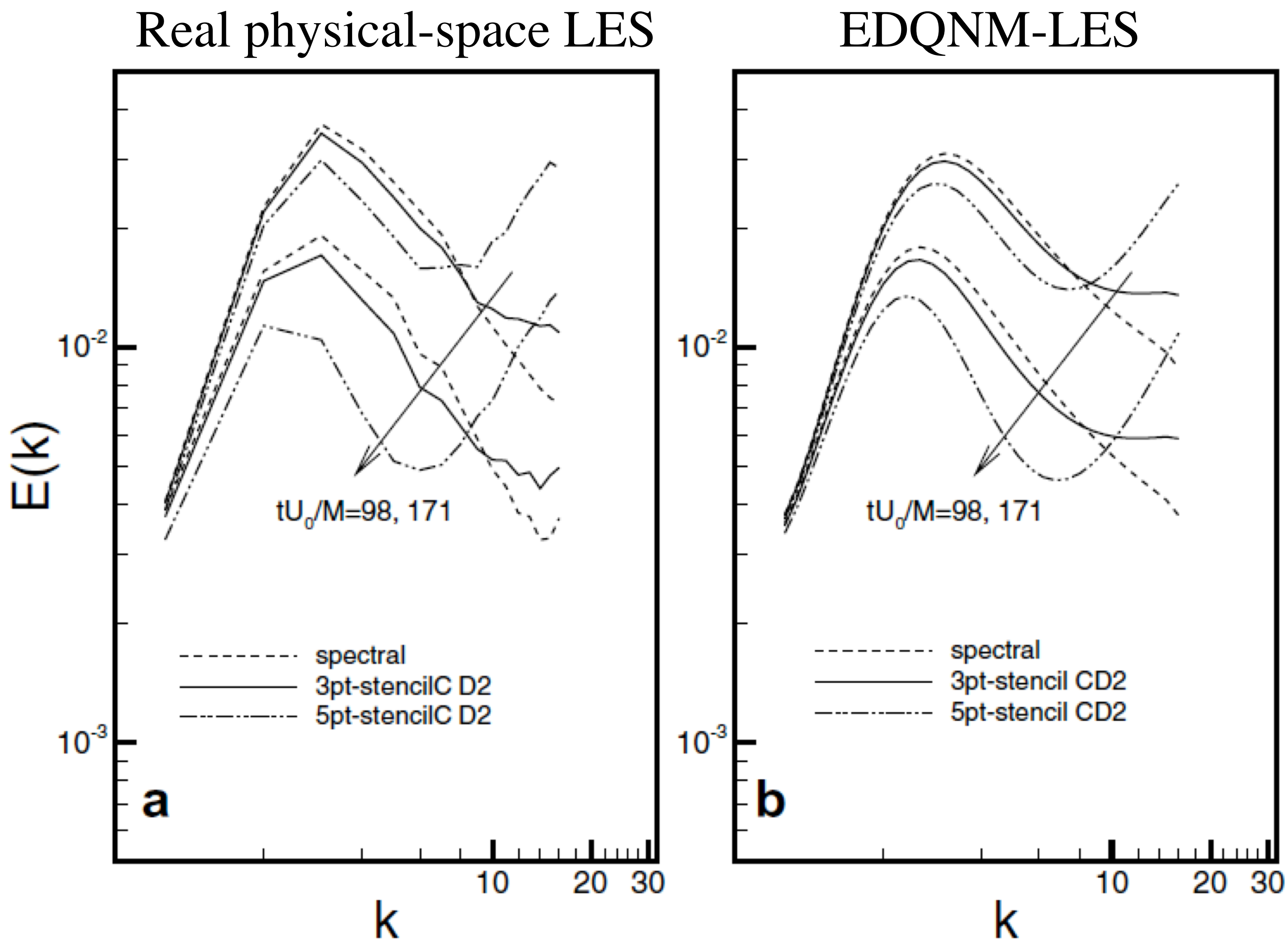

Sensitivity to viscous term discretization

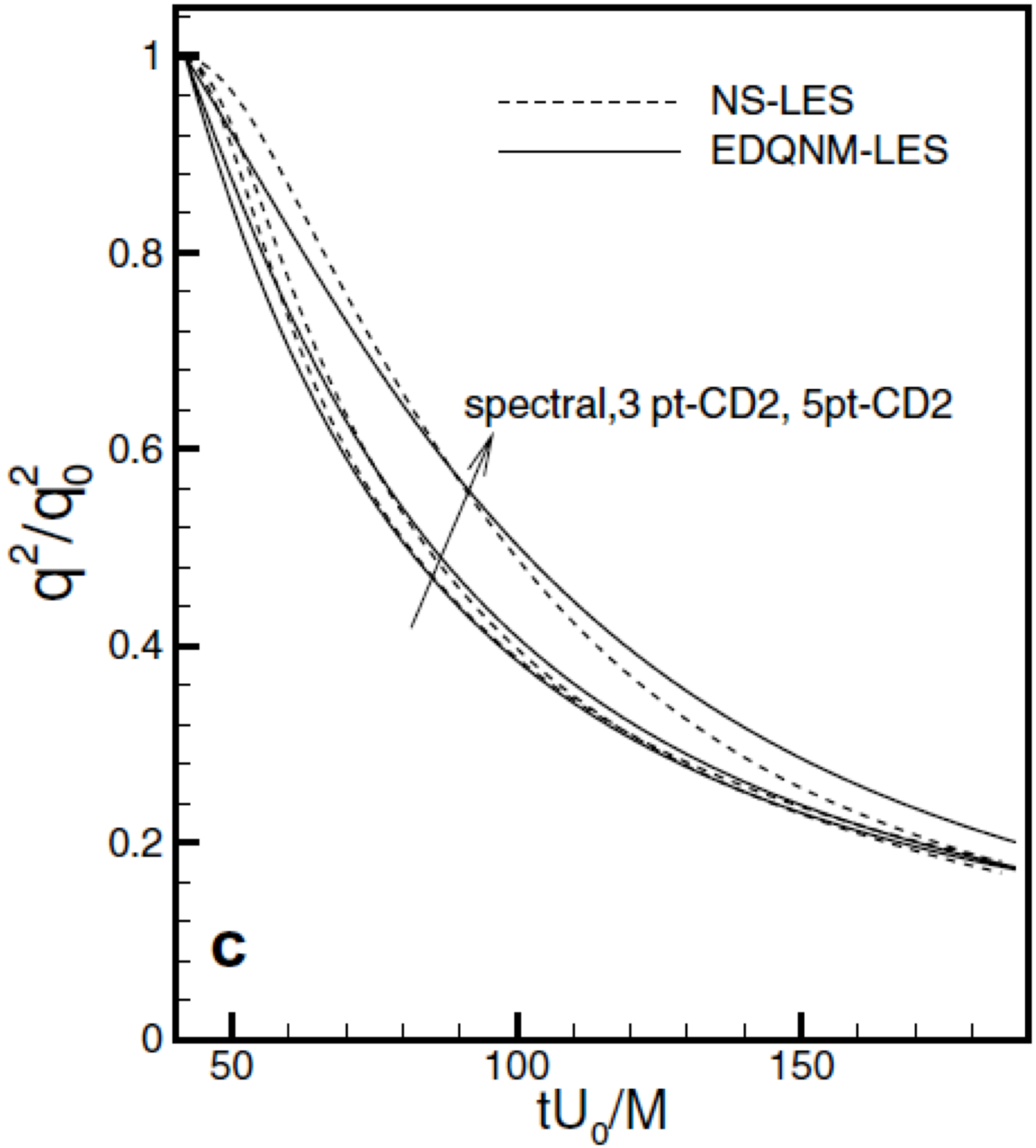

Sensitivity to aliasing errors

Real physical-space LES

EDQNM-LES

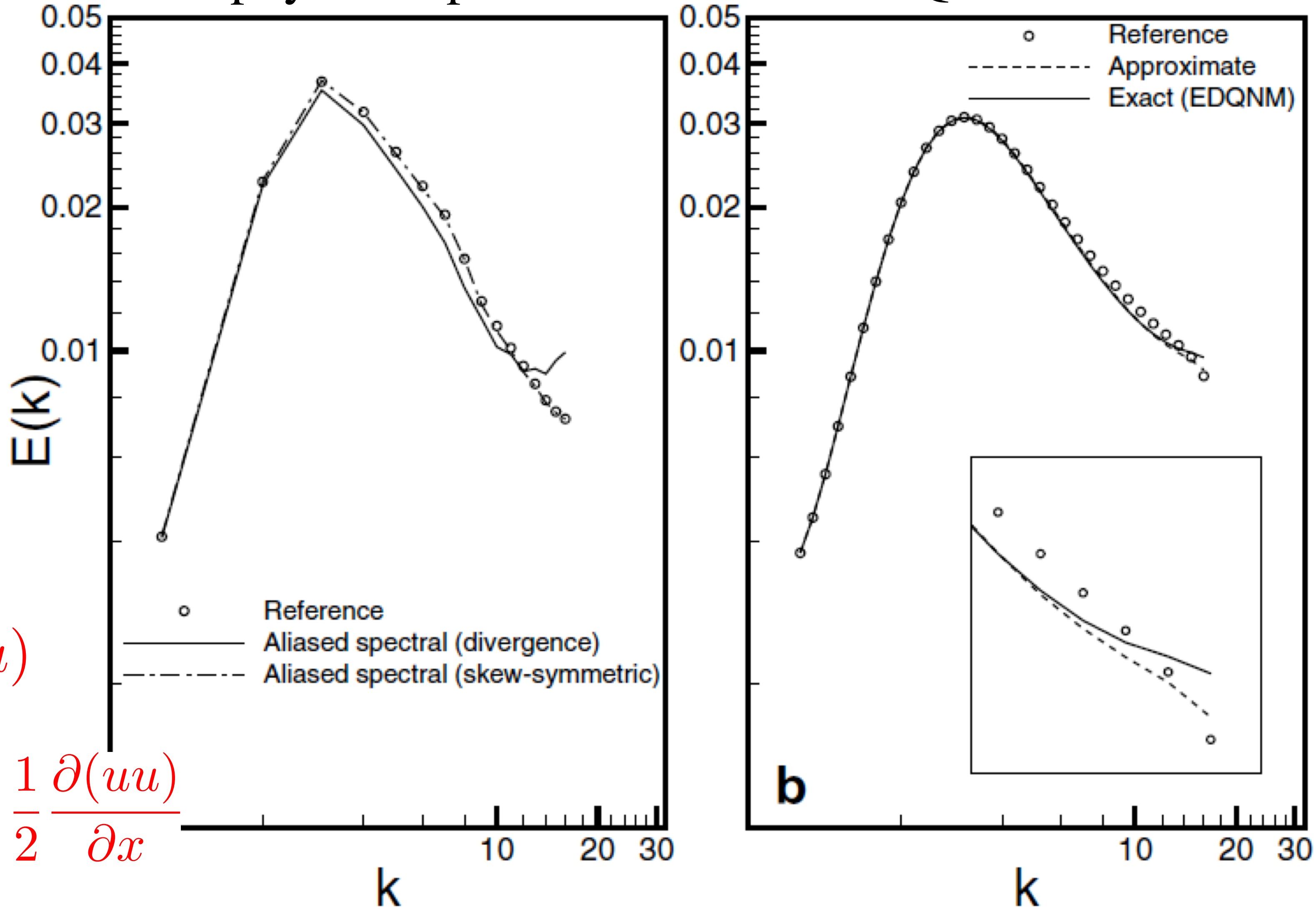

$$\frac{\partial}{\partial x}(uu)$$

$$\frac{1}{2}u\frac{\partial u}{\partial x}+\frac{1}{2}\frac{\partial (uu)}{\partial x}$$

Sensitivity to aliasing errors

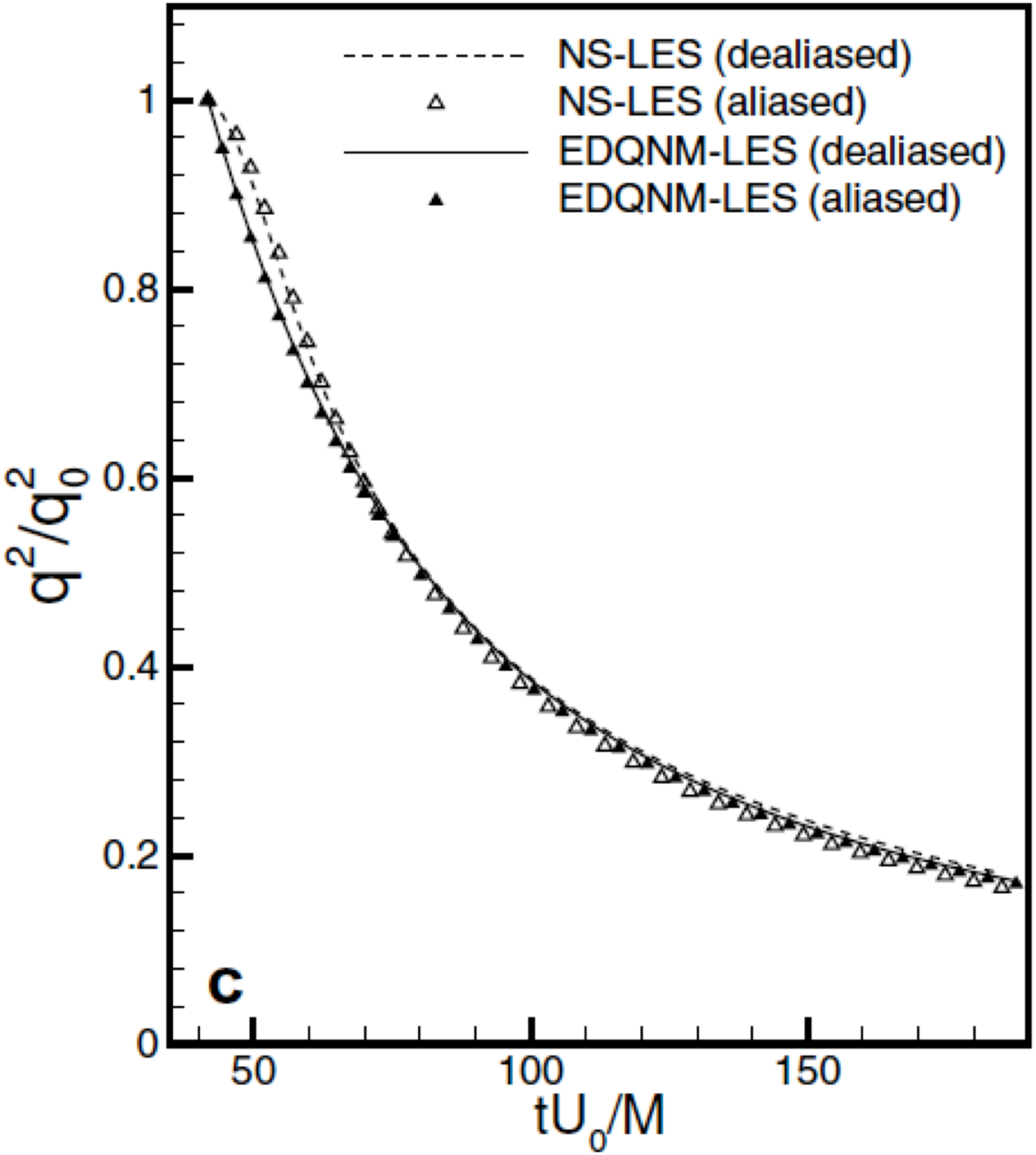

2nd-order vs. Spectral method

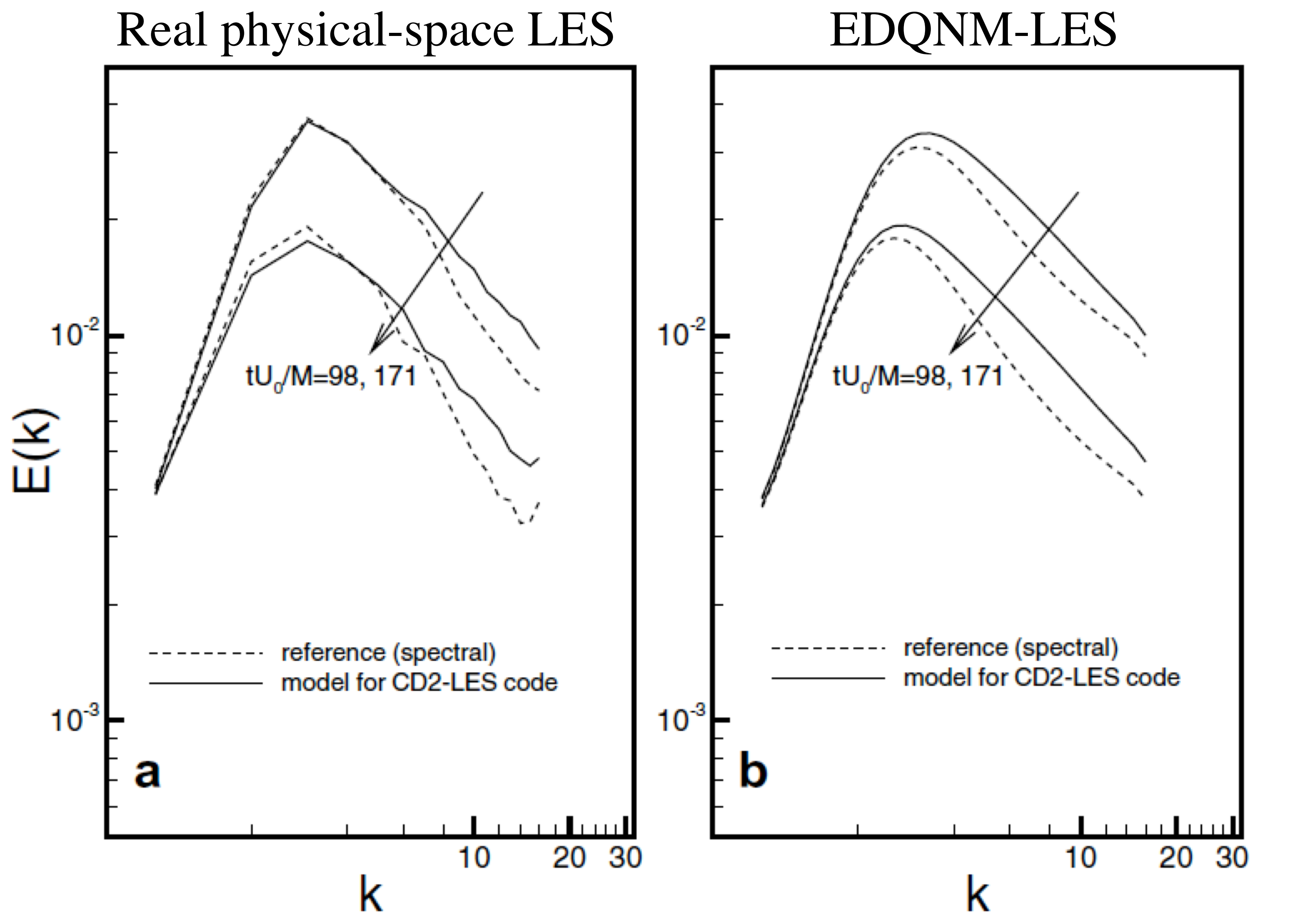

2^{nd}-order vs. Spectral method

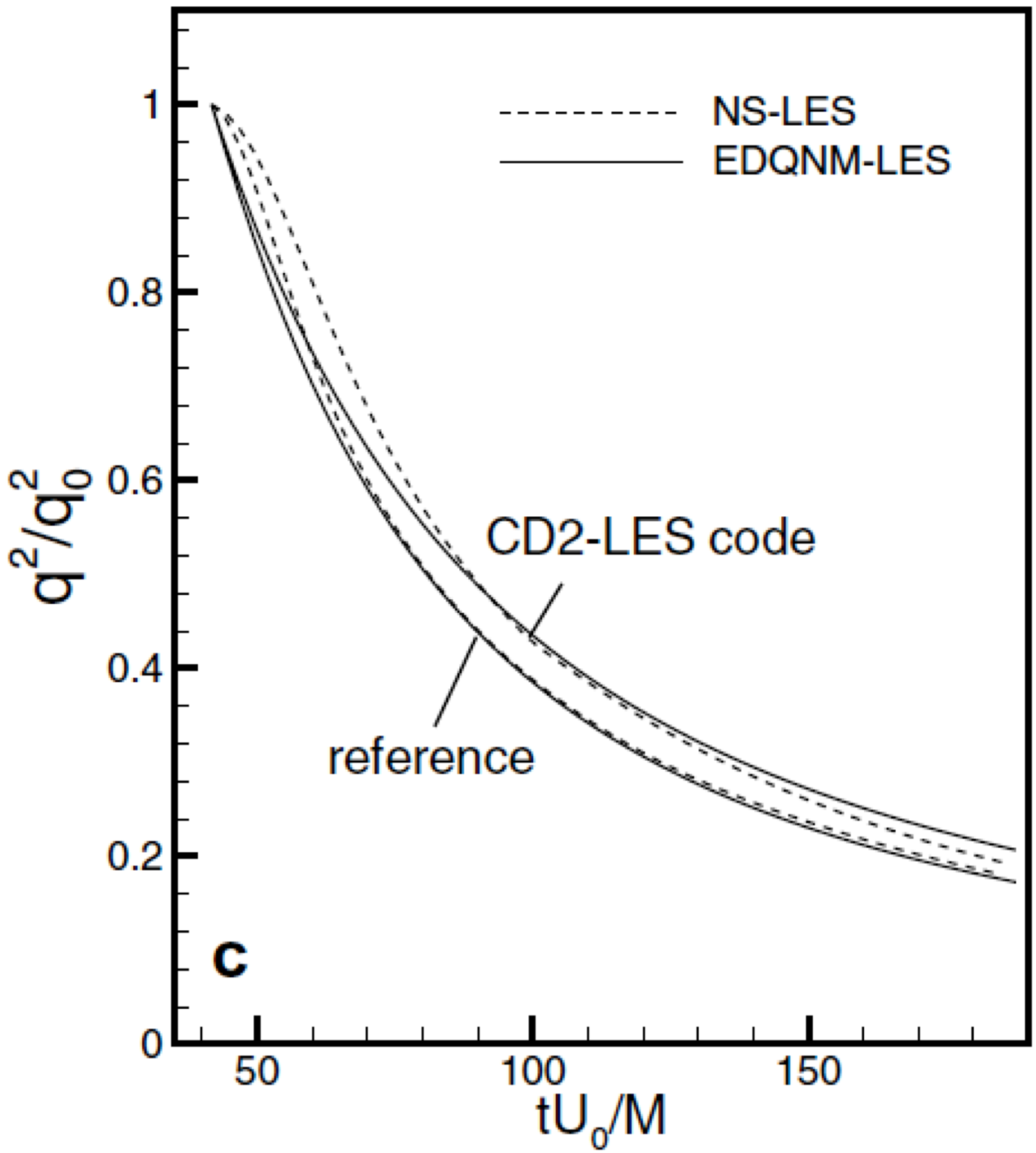

SGS model/numerics coupling

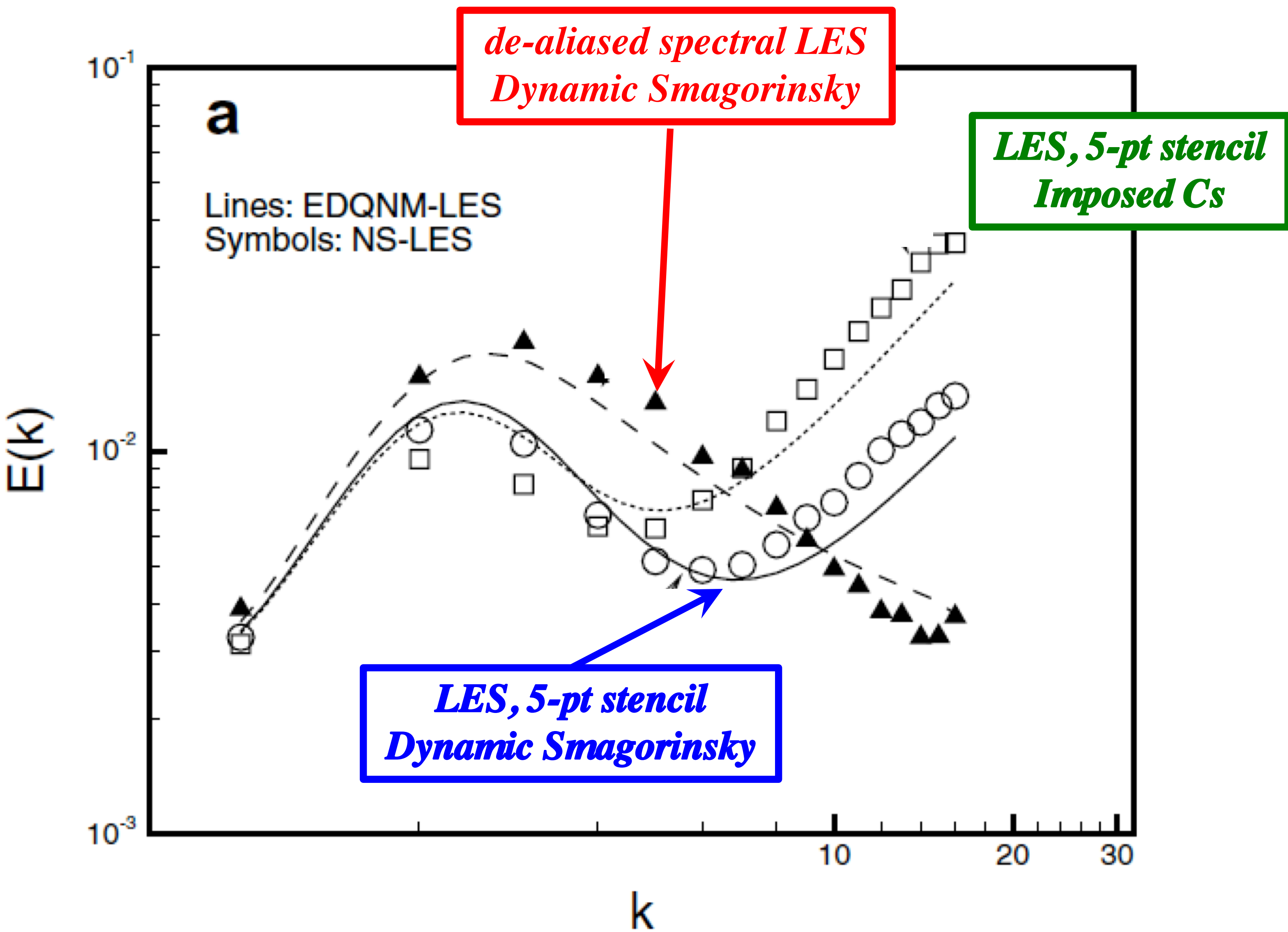

SGS model/numerics coupling

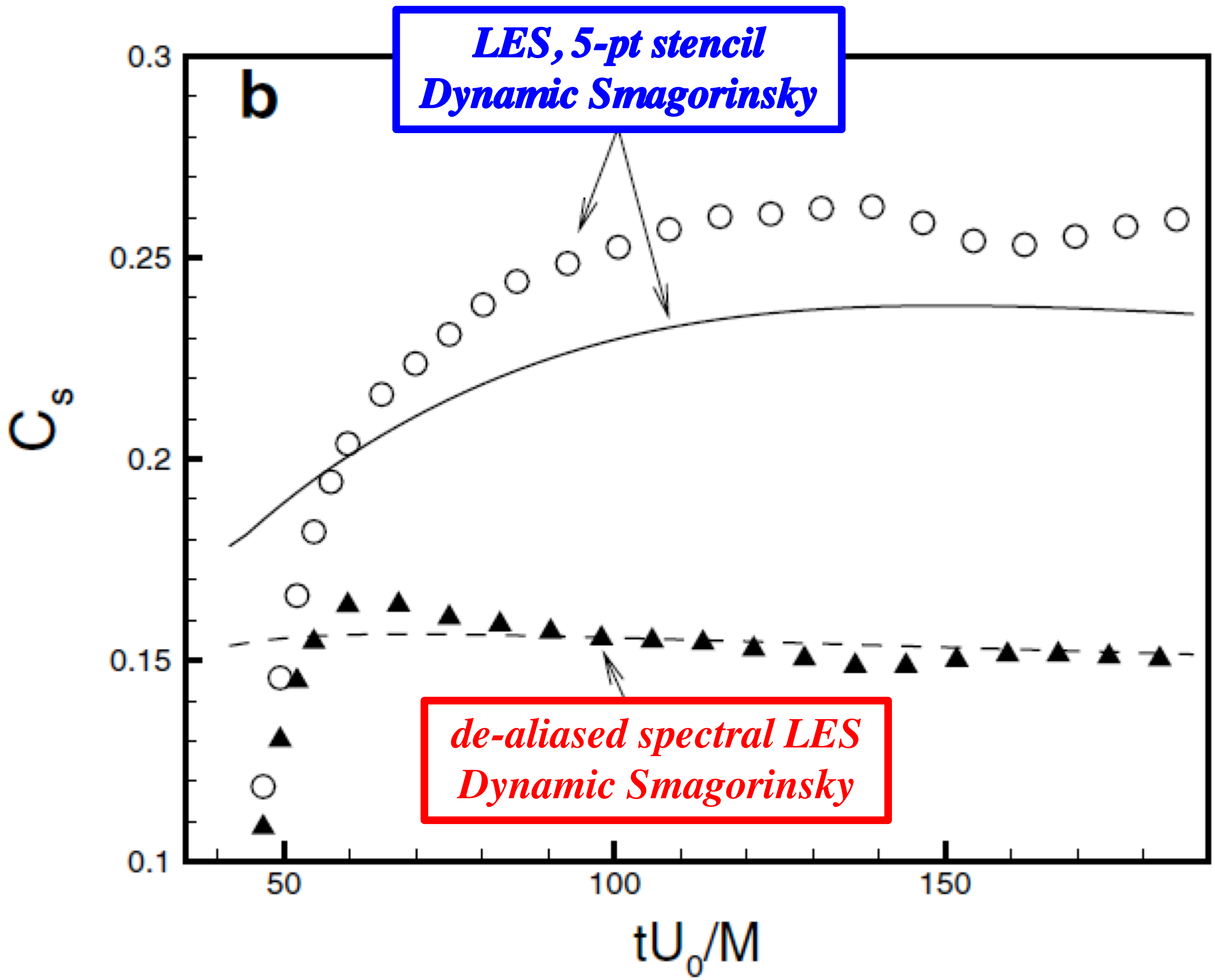

SGS model/numerics coupling

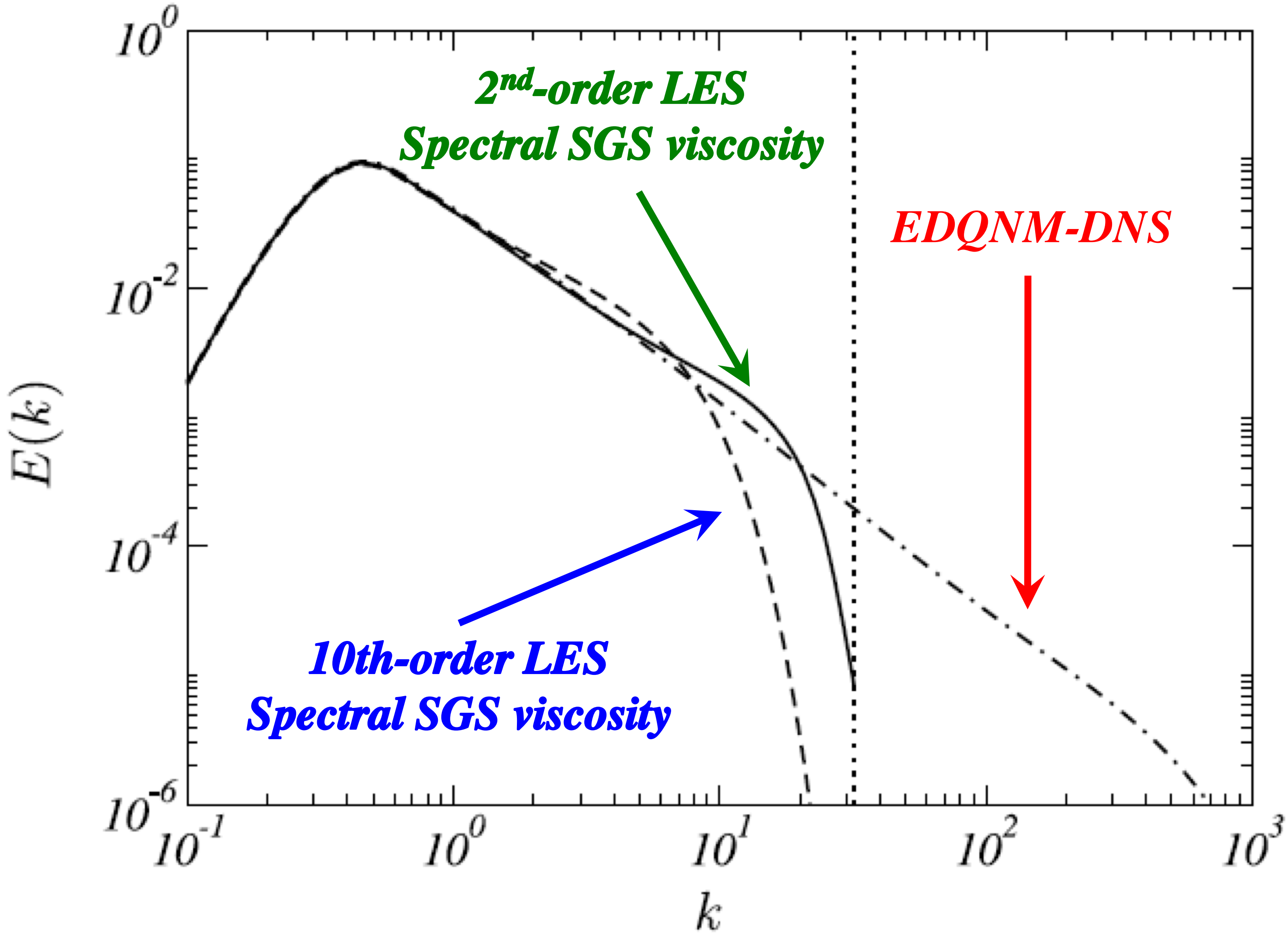

Static vs. Dynamic analysis

dynamic

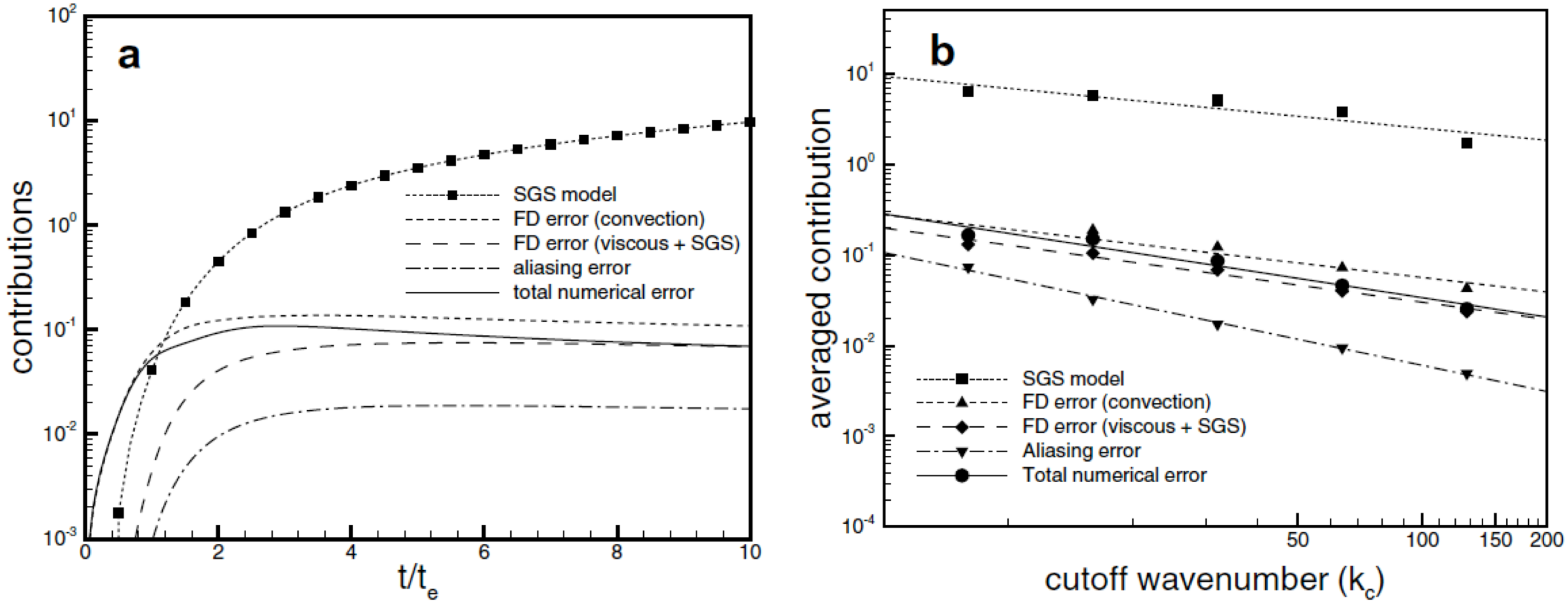

static

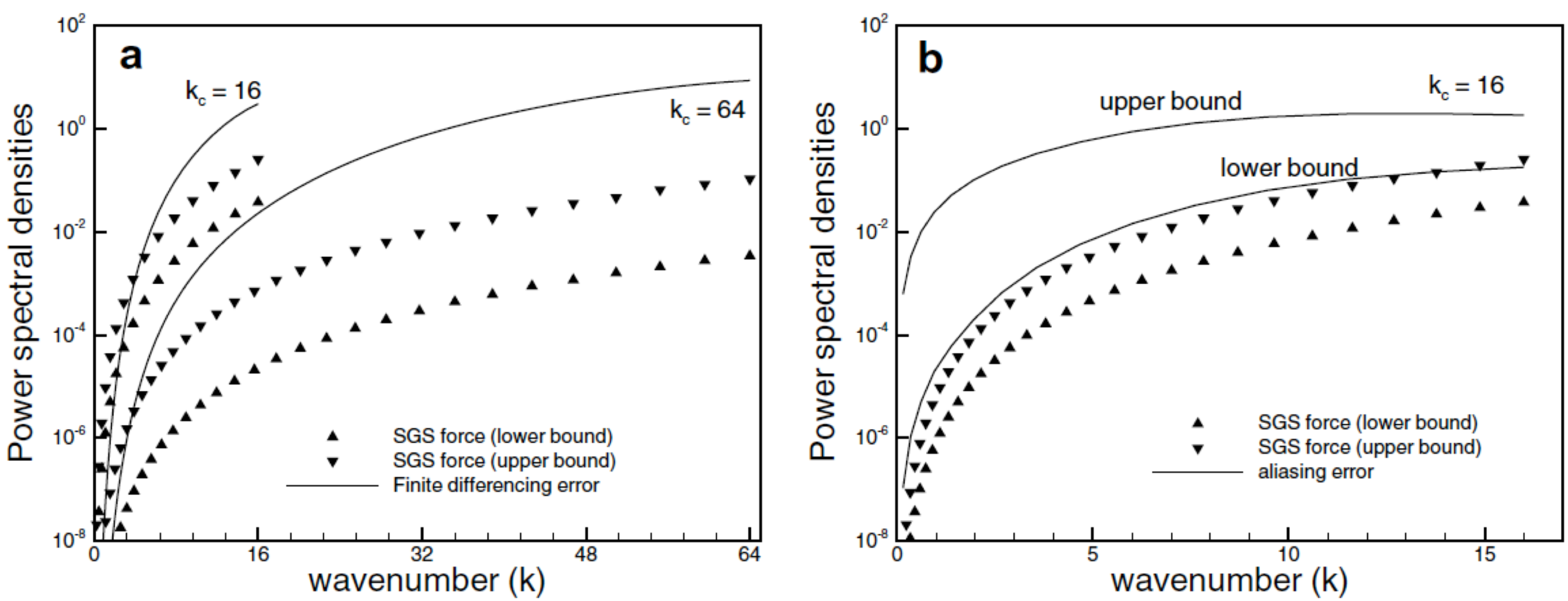

Effect of order of accuracy (*dynamic*)

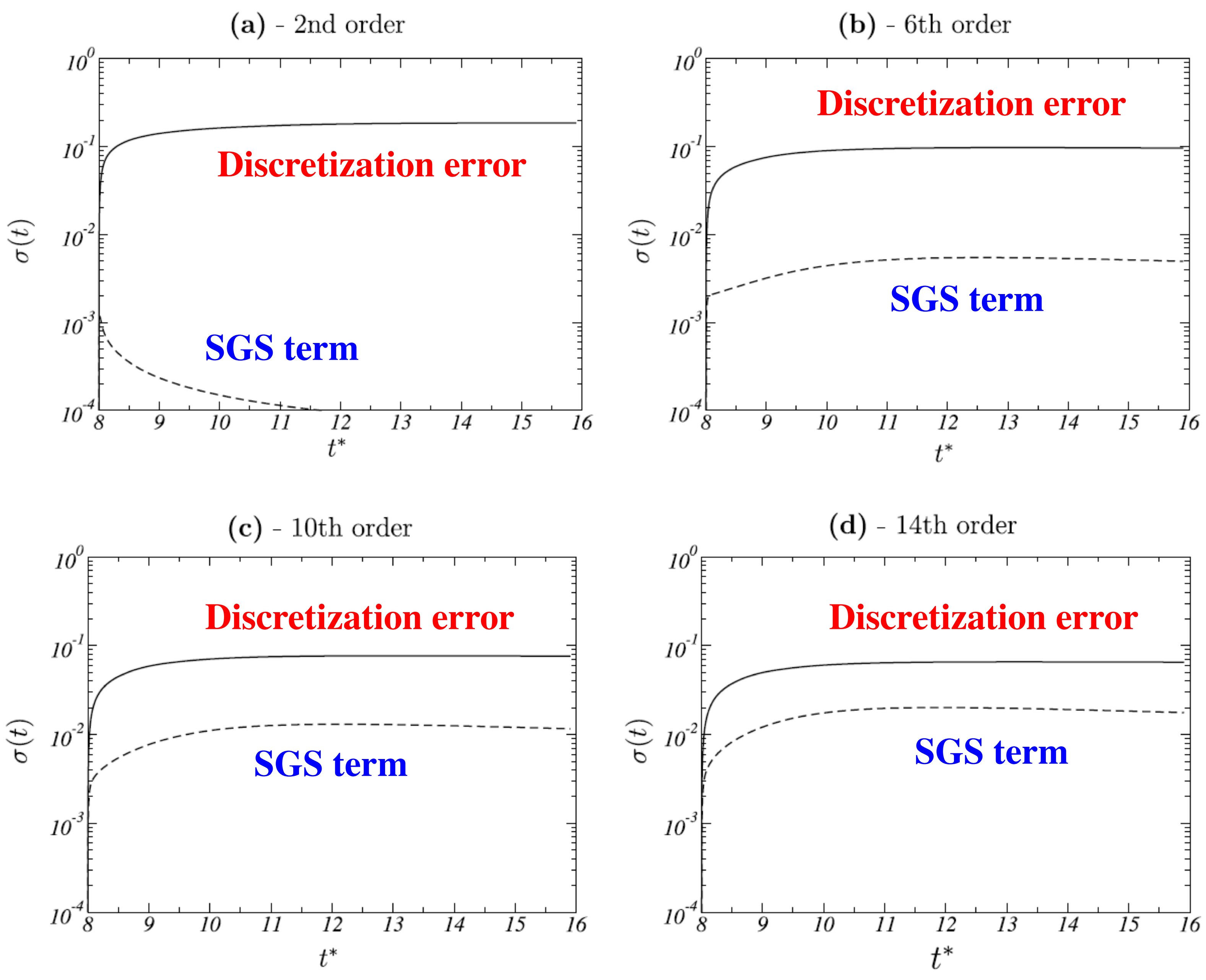

Channel flow case

Simulations of turbulent channel flow with various discretization schemes

Scheme	Nonlinear terms	SGS model	Stability
COM4	Divergence	○	↑
COM4	Skew-symmetric	○, ×	●
COM4	Advective	○ (×)	● (↑)
CUDZ	Divergence	○, ×	↓
CUD3	Divergence	○, ×	↓
CUD ($\alpha = 0.008$)	Divergence	○, ×	●
WENO3	Divergence	○, ×	↓

●, stable; ↑, numerically unstable; ↓, flow laminarizes.

Overshoot → no filter !

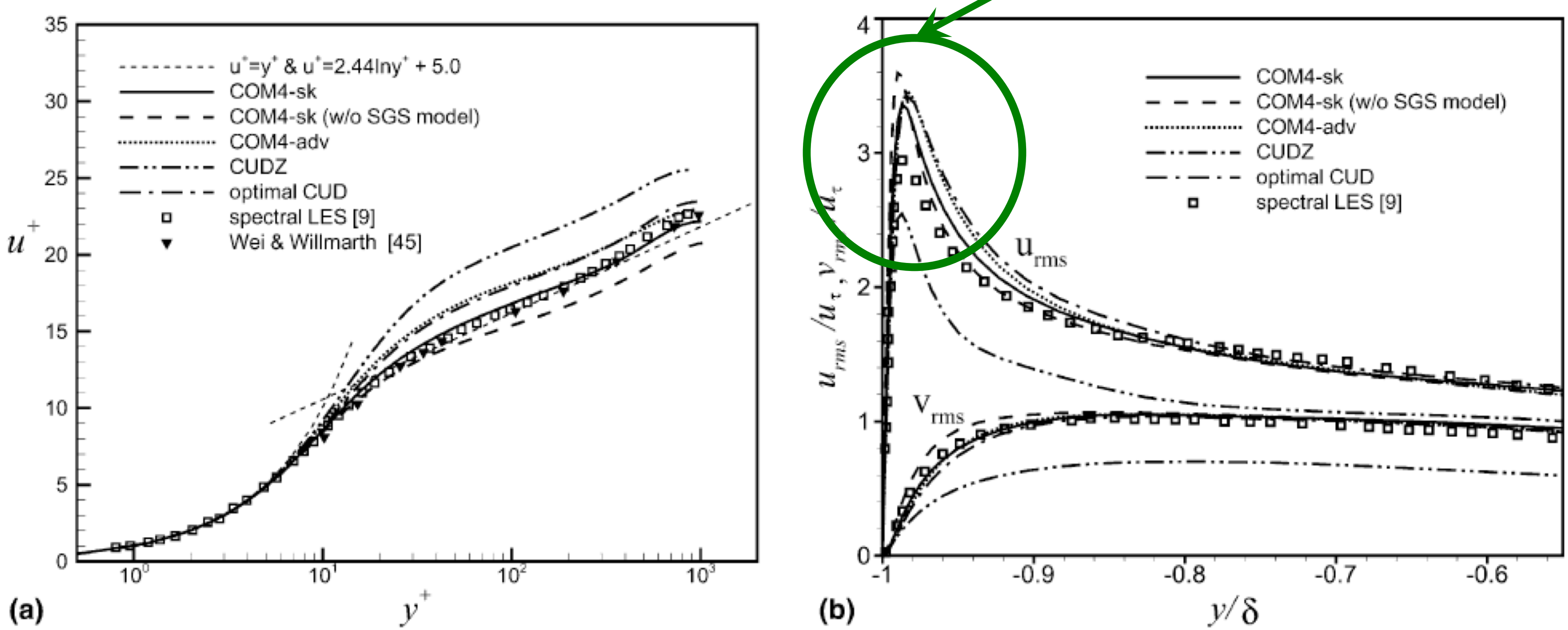

Channel flow case

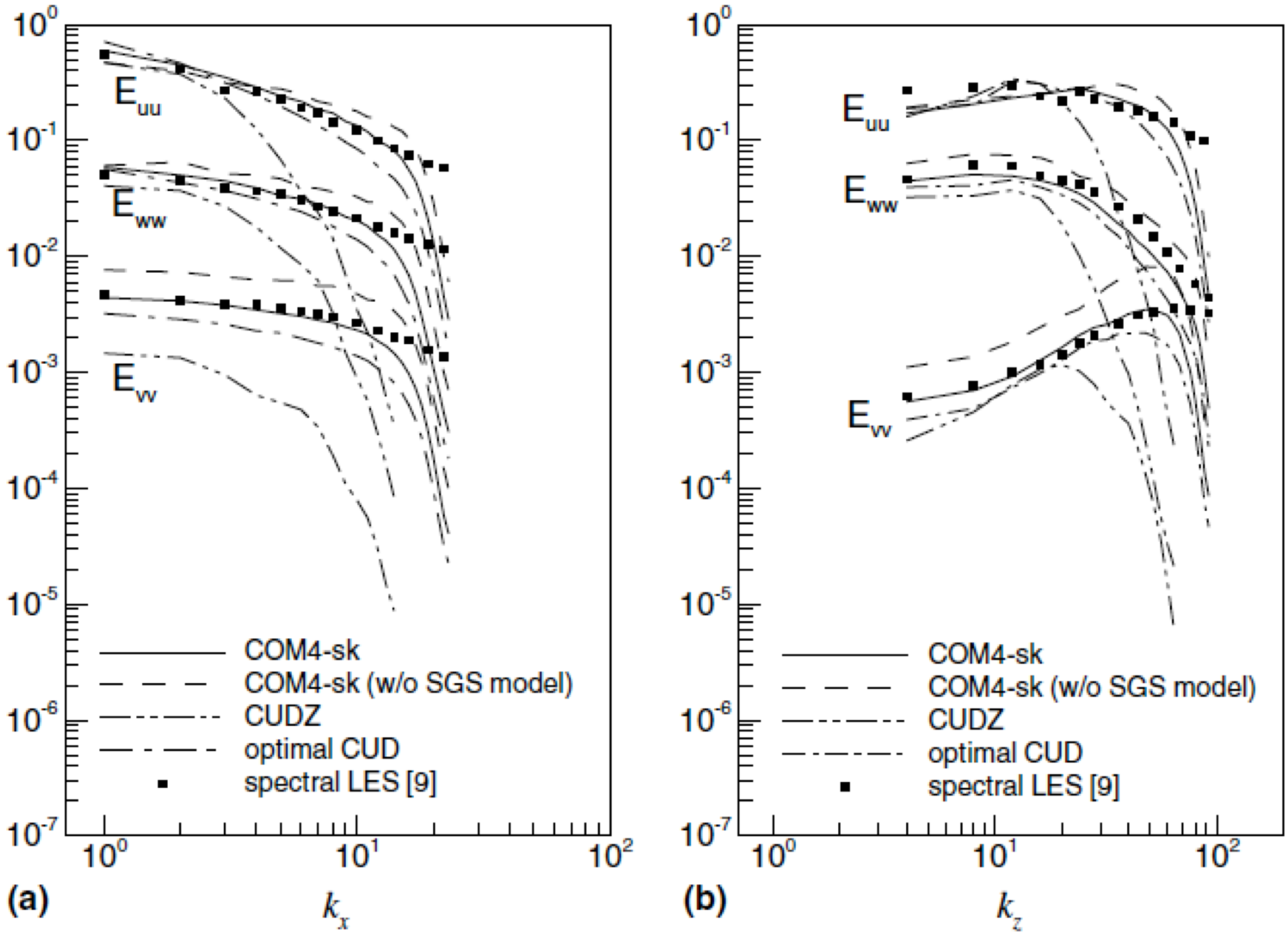

Channel flow case

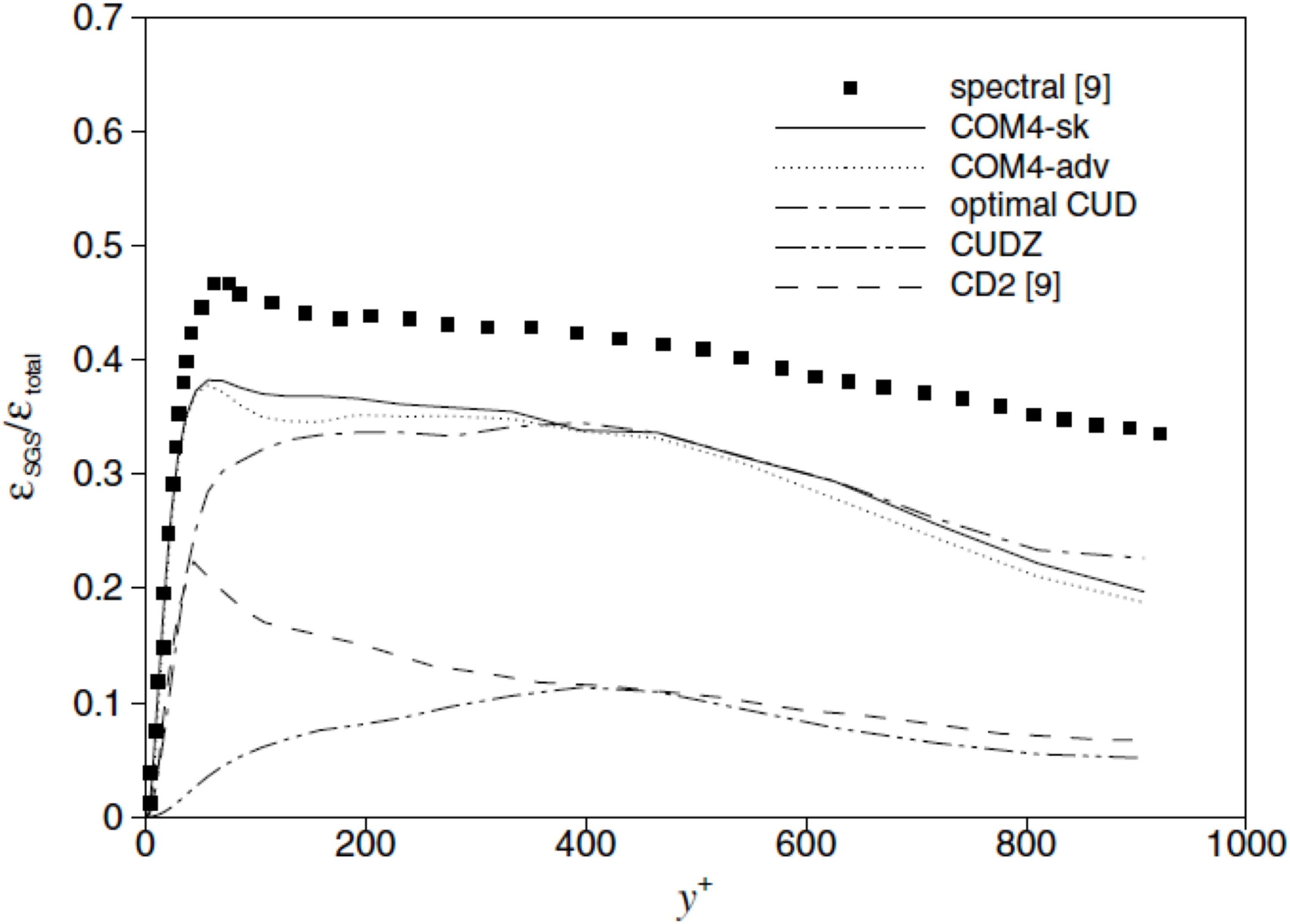

Skin friction error map (model-free)

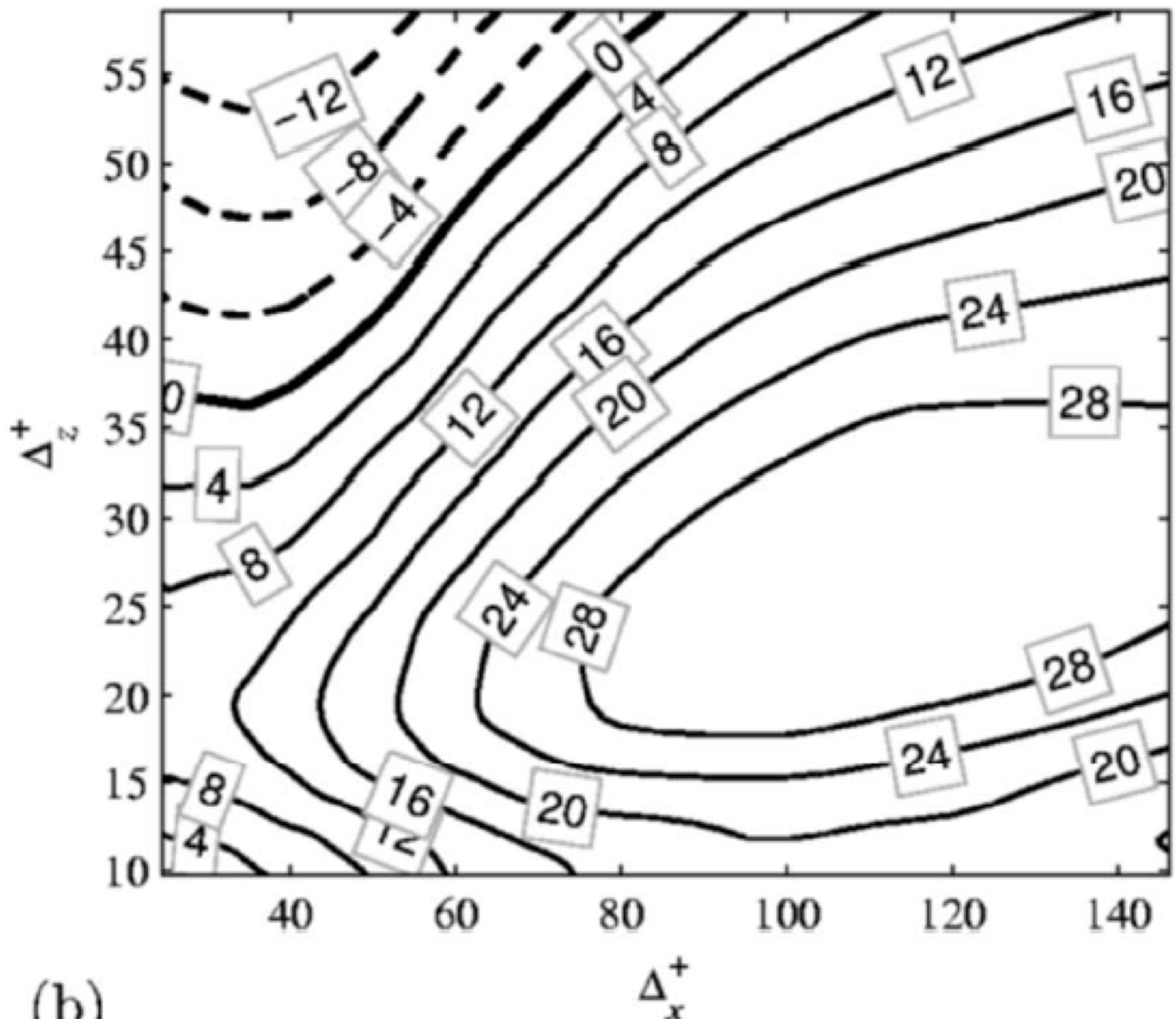

(b)

Zero error trajectories

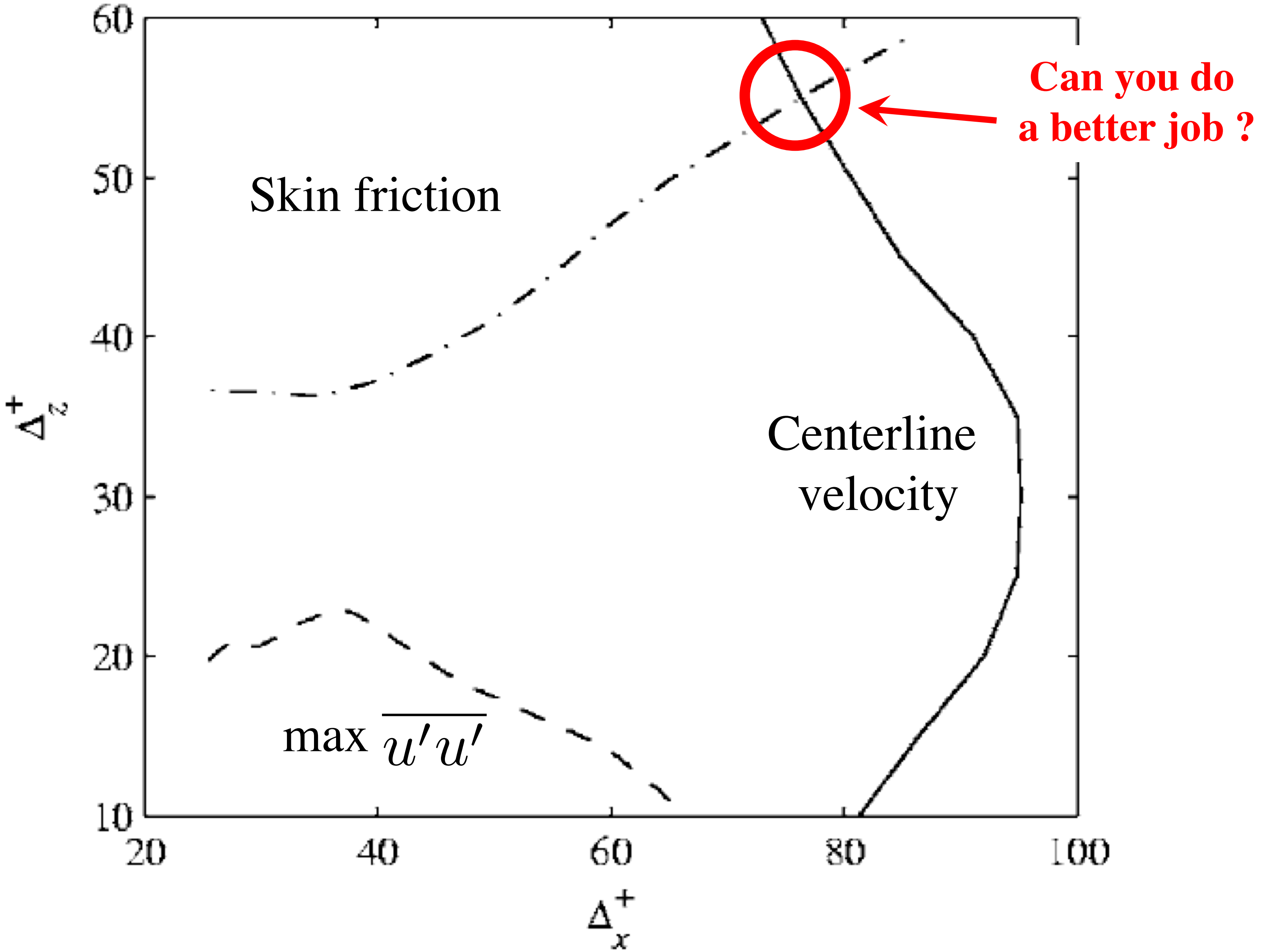

Circular cylinder (Re = 3900)

Flow parameters for the flow over a circular cylinder at $Re = 3900$

Data from	C_D	$-C_{p_b}$	St	L_{rec}/D	U_{min}
Run1	1.02	0.89	0.209	1.37	−0.33
Run2	1.04	0.93	0.209	1.26	−0.34
Run3	0.95	0.80	0.210	1.79	−0.27
Experiment [49–51]	0.99 ± 0.05	0.88 ± 0.05	0.215 ± 0.05	1.4 ± 0.1	-0.24 ± 0.1
UD7 (DSM) [19]	1.00	0.95	0.203	1.36	−0.32
UD7 (SM) [19]	0.96	0.81	0.209	1.74	−0.33
CD2 (DSM) [21]	1.00	0.93	0.207	1.40	−0.35
QUICK (SM) [22]	0.97	0.87	–	1.69	−0.24
B-spline (DSM) [47]	1.04	0.94	0.210	1.35	−0.37

Run1, COM4-sk (DSM); Run2, COM4-sk (no SGS model); Run3, CUDZ (DSM).

Circular cylinder (Re = 3900)

Compact scheme with dynamic Smagorinsky model

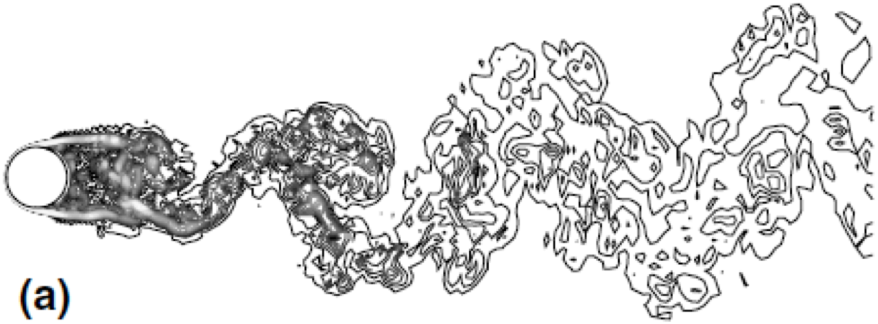

Compact scheme without Subgrid model

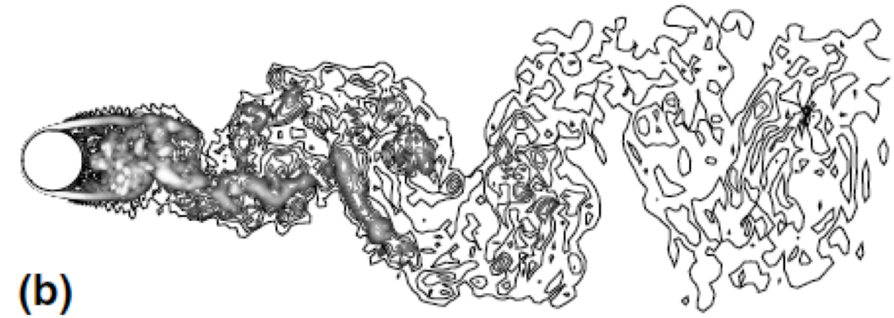

Compact upwind scheme without subgrid model

Circular cylinder (Re = 3900)

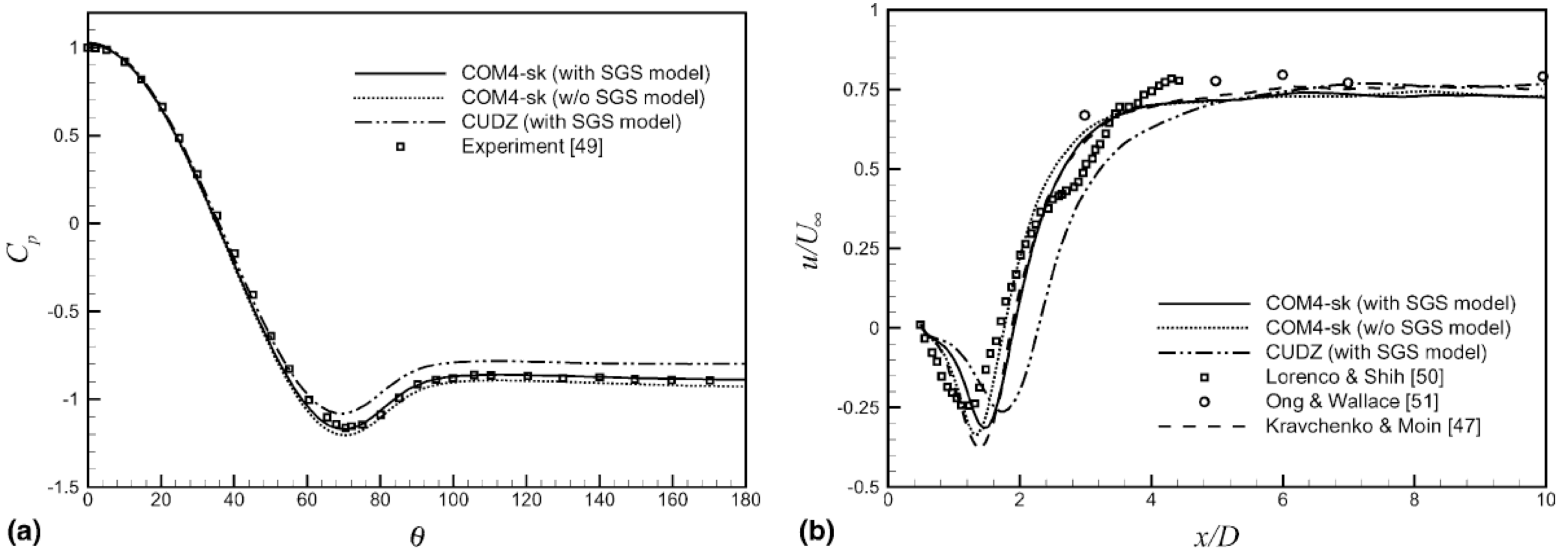

Circular cylinder (Re = 3900)

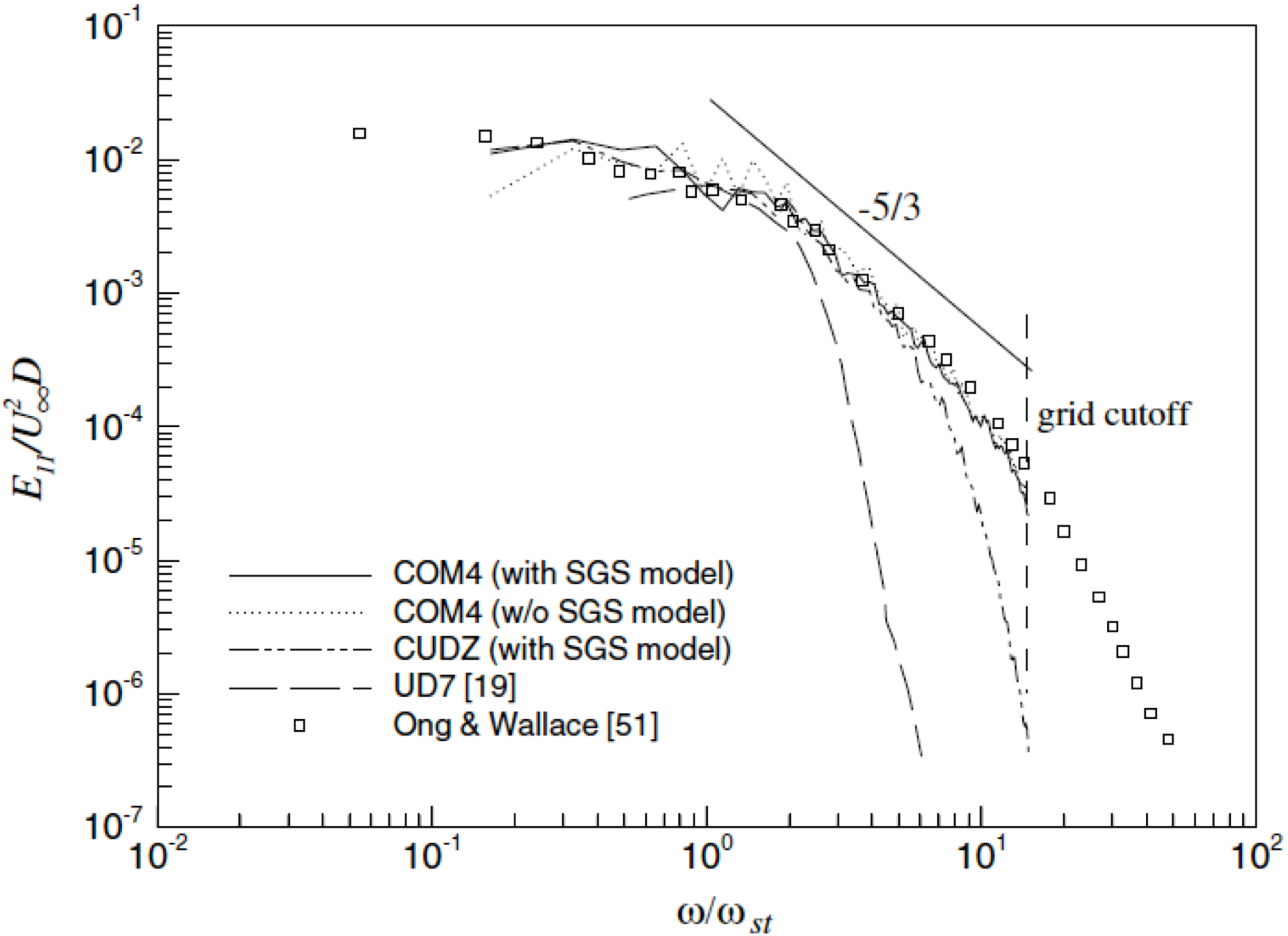

3. LES numerics:
beyond order of accuracy

Beyond order of accuracy

Order of acuracy:

- asymptotic behavior of numerical error when $h \longrightarrow 0$

but: h keeped as large as possible in practice

- LES solution has lot of kinetic energy at the cutoff

→ convergence of Taylor series expansions not obvious

e.g. $\overline{[u(x+r) - u(x)]^p} = O(r^p)?$

No ! Intermittency effect:

$$\Rightarrow \quad \overline{[u(x+r) - u(x)]^p} \sim (\varepsilon r)^{p/3} \Phi(p, r/L, Re)$$

What is now (commonly) agreed

- order of acuracy is not sufficient to describe LES numerics
- other features are important, such as
  - conservation of some invariant quantities (inviscid flows)

  ⇔ preservation of Kraichnan's detailed conservation properties

  ⇔ preservation of NS symmetries
- Low-order symmetry-preserving schemes may perform better than higher-order usual schemes
- Numerical scheme neutrality is physical-quantity-dependent
- No full-symmetry-group-preserving method known for Navier-Stokes !

- Partial error cancellation between discretization error and SGS error may occur

1-parameter symmetries of 3D incomp. NS

(Lie-group structure)

Time shift

$$(t,x,u,p) \longrightarrow (t+a,x,u,p)$$

Pressure shift

$$(t,x,u,p) \longrightarrow (t,x,u,p+\xi(t))$$

Rotations

$$(t,x,u,p) \longrightarrow (t,\mathcal{R}x,\mathcal{R}u,p)$$

Generalized Galilean Transformations

$$(t,x,u,p) \longrightarrow (t,x+\alpha(t),u+\dot{\alpha}(t),p-\rho x\ddot{\alpha}(t))$$

Rescaling (I)

$$(t,x,u,p) \longrightarrow (a^2 t,ax,u/a,p/a^2)$$

Rescaling (II)

$$(t,x,u,p,\nu) \longrightarrow (t,ax,au,a^2 p,a^2\nu)$$

More symmetries of 3D incomp. NS

Mirror symmetry

$$(t,x,u,p) \longrightarrow (t,\Lambda x,\Lambda u,p)$$

2D Material frame indifference (2D flow only)

$$(t,x,u,p) \longrightarrow (t,\mathcal{R}_{2D}(\omega,t)x,\mathcal{R}_{2D}(\omega,t)u,p-3\omega\psi+\omega^2|x|^2/2)$$

Time reversal (inviscid flow only)

$$(t,x,u,p) \longrightarrow (-t,x,-u,p)$$

Aix*Marseille université

Verstappen's method: fundamentals

Navier-Stokes momentum equation (incompressible flow)

$$\frac{\partial}{\partial t}u + \underbrace{(u \cdot \nabla)u}_{C(u,u)} + \nabla p - \frac{1}{Re}\underbrace{\nabla \cdot \nabla u}_{\Delta u} = 0$$

Skew-symmetry of pressure & convection terms

$$(u \cdot \nabla)^* = -(u \cdot \nabla), \qquad \nabla^* = -\nabla$$

$$(\nabla p, u) = -(p, \nabla \cdot u), \qquad \underbrace{((u \cdot \nabla)v, w)}_{(C(u,v),w)} = -\underbrace{(v, (u \cdot \nabla)w)}_{(v,C(u,w))}$$

Verstappen's method: fundamentals

Global kinetic energy equation

$$\frac{d}{dt}(u,u) = -\frac{2}{Re}(\nabla u, \nabla u) \leq 0$$

Global vorticity equation

$$\frac{d}{dt}\frac{1}{2}(\omega,\omega) = -\frac{1}{Re}|\Delta u|^2 - (C(u,u), \Delta u)$$

Invariant quantities (inviscid flows/Kraichnan's detailed conservation)

- **2D: kinetic energy, vorticity**
- **3D: kinetic energy, helicity**

Idea: numerical schemes which preserve invariants/skew-symmetry

Verstappen's method: links with LES

Momentum equation with filtered convection term

$$\frac{\partial}{\partial t}\bar{u} + C_n(\bar{u},\bar{u}) + \nabla\bar{p} - \frac{1}{Re}\Delta\bar{u} = 0$$

Increasing-order filtered skew-symmetry-preserving nonlinear terms

$$\bar{\phi} = \tilde{\phi} + \phi'$$

Explicit symmetric (self-adjoint) filter

$$\begin{aligned}
C_2(u,v) &= \widetilde{C(\tilde{u},\tilde{v})}\\
C_4(u,v) &= C(\tilde{u},\tilde{v}) + \widetilde{C(\tilde{u},v')} + \widetilde{C(u',\tilde{v})}\\
C_6(u,v) &= C(\tilde{u},\tilde{v}) + C(\tilde{u},v') + C(u',\tilde{v}) + \widetilde{C(u',v')}
\end{aligned}$$

Verstappen's method: links with LES

Links with Adams' Approximate Deconvolution Method

$$u^\star = Q \star \bar{u} = u + 0(h^n) \simeq u$$
$$\frac{\partial}{\partial t}\bar{u} + \overline{C(u^\star, u^\star)} + \nabla \bar{p} - \frac{1}{Re}\Delta \bar{u} = 0$$

$$\overline{C(Q\star\bar{u}, Q\star\bar{u})} = \widetilde{C(\tilde{\bar{u}}, \tilde{\bar{u}})} + O(h^2)$$

Links with tensor diffusivity model

$$C_n(\bar{u}, \bar{u}) = C(\bar{u}, \bar{u}) - \frac{1}{12}\delta^2 \mathrm{div}(\nabla\bar{u}\cdot\nabla\bar{u}) + O(h^4, h^n)$$

Verstappen's method: plane channel flow

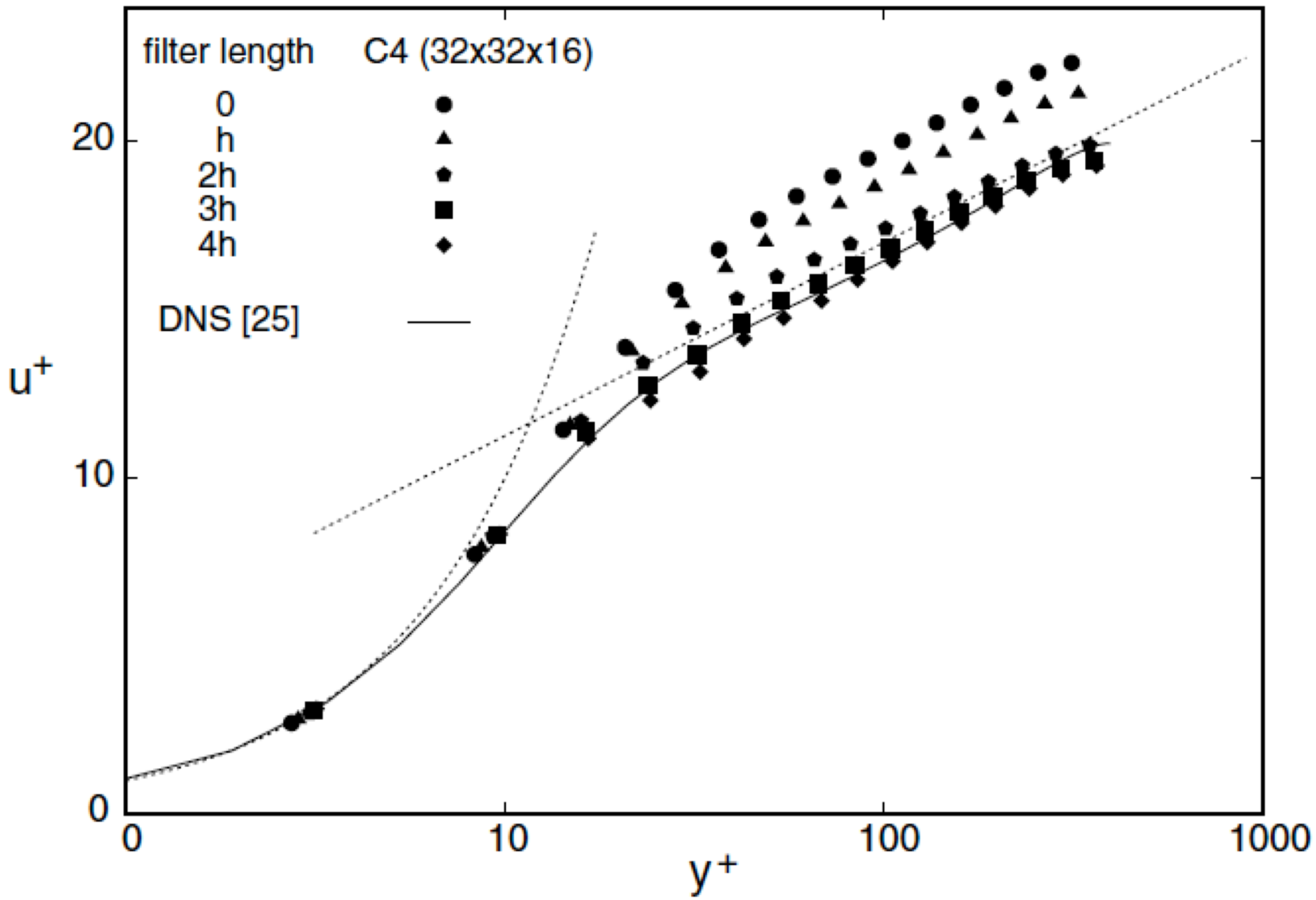

Verstappen's method: plane channel flow

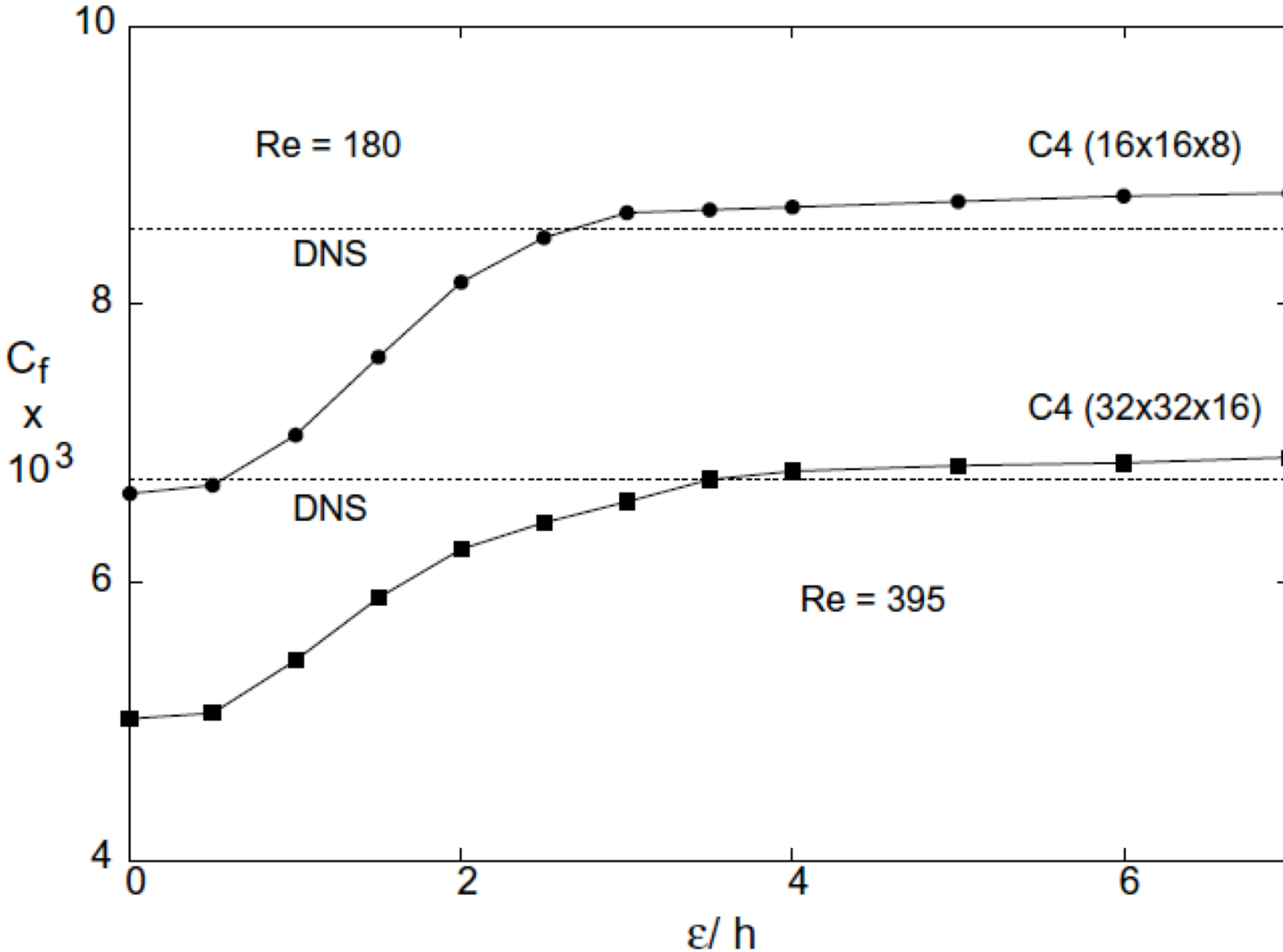

Verstappen's method: plane channel flow

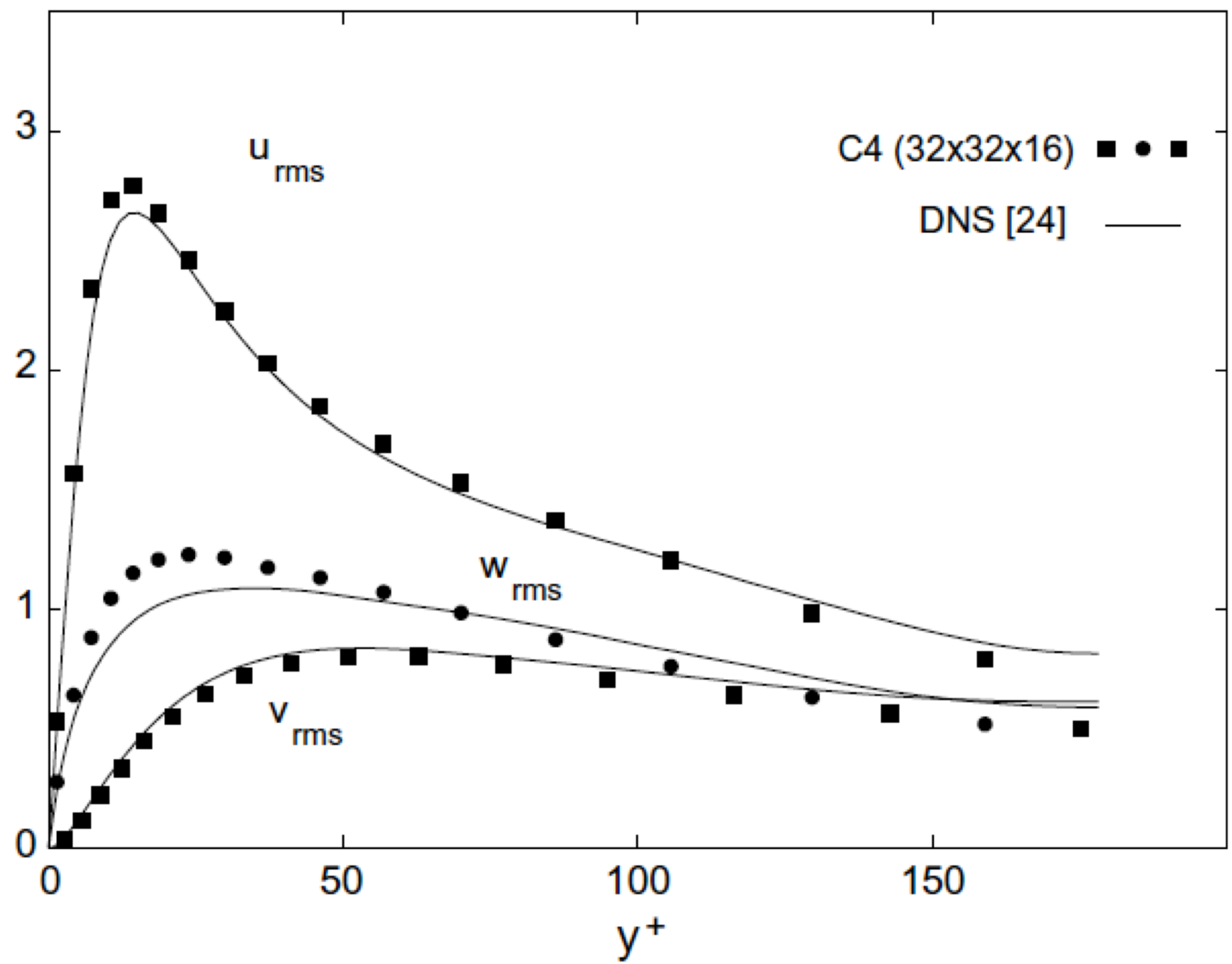

Compressible flows

Conservative variable formulation

$$\frac{\partial \rho}{\partial t} + \frac{\partial \rho u_i}{\partial x_i} = 0$$

$$\frac{\partial \rho u_i}{\partial t} + \frac{\partial \rho u_i u_j}{\partial x_j} + \frac{\partial p}{\partial x_i} = \frac{\partial \tau_{ij}}{\partial x_j}$$

$$\frac{\partial E}{\partial t} + \frac{\partial E u_j}{\partial x_j} + \frac{\partial p u_i}{\partial x_i} = \frac{\partial \tau_{ij} u_i}{\partial x_j} + \frac{\partial}{\partial x_i}\left(\kappa \frac{\partial T}{\partial x_i}\right)$$

$$\tau_{ij} = \mu\left(\frac{\partial u_i}{\partial x_j} + \frac{\partial u_j}{\partial x_i}\right) - \frac{2}{3}\mu \frac{\partial u_k}{\partial x_k}\delta_{ij}, \qquad E = \rho\frac{u_i u_i}{2} + \rho C_v T$$

Compressible flows

- **Problems**:
  - no scalar invariant directly appearing
  - splitting of fluctuations into different physical modes
    - Kovasznay: acoustic, vortical & entropy modes
    - Helmholtz: solenoidal & dilatational modes

  → transfers between modes

- **Possible solution**: looking at 2^{nd} law of thermodynamics/entropy

Entropy-based eqs.

$$\frac{\partial \rho s}{\partial t} + \frac{\partial \rho s u_j}{\partial x_j} = \frac{1}{T}\left[\tau_{ij}\frac{\partial u_i}{\partial x_j} + \frac{\partial}{\partial x_i}\left(\kappa\frac{\partial T}{\partial x_i}\right)\right]$$
$$= \frac{\partial}{\partial x_i}\left(\frac{\kappa}{T}\frac{\partial T}{\partial x_i}\right) + \frac{\tau_{ij}}{T}\frac{\partial u_i}{\partial x_j} + \frac{\kappa}{T^2}\frac{\partial T}{\partial x_i}\frac{\partial T}{\partial x_i}$$

$$\frac{\partial \rho s^2}{\partial t} + \frac{\partial \rho s^2 u_j}{\partial x_j} = \frac{2s}{T}\left[\tau_{ij}\frac{\partial u_i}{\partial x_j} + \frac{\partial}{\partial x_i}\left(\kappa\frac{\partial T}{\partial x_i}\right)\right]$$

Global invariants in homogeneous flows:

$$\overline{\rho s}, \quad \overline{\rho s^2}$$

Entropy-conservation-based schemes

Skew-symmetric splittings

Quadratic nonlinear term splitting (also in incompressible flows)

$$\frac{\partial a u_j}{\partial x_j} \longrightarrow \frac{1}{2}\left(\frac{\partial a u_j}{\partial x_j} + a\frac{\partial u_j}{\partial x_j} + u_j\frac{\partial a}{\partial x_j}\right)$$

Entropy-consistent cubic nonlinear term splitting

$$\frac{\partial \rho a u_j}{\partial x_j} \longrightarrow \frac{1}{2}\left(\frac{\partial \rho a u_j}{\partial x_j} + a\frac{\partial \rho u_j}{\partial x_j} + \rho u_j\frac{\partial a}{\partial x_j}\right)$$

Other cubic nonlinear term splitting

$$\frac{\partial \rho a u_j}{\partial x_j} \longrightarrow \frac{1}{2}\left(\frac{\partial \rho a u_j}{\partial x_j} + \rho a\frac{\partial u_j}{\partial x_j} + u_j\frac{\partial \rho a}{\partial x_j}\right)$$

Honein's method: model-free simulation

Honein's entropy-preserving method

Internal energy entropy-preserving equation

$$\frac{\partial \rho e}{\partial t} + e\left(\gamma - \frac{s}{2C_v}\right)\frac{\partial \rho u_j}{\partial x_j} + \frac{e}{2C_v}\frac{\partial \rho s u_i}{\partial x_i} + \frac{\rho e u_i}{2C_v}\frac{\partial s}{\partial x_i} = \tau_{ij}\frac{\partial u_i}{\partial x_j} + \frac{\partial}{\partial x_i}\left(\kappa\frac{\partial T}{\partial x_i}\right)$$

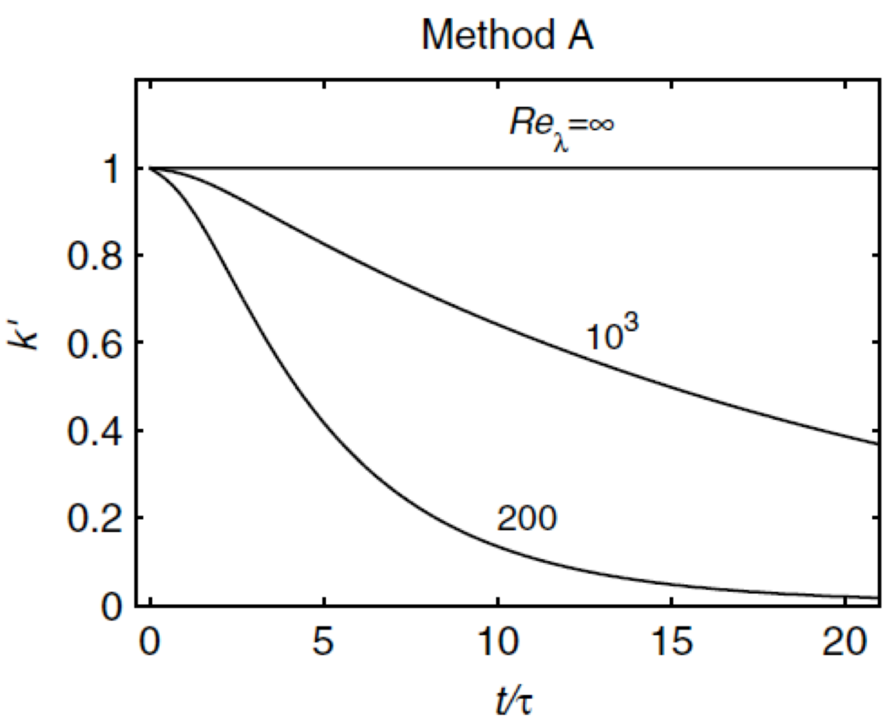

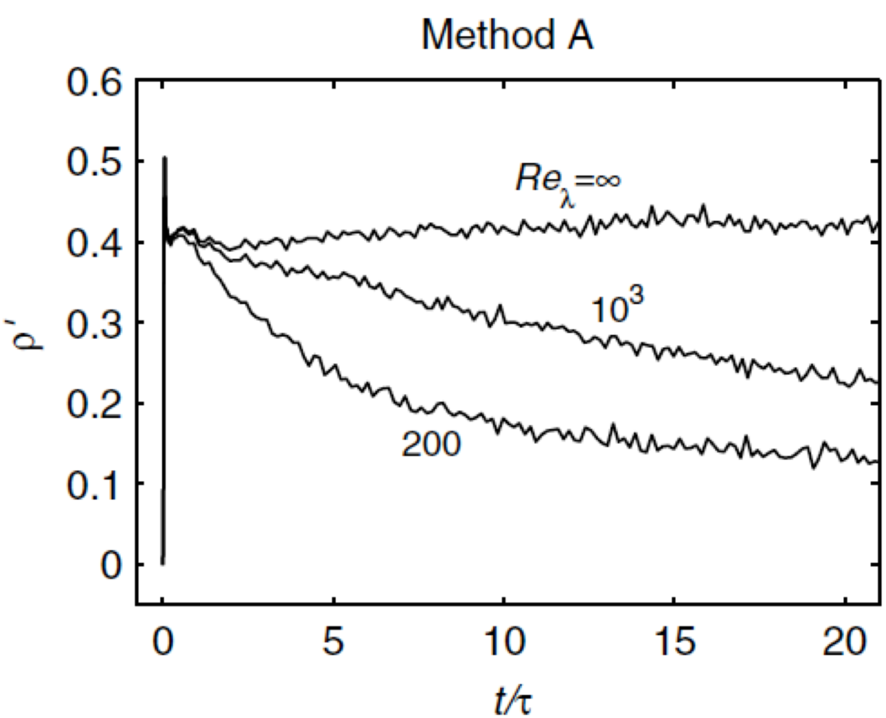

Honein's method: model-free simulation

Yee's entropy-splitting method

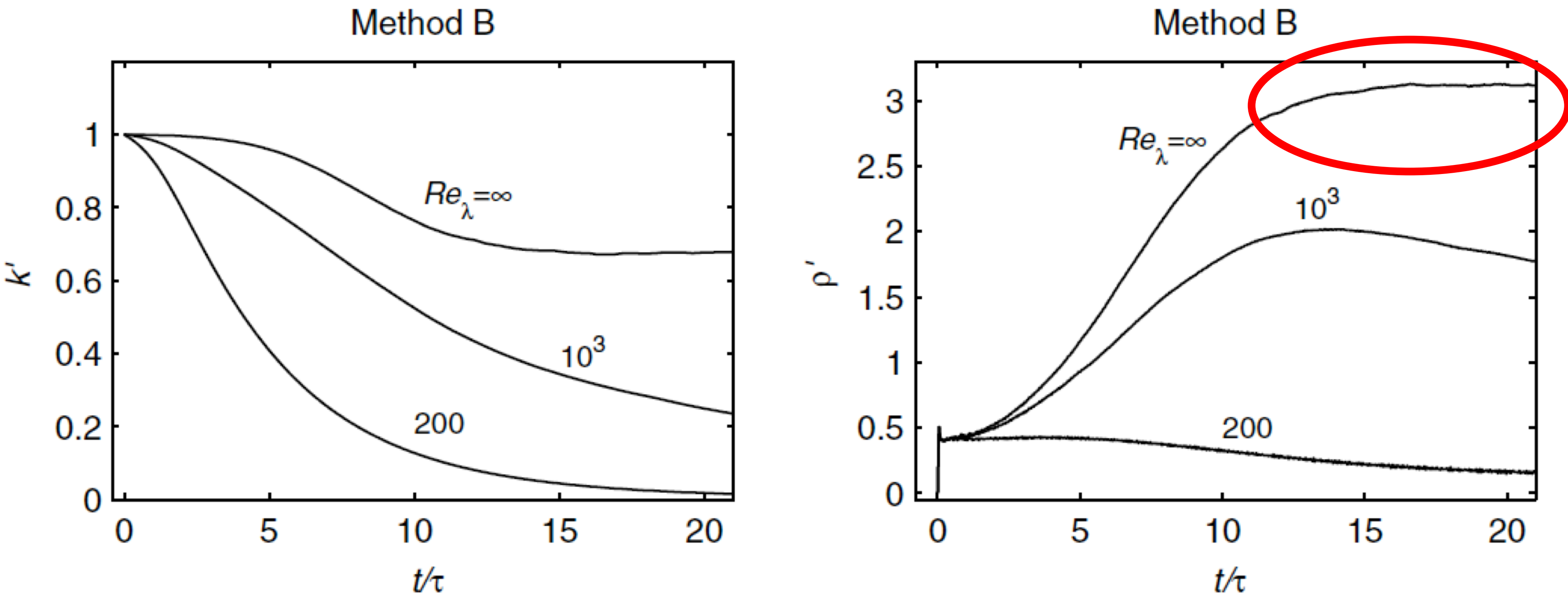

Honein's method: model-free simulation

Honein's splitting & usual internal energy equation

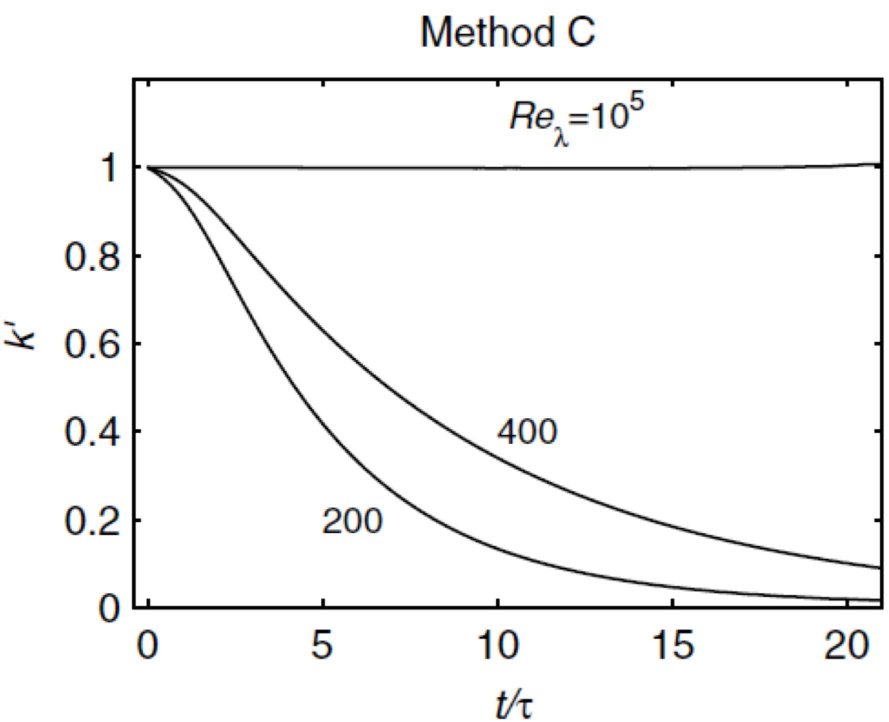

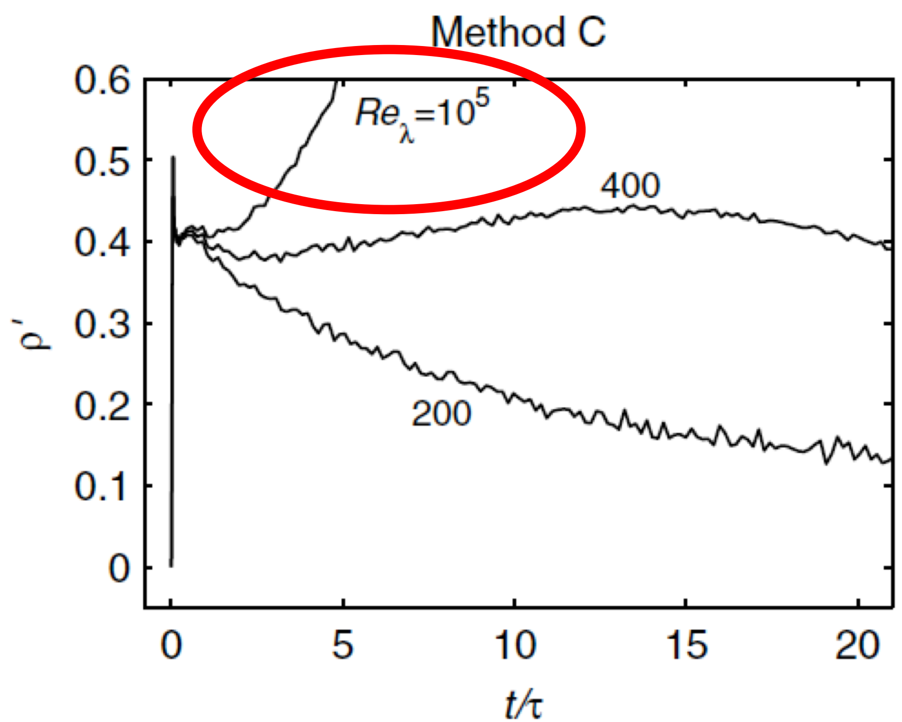

Honein's method: model-free simulation

Staggered grid method

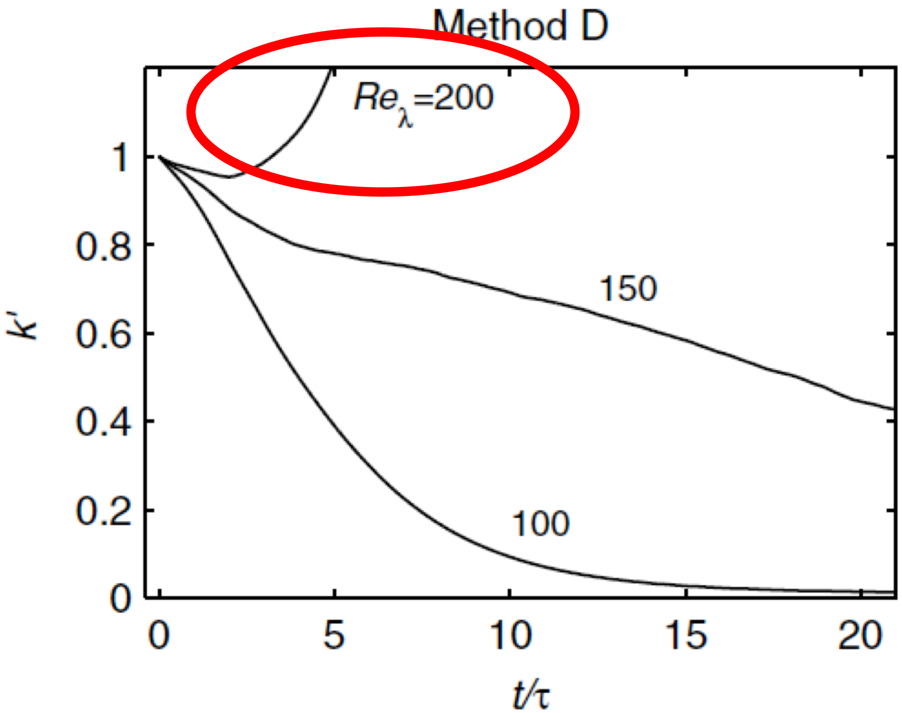

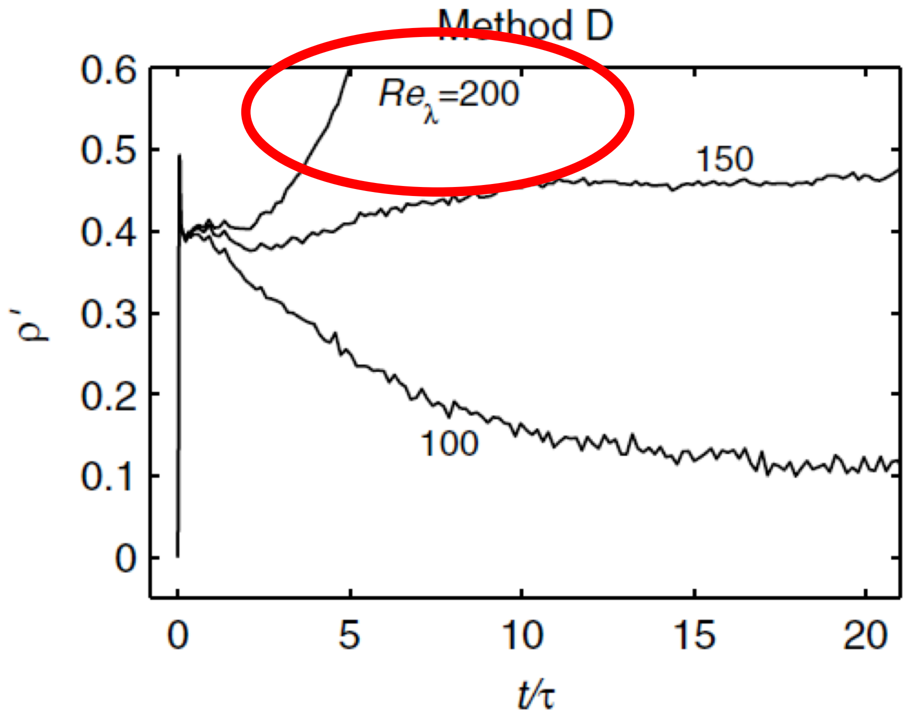

Honein's method: model-free simulation

Conservative formulation & bad cubic splitting

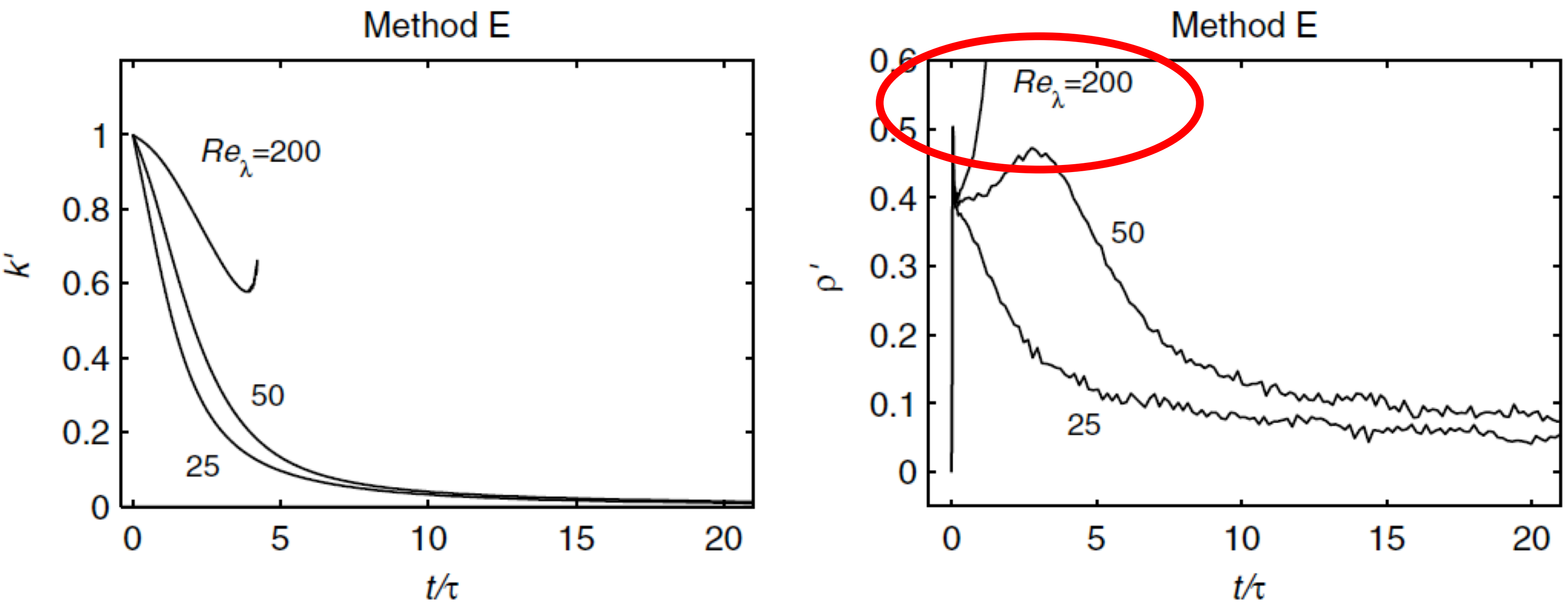

Honein's method: model-free vs. LES

Honein's entropy-preserving method

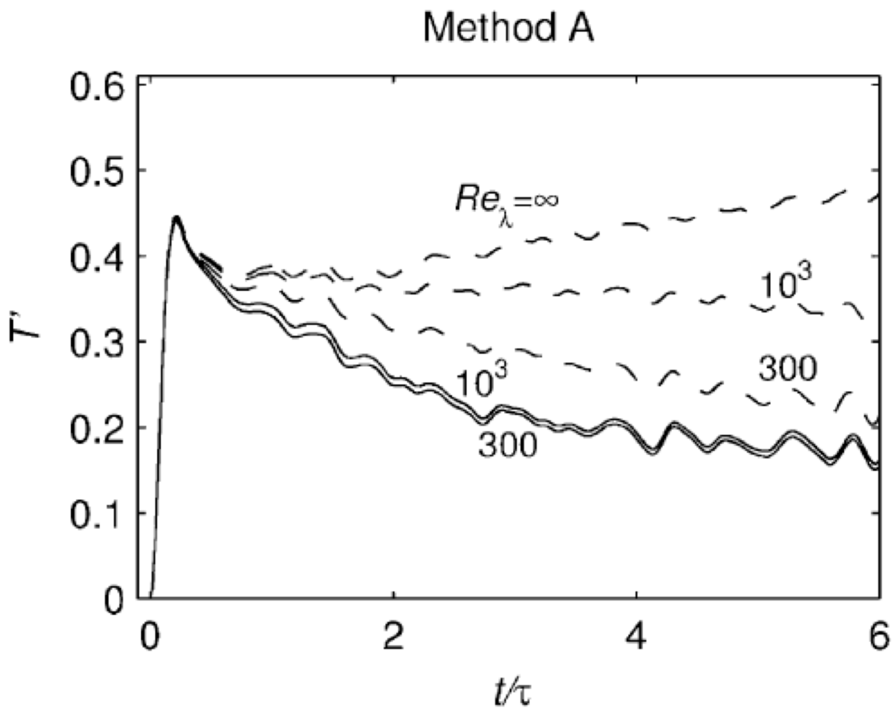

Yee's entropy-splitting method

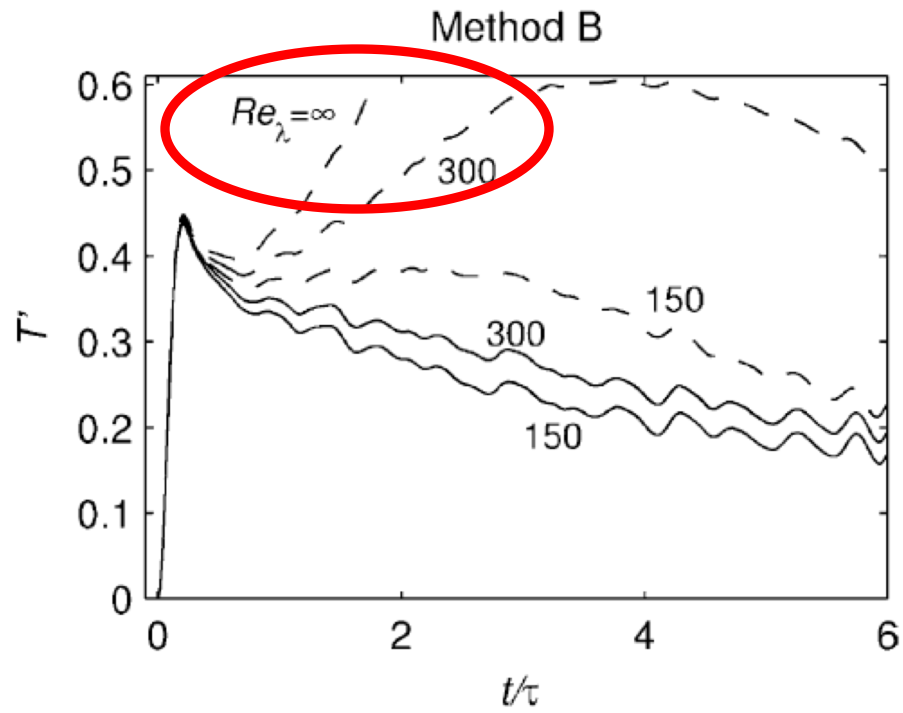

Solid line: LES   Dashed: model-free

Honein's method: model-free vs. LES

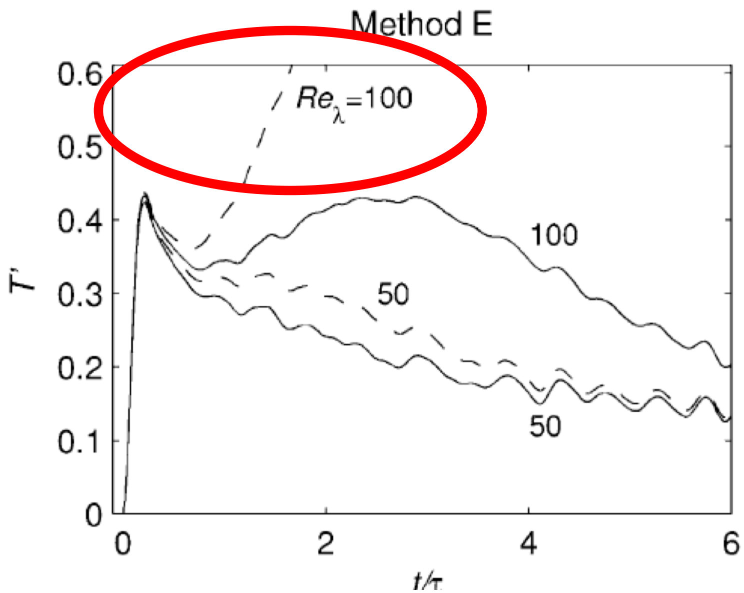

Conservative formulation & bad cubic splitting

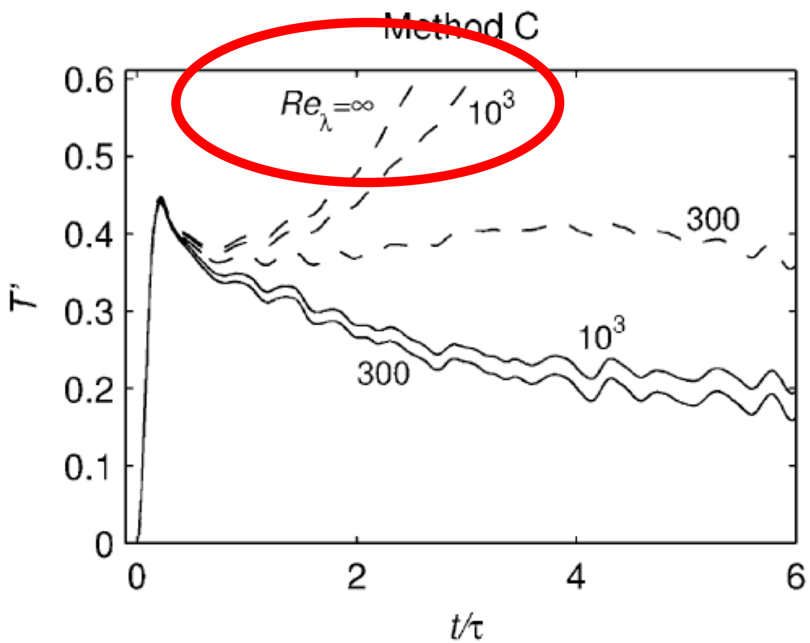

Honein's splitting & usual internal energy equation

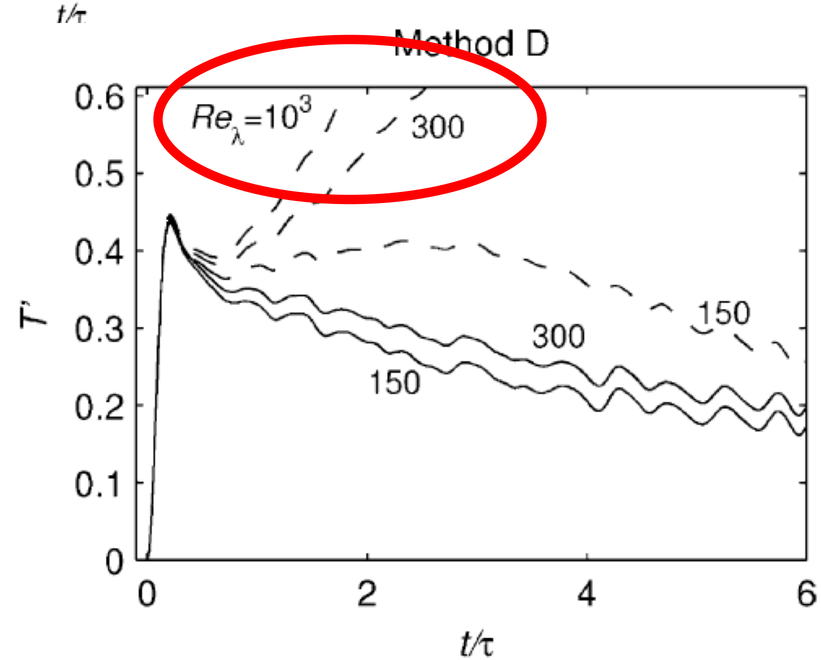

Staggered grid method

Order of accuracy vs. Global reliability

How to measure the accuracy of LES results ?

- need for a quantitative error norm
- need for reference data (accuracy ≠ sensitivity)
- sensitivity important for robustness evaluation
- several quantities predicted at the same time → unique error ?

Single-objective error norms

L2-type error norms

$$D_p(N,C_s) = \left[\frac{\int_0^T \left\{ \int_0^{k_c} k^p (E_{LES}(k,t) - E_{DNS}(k,t)) dk \right\}^2 dt}{\int_0^T \left\{ \int_0^{k_c} k^p E_{DNS}(k,t) dk \right\}^2 dt} \right]^{1/2}$$

Physical-quantity-based error norms

$$d_p(N,C_s) = \left[\frac{\int_0^T \int_0^{k_c} k^p (E_{LES}(k,t) - E_{DNS}(k,t))^2 dk dt}{\int_0^T \int_0^{k_c} k^p E_{DNS}^2(k,t) dk dt} \right]^{1/2}$$

$$L = \int_0^{+\infty} k^{-1} E(k) dk, \quad K = \int_0^{+\infty} E(k) dk, \quad \varepsilon = 2\nu \int_0^{+\infty} k^2 E(k) dk$$

Error surfaces

(Smagorinsky model, Re_λ=100)

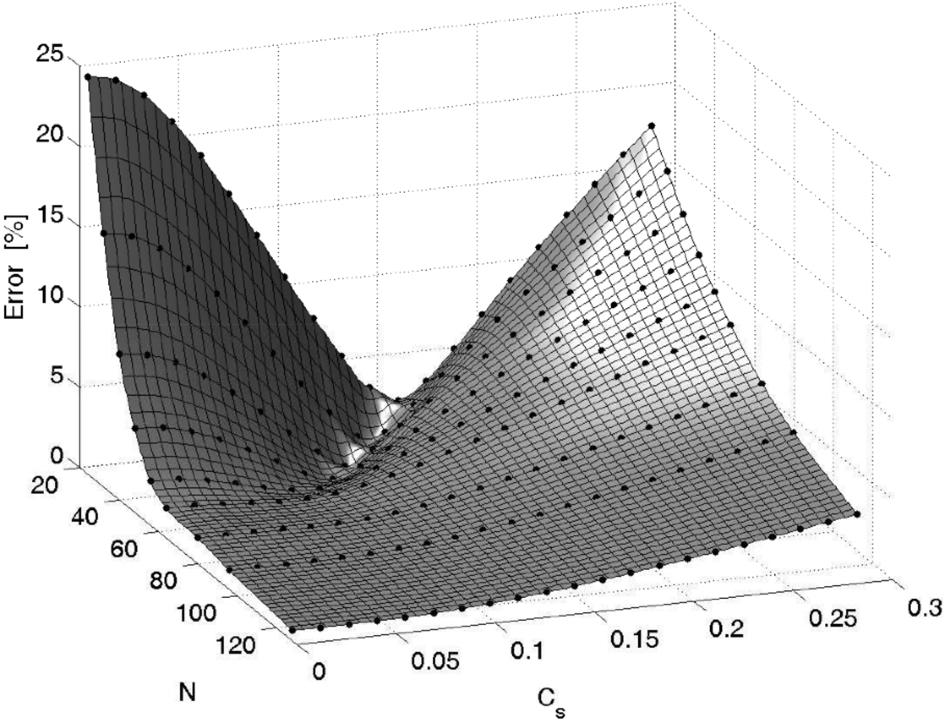

Resolved kinetic energy

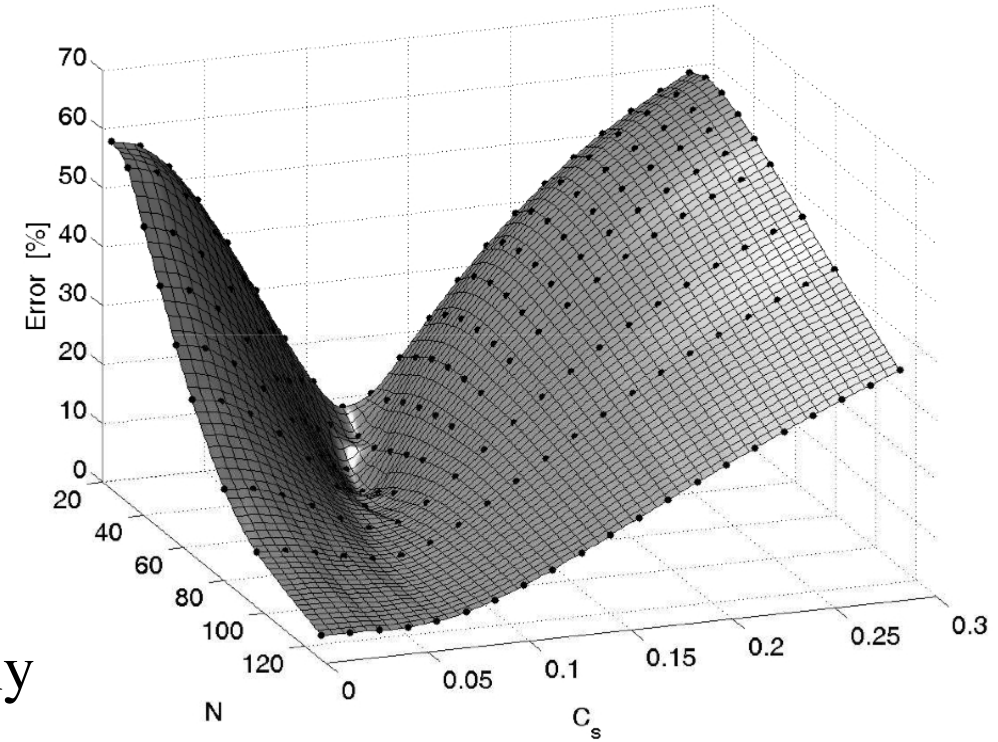

Resolved enstrophy

Multi-objective error norms

L2-type error norms

$$\tilde{D}(N, C_s) = \frac{\sum_p \left[D_p(N, C_s) / D_p(N, \hat{C}_s^{(p)}(N)) \right]}{\sum_p \left[1 / D_p(N, \hat{C}_s^{(p)}(N)) \right]}$$

Physical error norms

$$\tilde{d}(N, C_s) = \frac{\sum_p \left[d_p(N, C_s) / d_p(N, \hat{C}_s^{(p)}(N)) \right]}{\sum_p \left[1 / d_p(N, \hat{C}_s^{(p)}(N)) \right]}$$

Best LES solution on the same grid (optimal Cs)

Near-optimal LES: L2 error norm

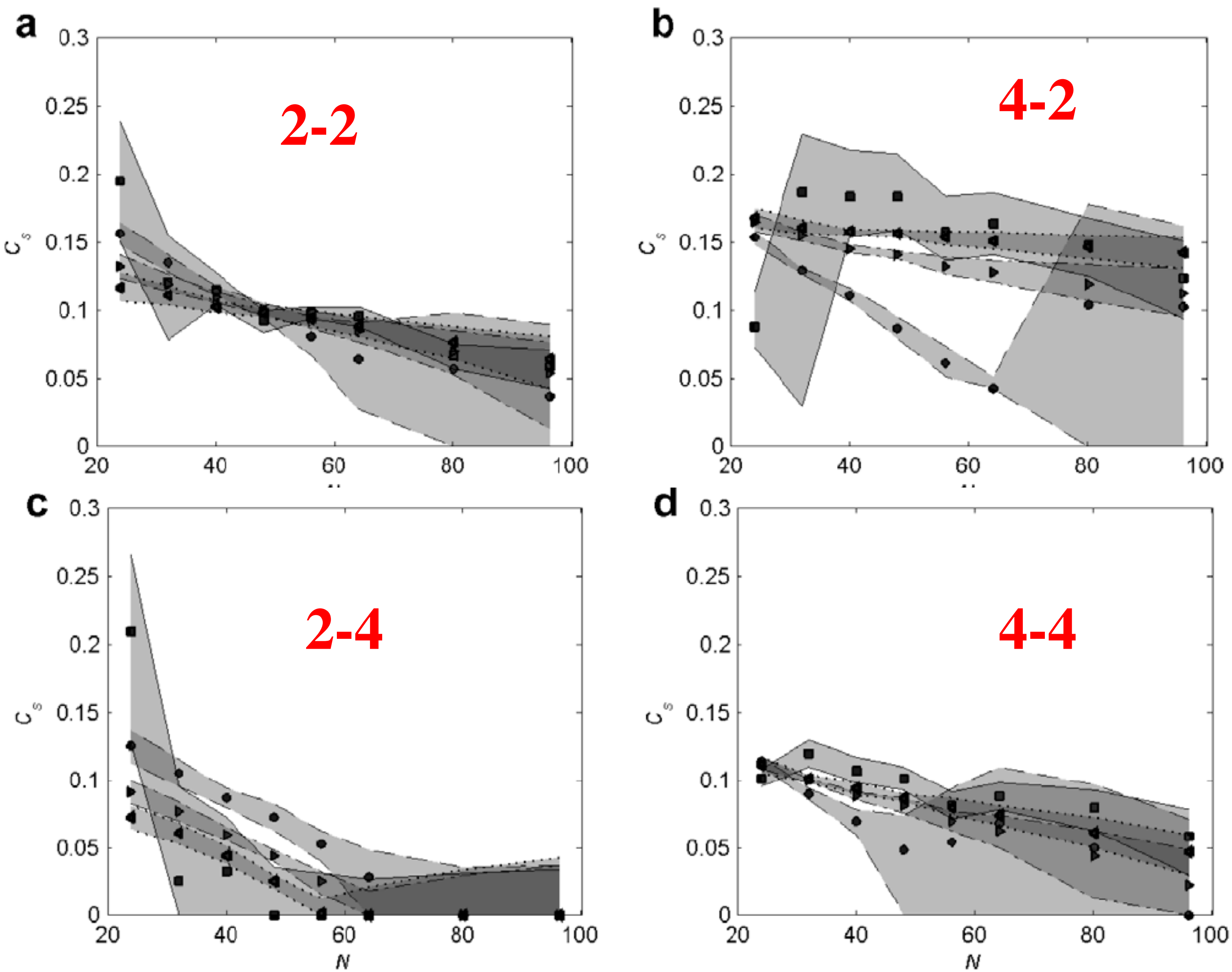

Near-optimal LES: physical error norm

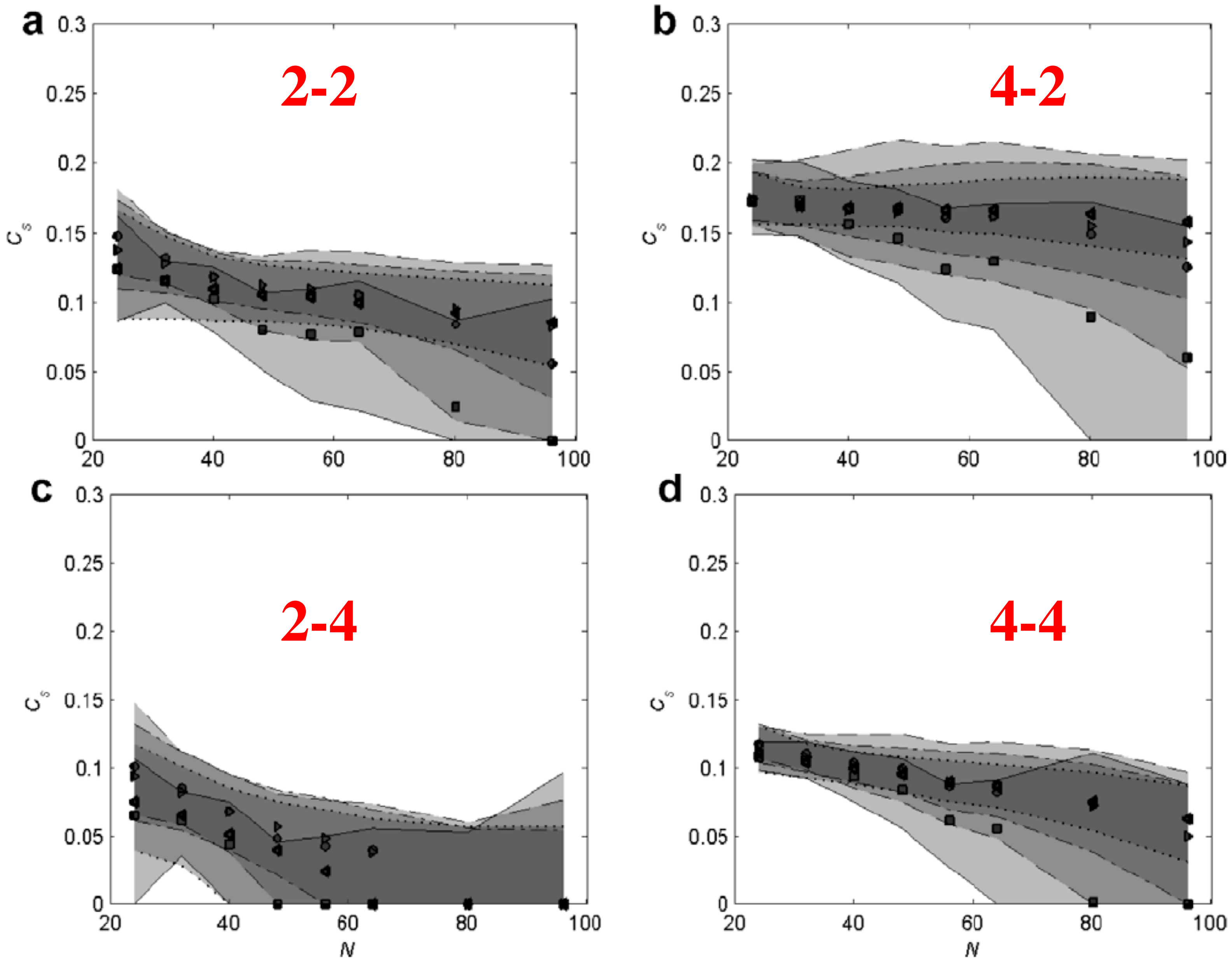

Multi-objective optimal Smagorinsky constant

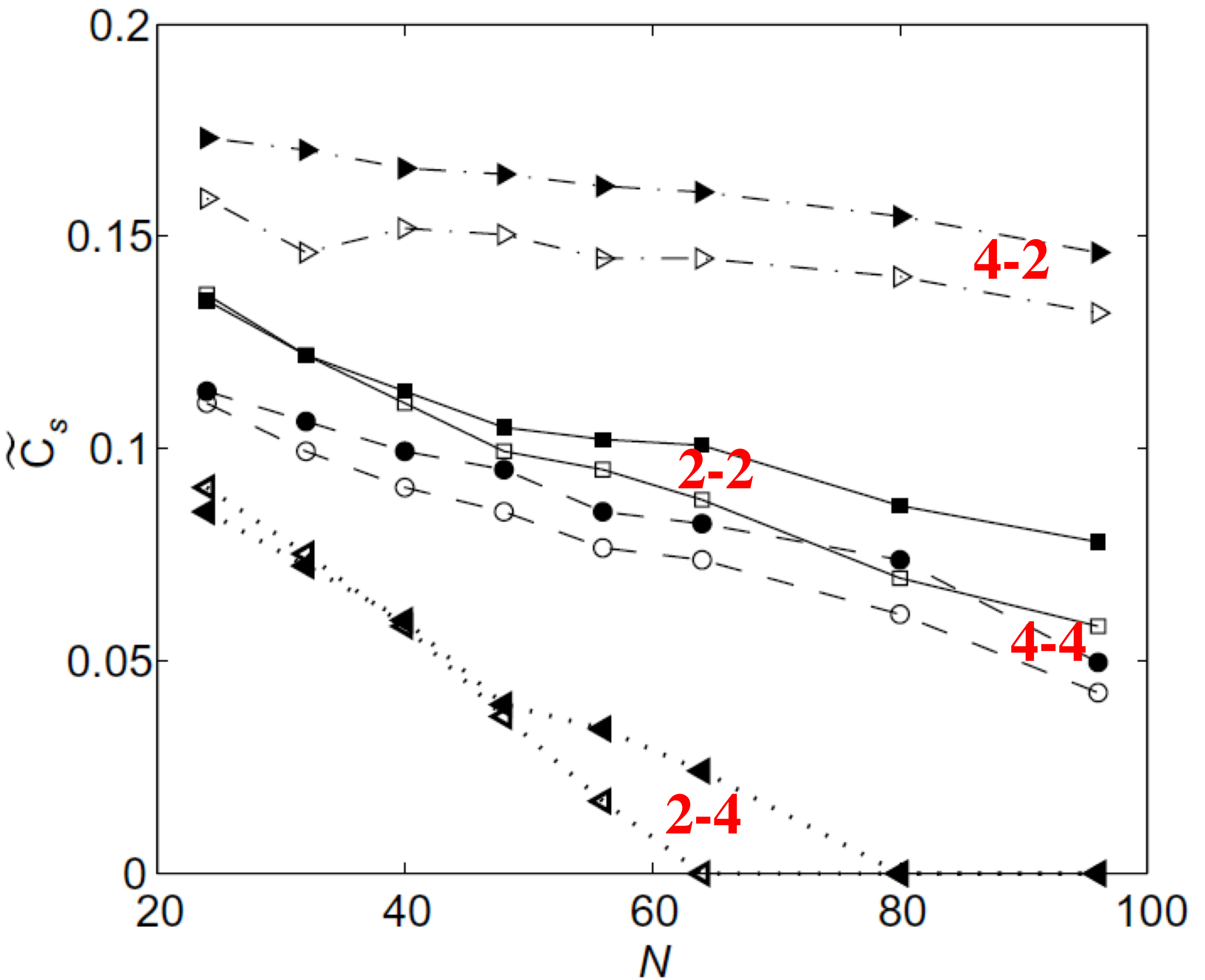

Multi-objective optimal LES: single obj. errors

p=-1

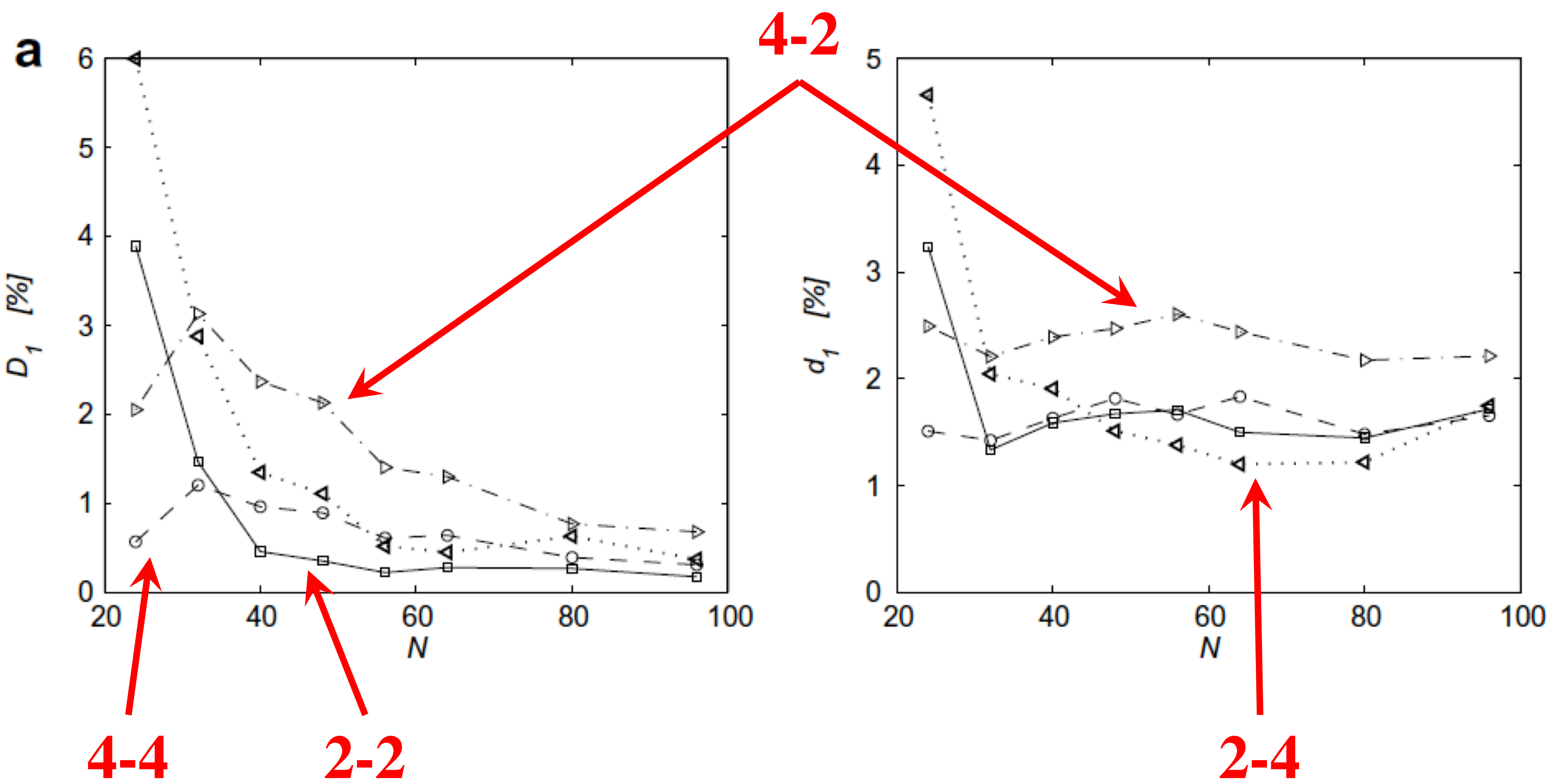

Multi-objective optimal LES: single obj. errors

p=0

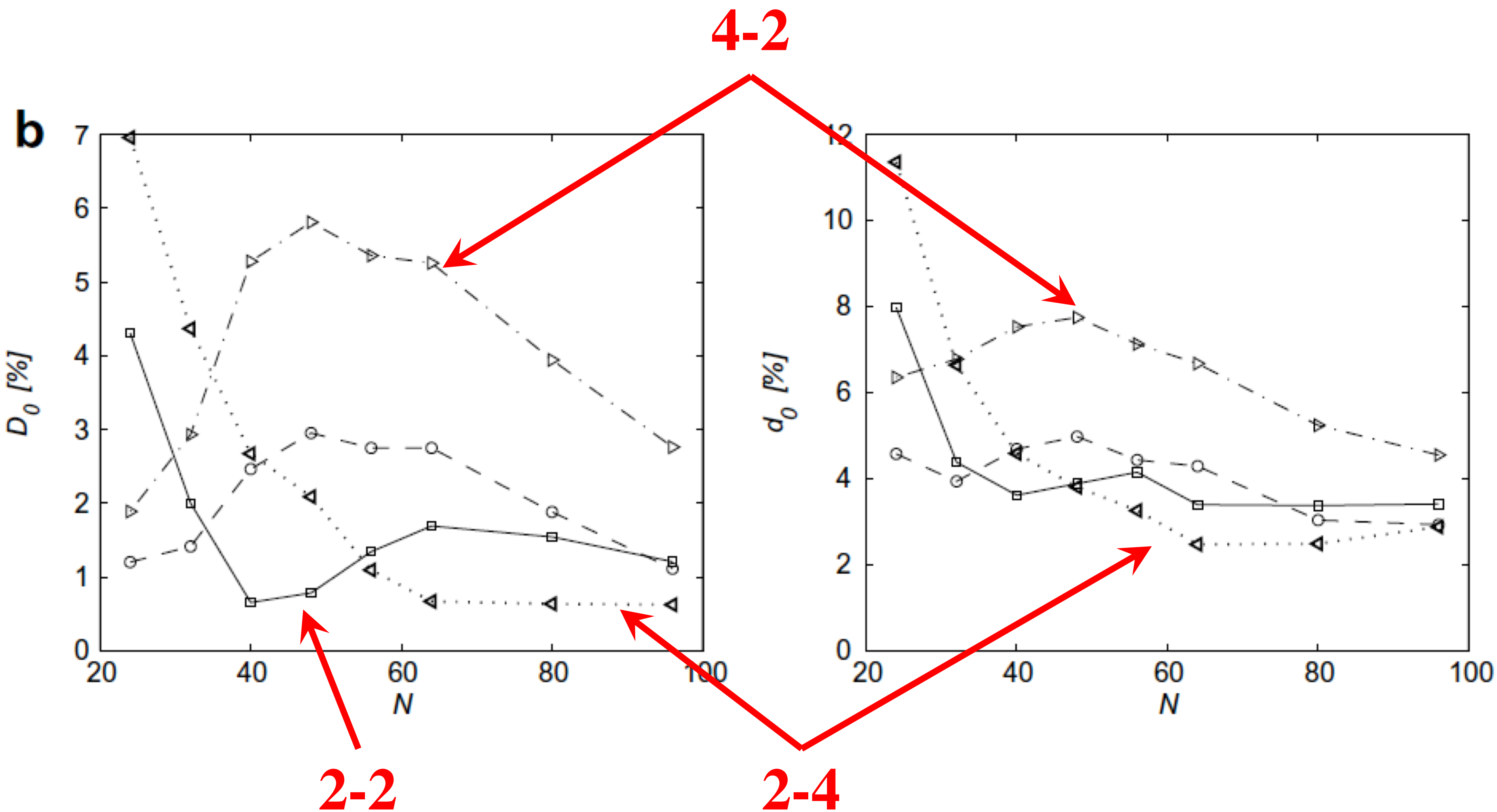

Multi-objective optimal LES: single obj. errors

p=1

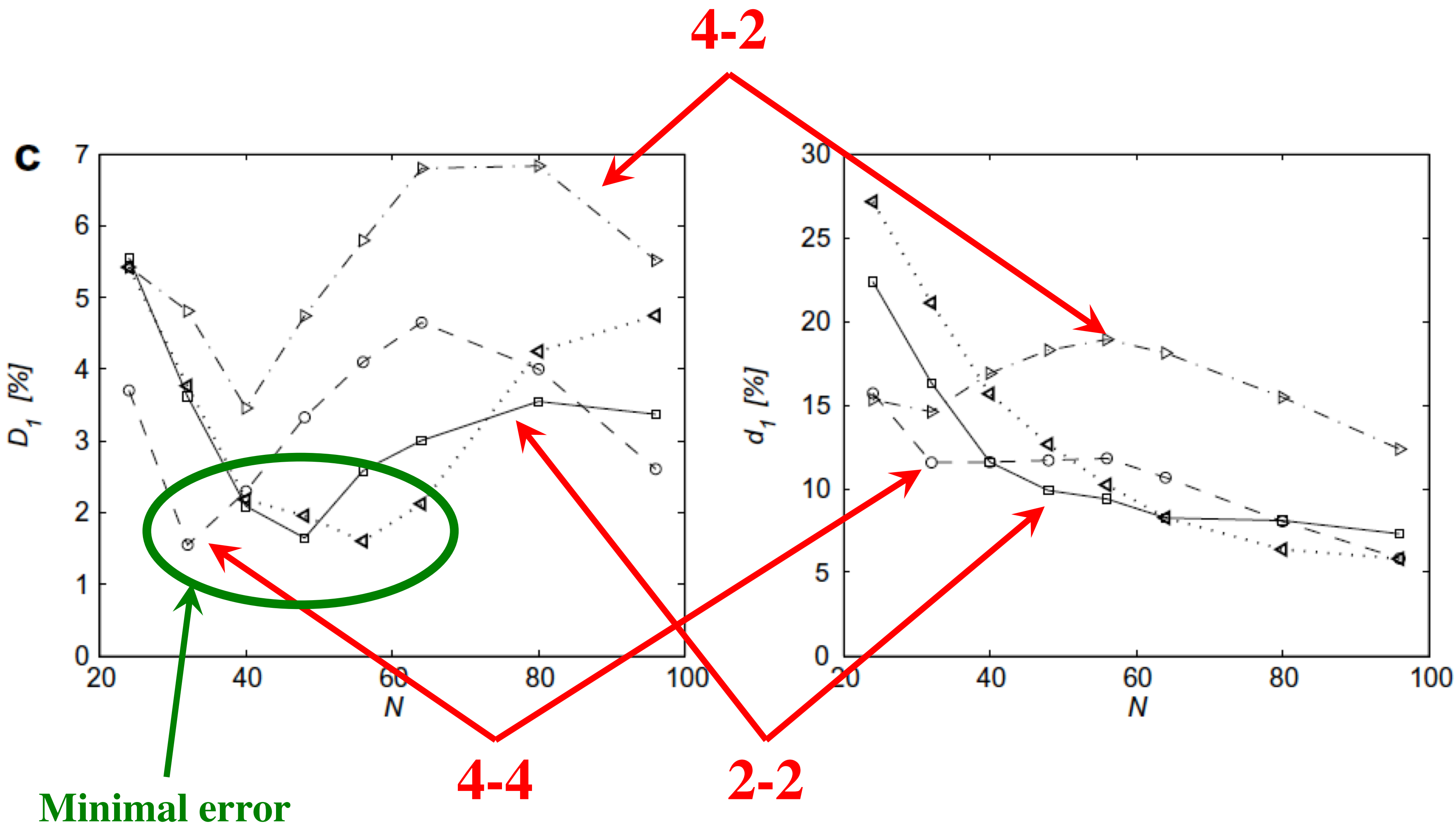

Multi-objective optimal LES: single obj. errors

p=2

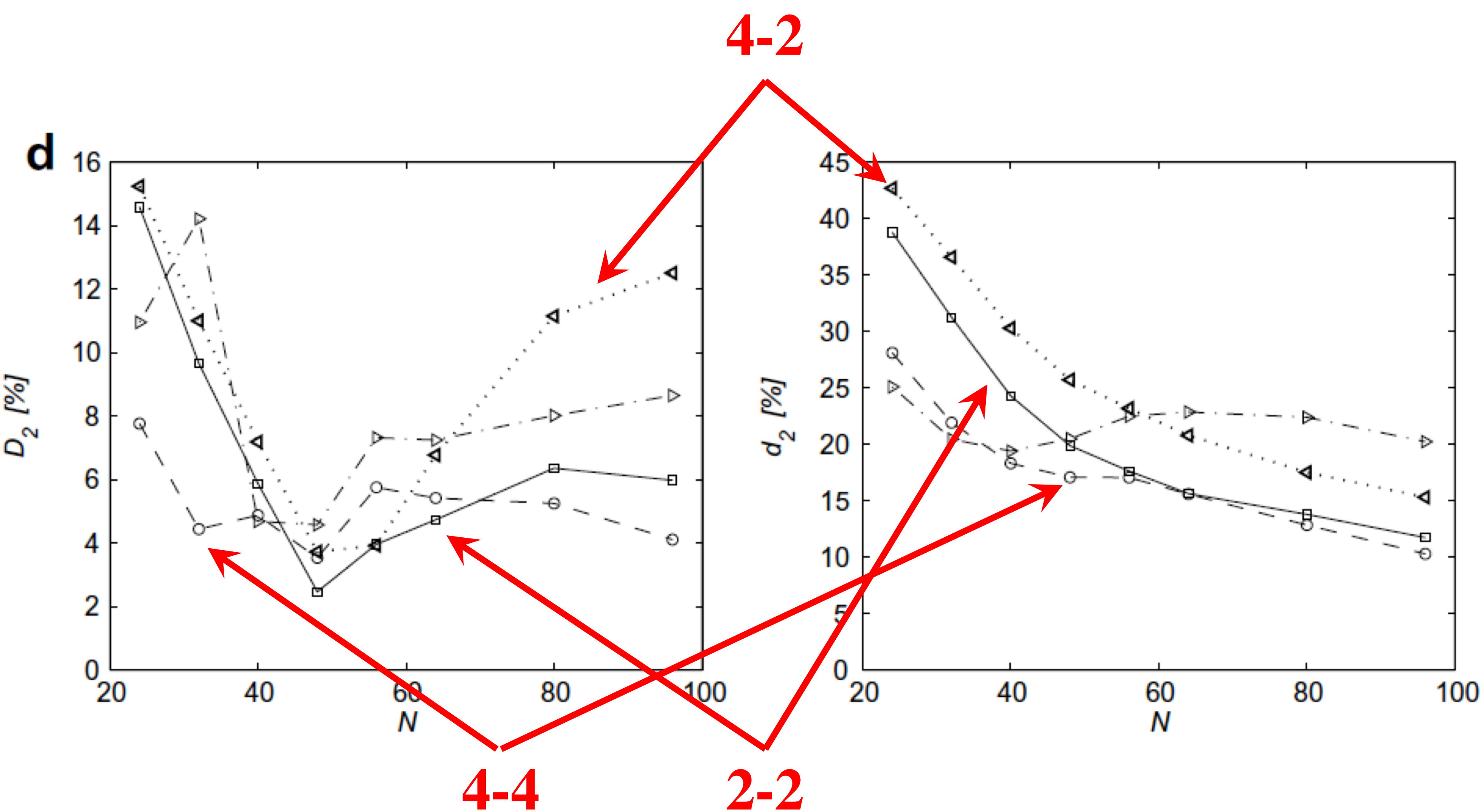

4. Response surface analysis & uncertainty quantification tools

Dealing with complex flow LES

(Jouhaud & Sagaut, J. Fluid Engng, 2008)

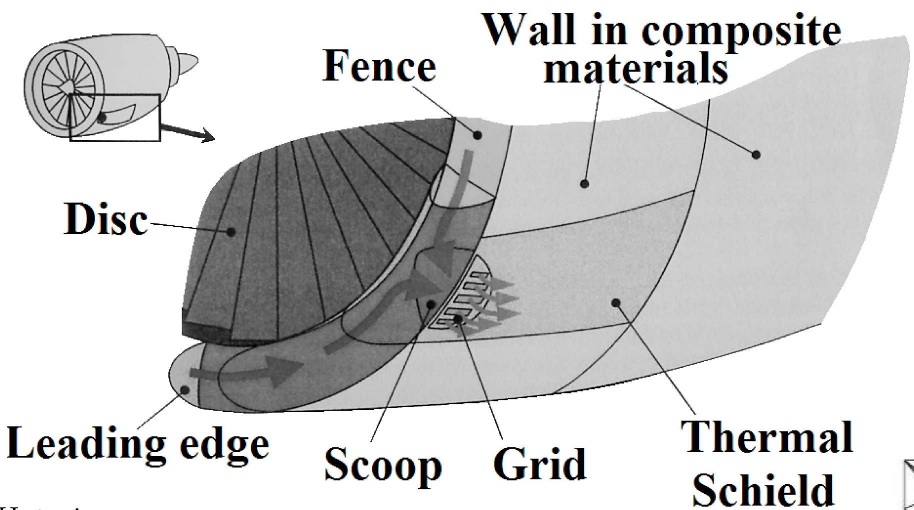

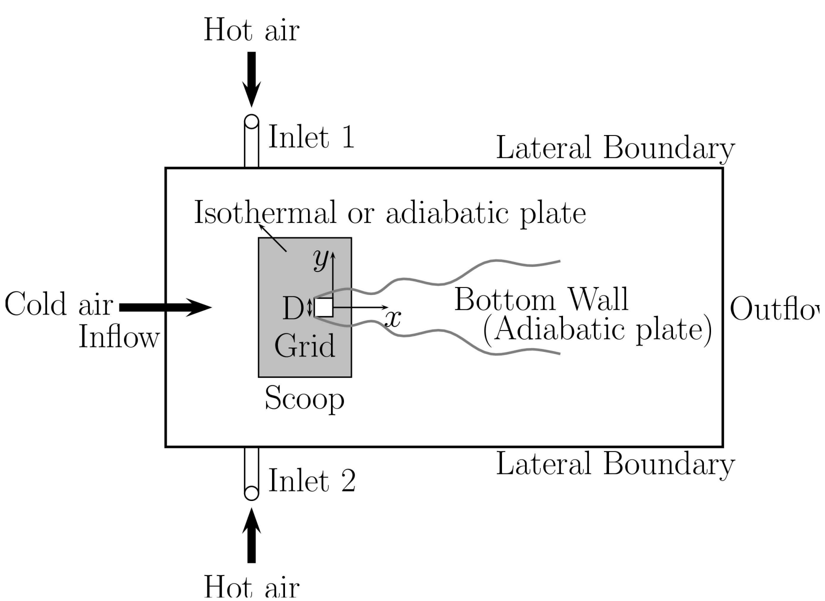

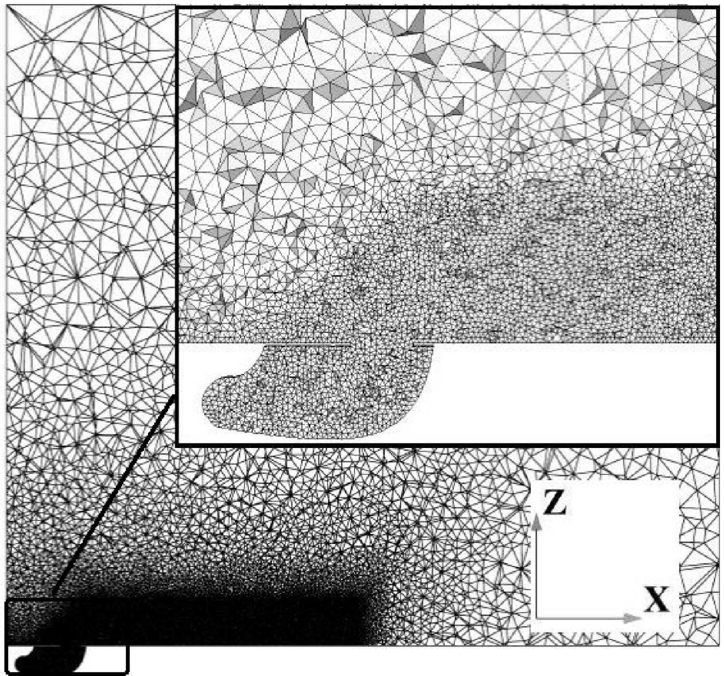

Putting error bars on LES data

- In complex configurations:
  - optimal values of subgrid models are not known
  - best tuning of artificial viscosity parameter not known

➪ these two parameters are considered as uncertain parameters

➪ comparison with experimental data should account for possible numerical result variability

Response surface via Kriging

- Optimal linear unbiaised statistical predictor
- Based on sampling points (1 sample = 1 usual simulation)
- Several variants have been developed (cokriging, …)
- Kriging methods also provide an estimation of the interpolation error
- Sampling points can be generated dynamically to minimize the interpolation error (adaptive refinement)

Basic Kriging Method

Estimator at position x

Estimated function at position x_s

$$\hat{f}(x) = c^T(x, x_s)C^{-1}(x, x_s)f(x_s)$$

Covariance vector **Covariance matrix**

$$c(x, x_s) = \begin{pmatrix} Cov(x, x_1) \\ \dots \\ Cov(x, x_n) \end{pmatrix}$$

$$C(x_s, x_s) = \begin{pmatrix} \sigma^2 & Cov(x_1, x_2) \dots & Cov(x_1, x_n) \\ Cov(x_2, x_1) & \sigma^2 & \dots Cov(x_2, x_n) \\ \dots & \dots & \dots & \dots \\ Cov(x_n, x_1) & Cov(x_n, x_2) \dots & \sigma^2 \end{pmatrix}$$

a priori covariogram function: $Cov(y, z) = \sigma^2 \exp(-|y - z|)$

Mean flow predicted by LES

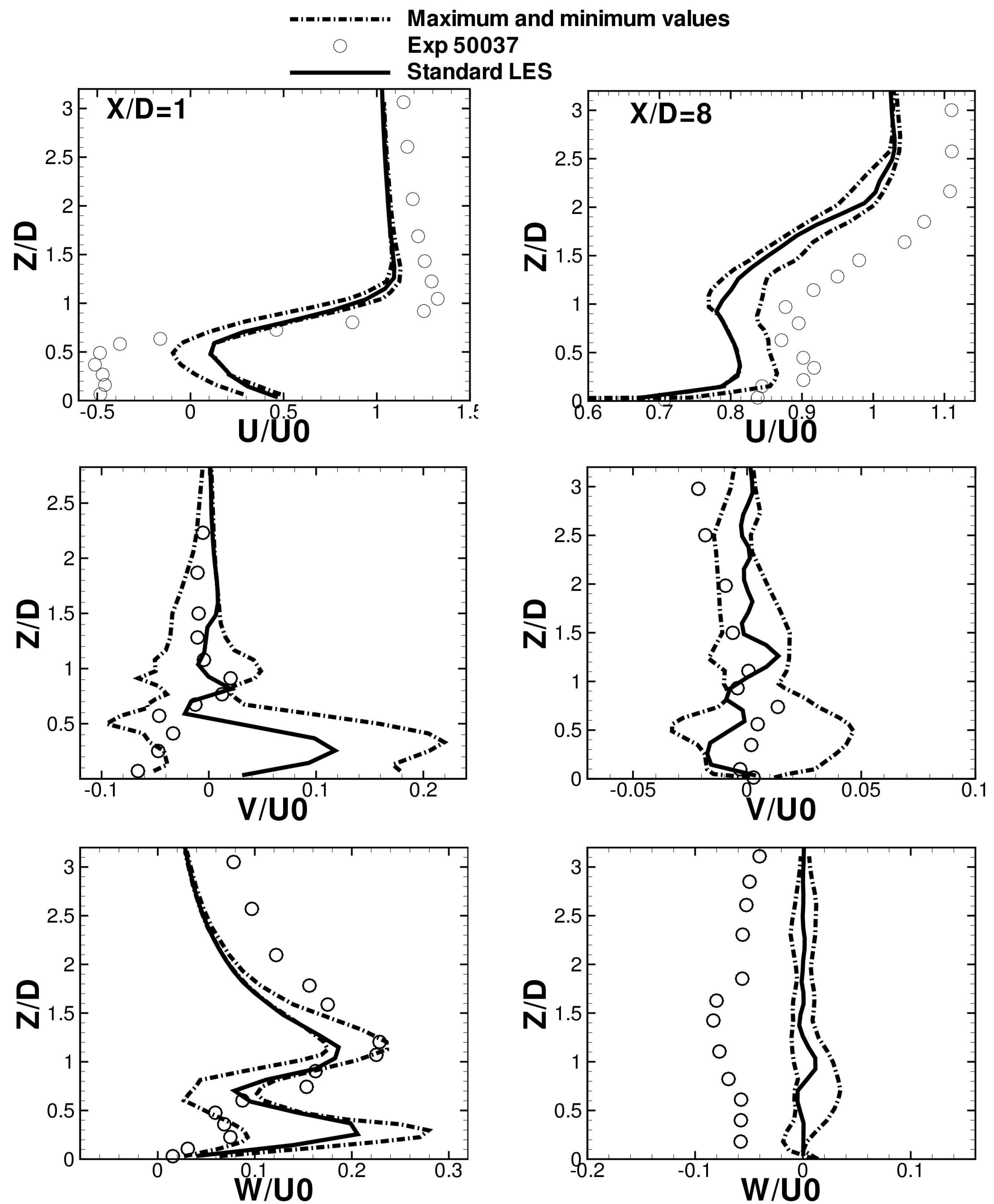

Mean temperature field

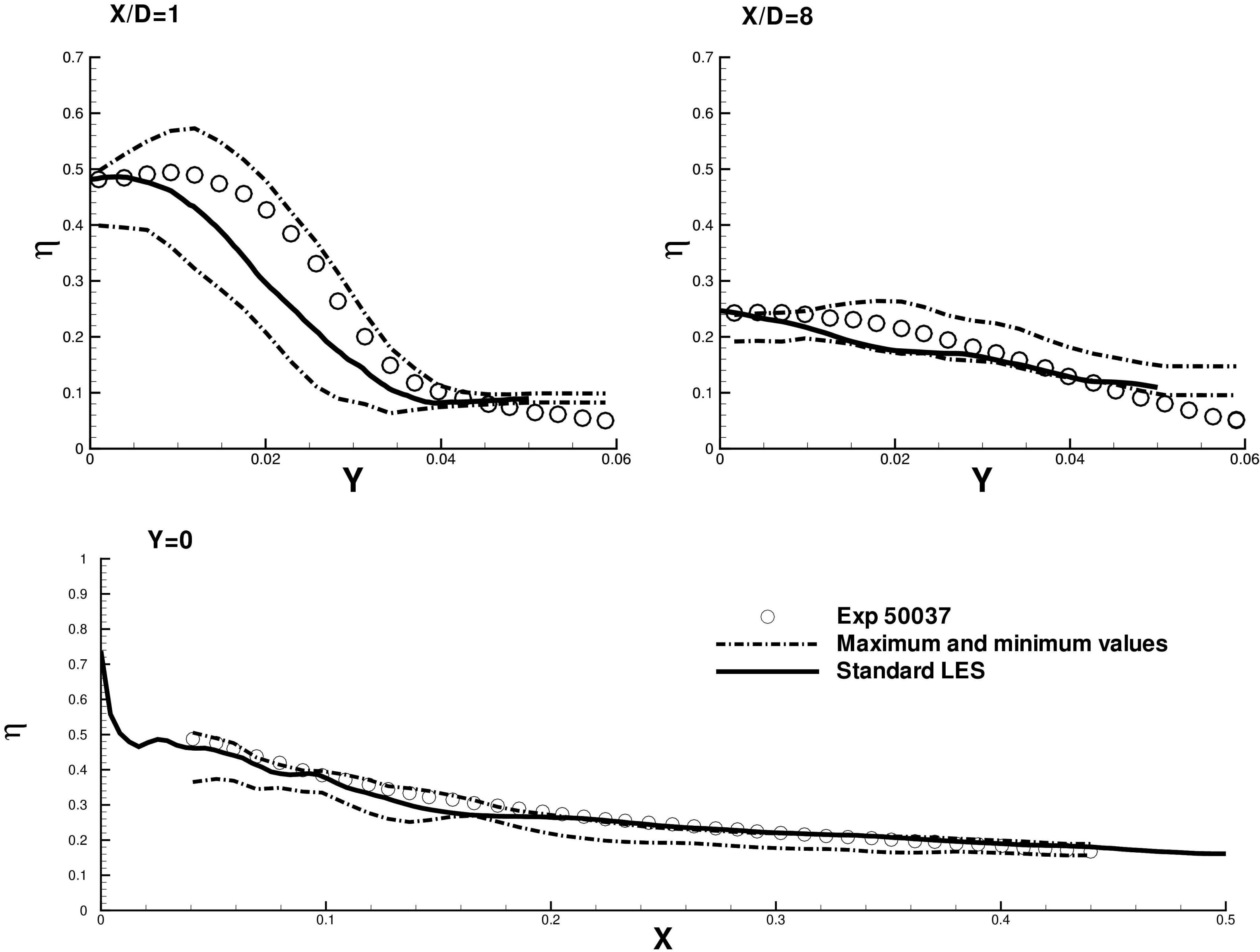

Defining the best LES solution

Which solution is the best LES solution ?

- If some experimental data are available:
  - some error functions can be defined
  - solutions with the lowest error norm can be identified

  ➪ « clean » definition of the best/opimal LES solution(s)

- « best » LES a priori depends on the error measure

Error map

Kriging-based response surface of error at X/D=8

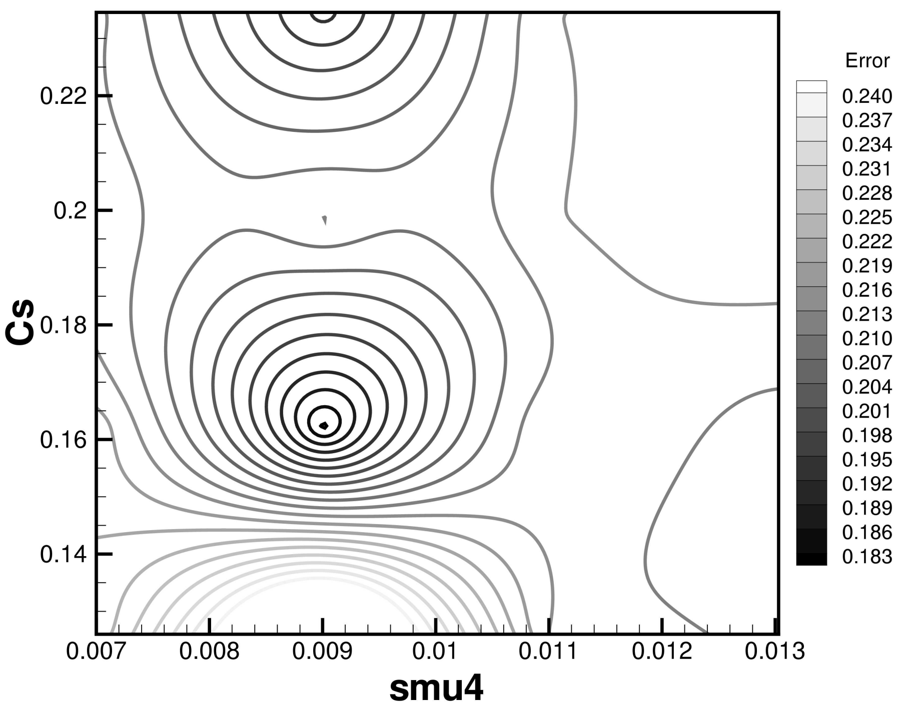

L_1 norm

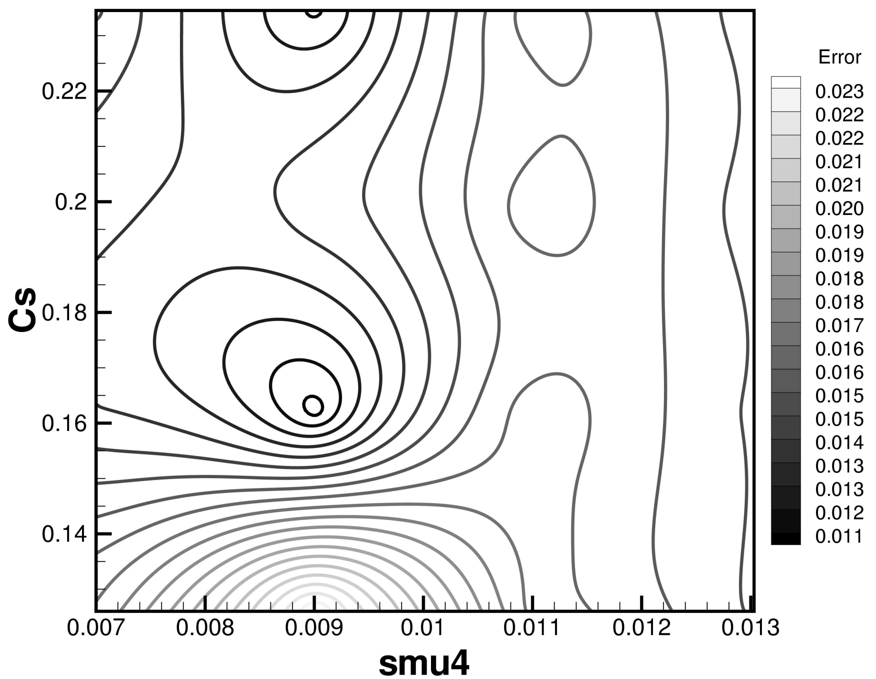

L_2 norm

Error map (cont'd)

Kriging-based response surface of global error at both locations X/D=8 and X/D=1

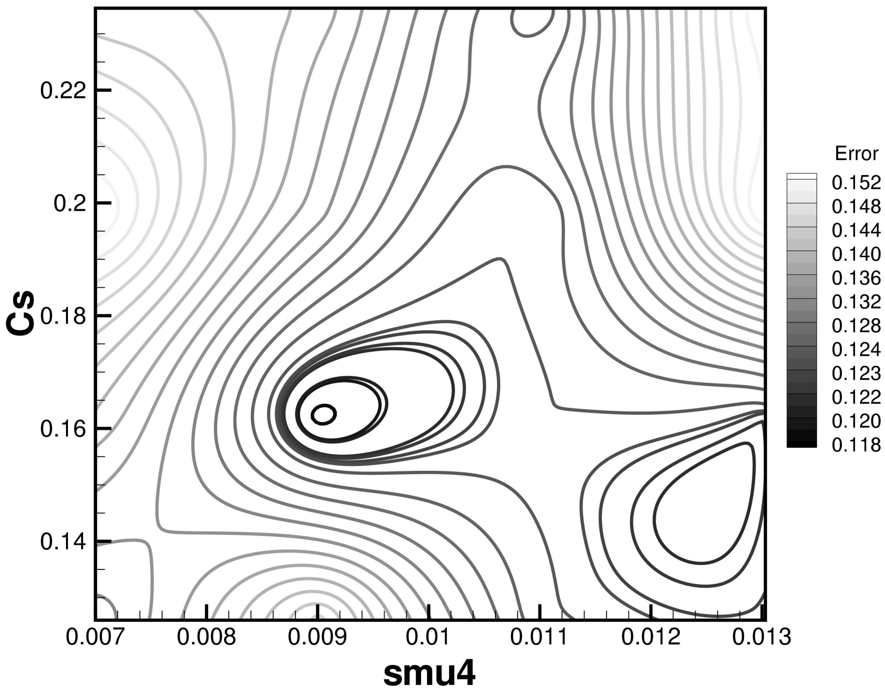

L_1 norm

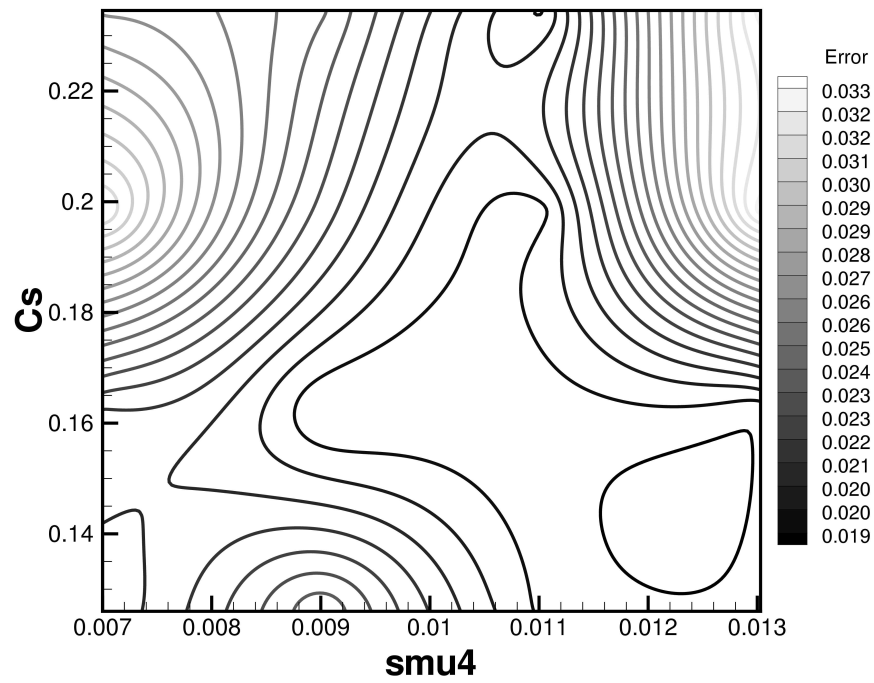

L_2 norm

Best LES solution

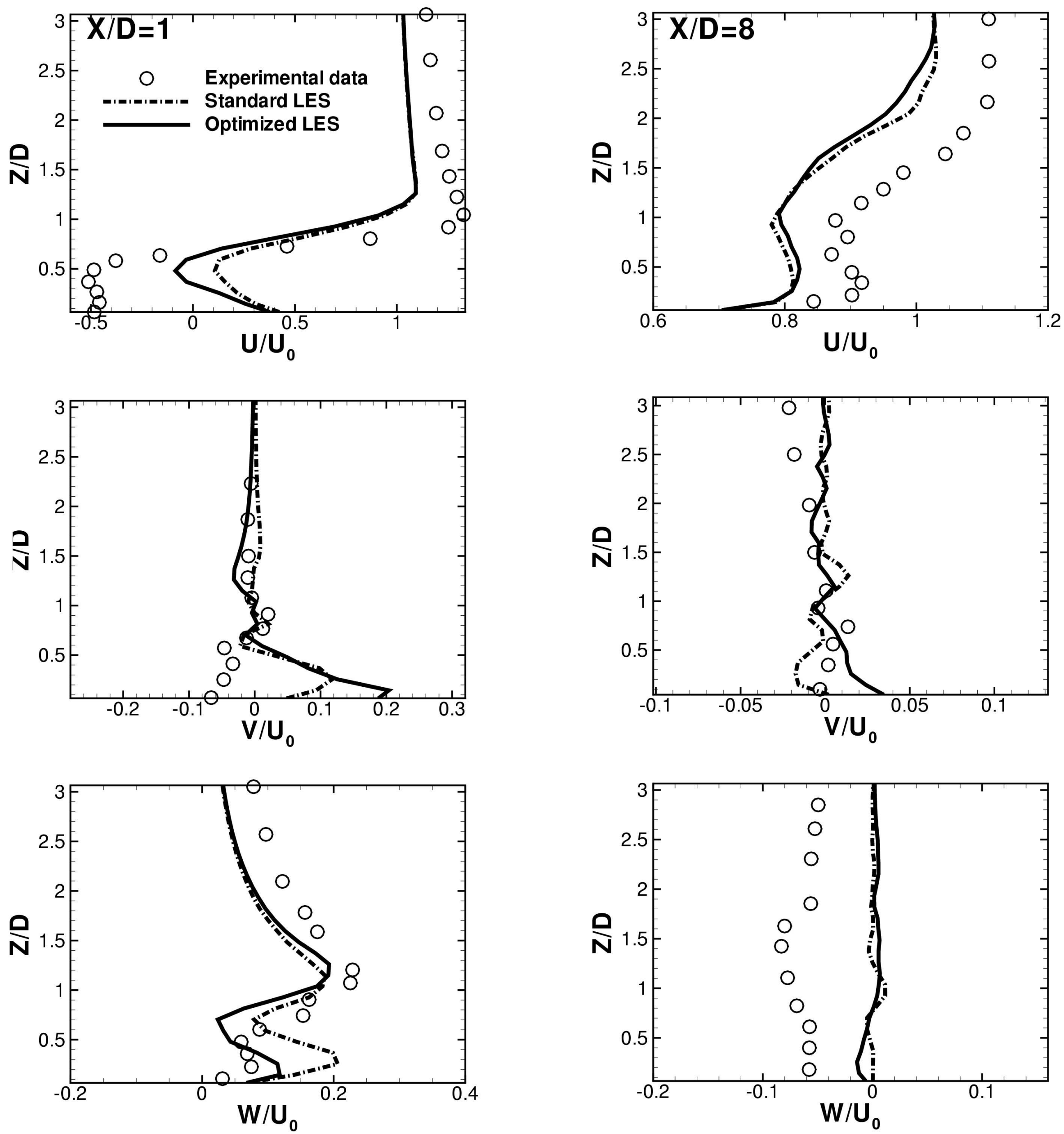

Best LES solution

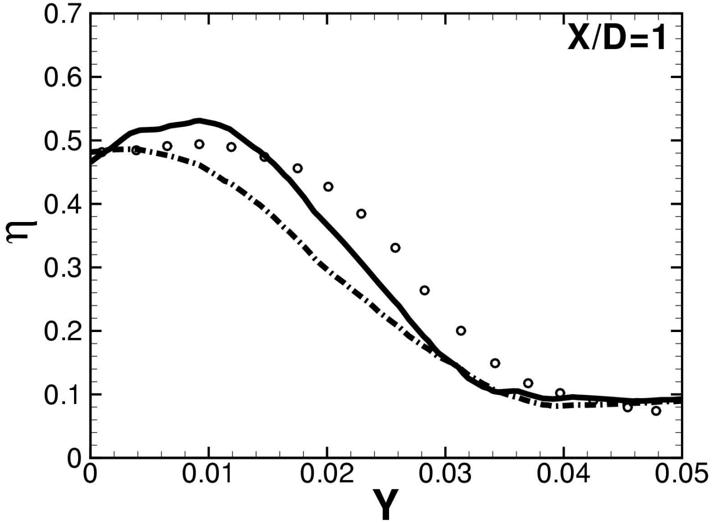

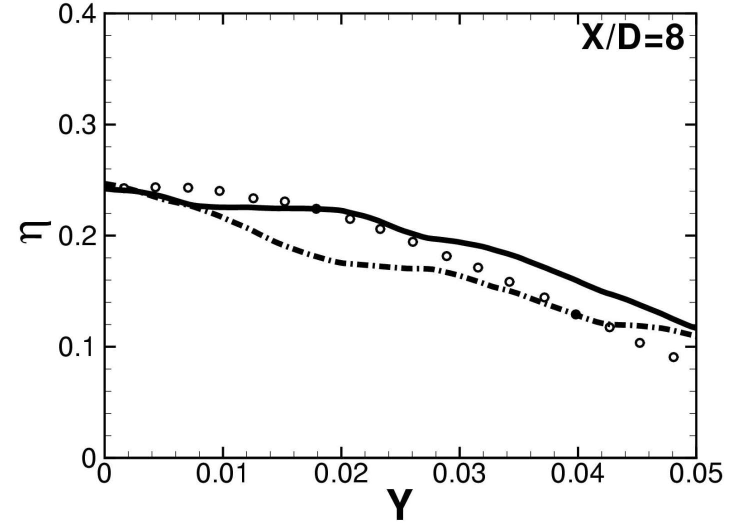

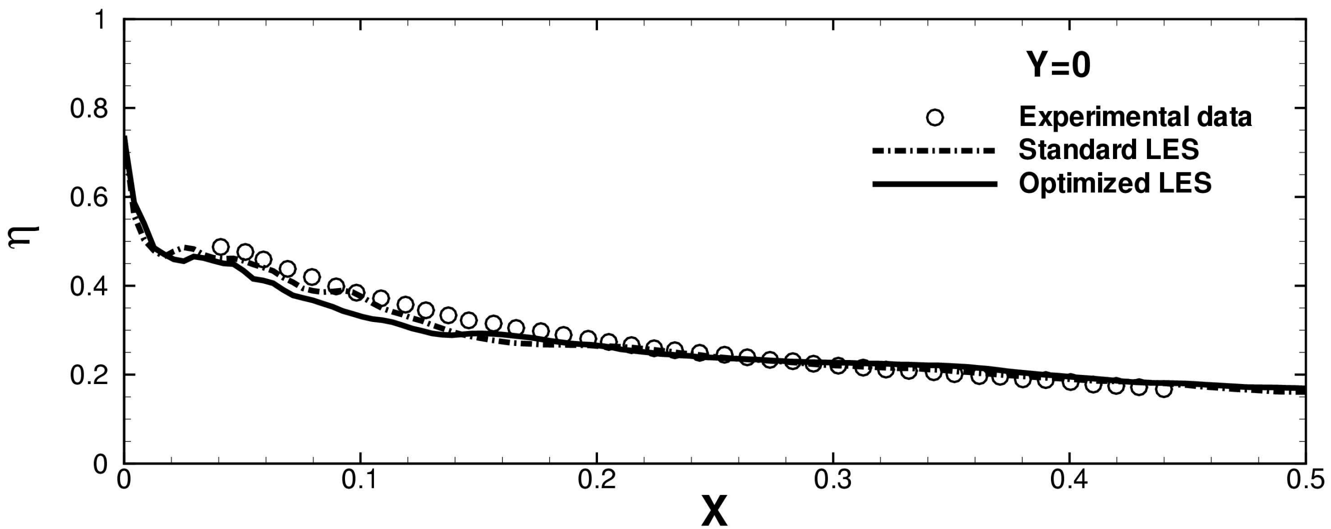

Aix*Marseille université

2. Uncertainty in inflow BC

[Ko, J., Lucor, D., Sagaut, P. (2008) Phys. Fluids 20, 077102]

- Spatially developing shear flows very sensitive to inflow BC
- Dispersion in CFD results (jets, …)
- Case study: 2D mixing layer with stochastic inflow BC

$$u_{\text{in}}(y,t) = \overline{u}_{\text{in}}(y) + \sum_{i=1}^{N} \varepsilon_i \left[f(y)\sin(\omega_i t) + \gamma_i \right]$$

$$v_{\text{in}}(y,t) = \overline{v}_{\text{in}}(y) + \sum_{i=1}^{N} \frac{\varepsilon_i}{i} \left[g(y)\sin(\omega_i t) + \gamma_i \right]$$

Present results: $N = 2 \quad \varepsilon_1 + \varepsilon_2 = U/10$

2. Deterministic views

Fundamental mode forcing

1st subharmonic mode forcing

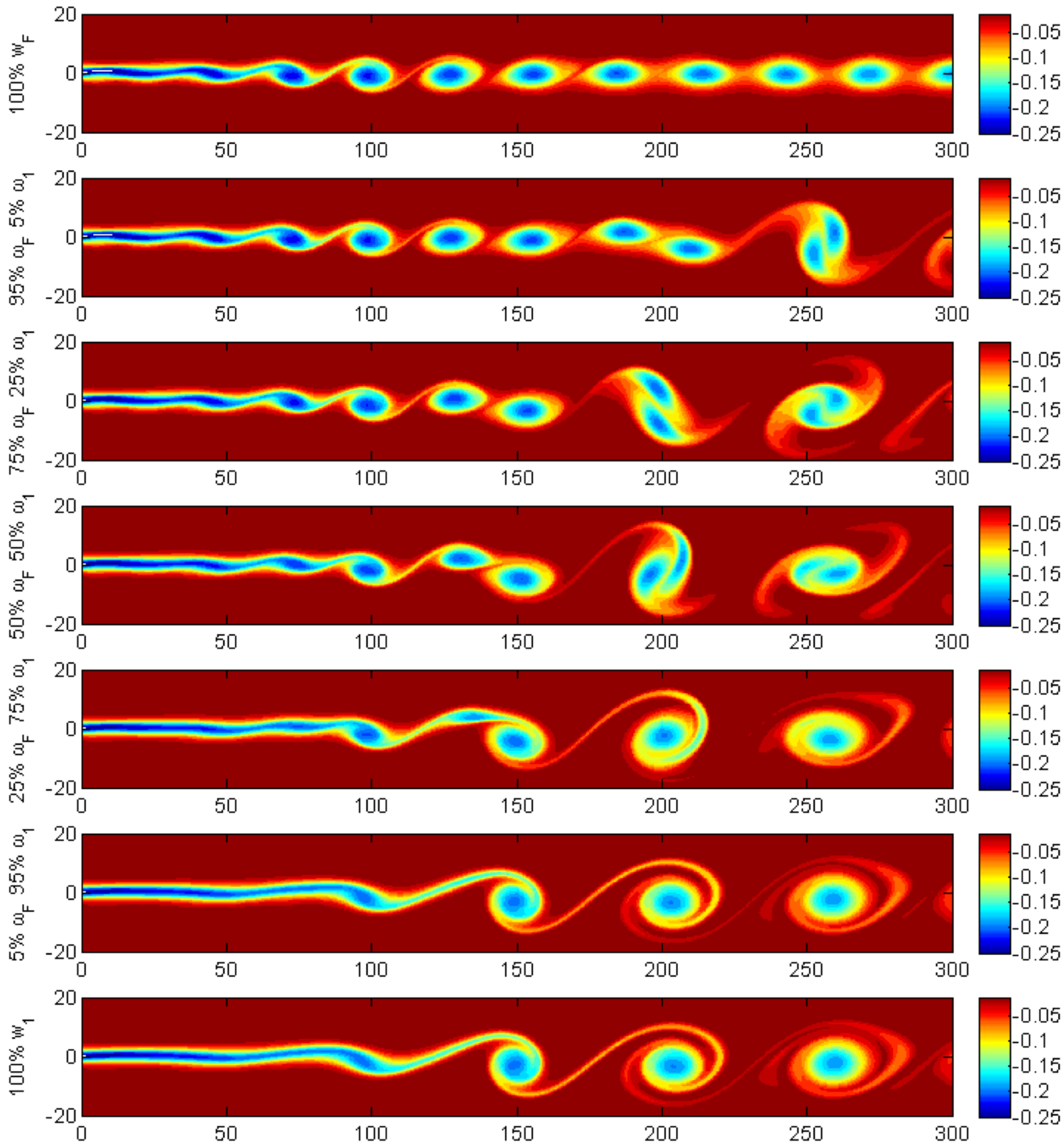

$$\varepsilon_2 = 0$$

$$\varepsilon_1 = 0$$

NI-gPC expansion convergence

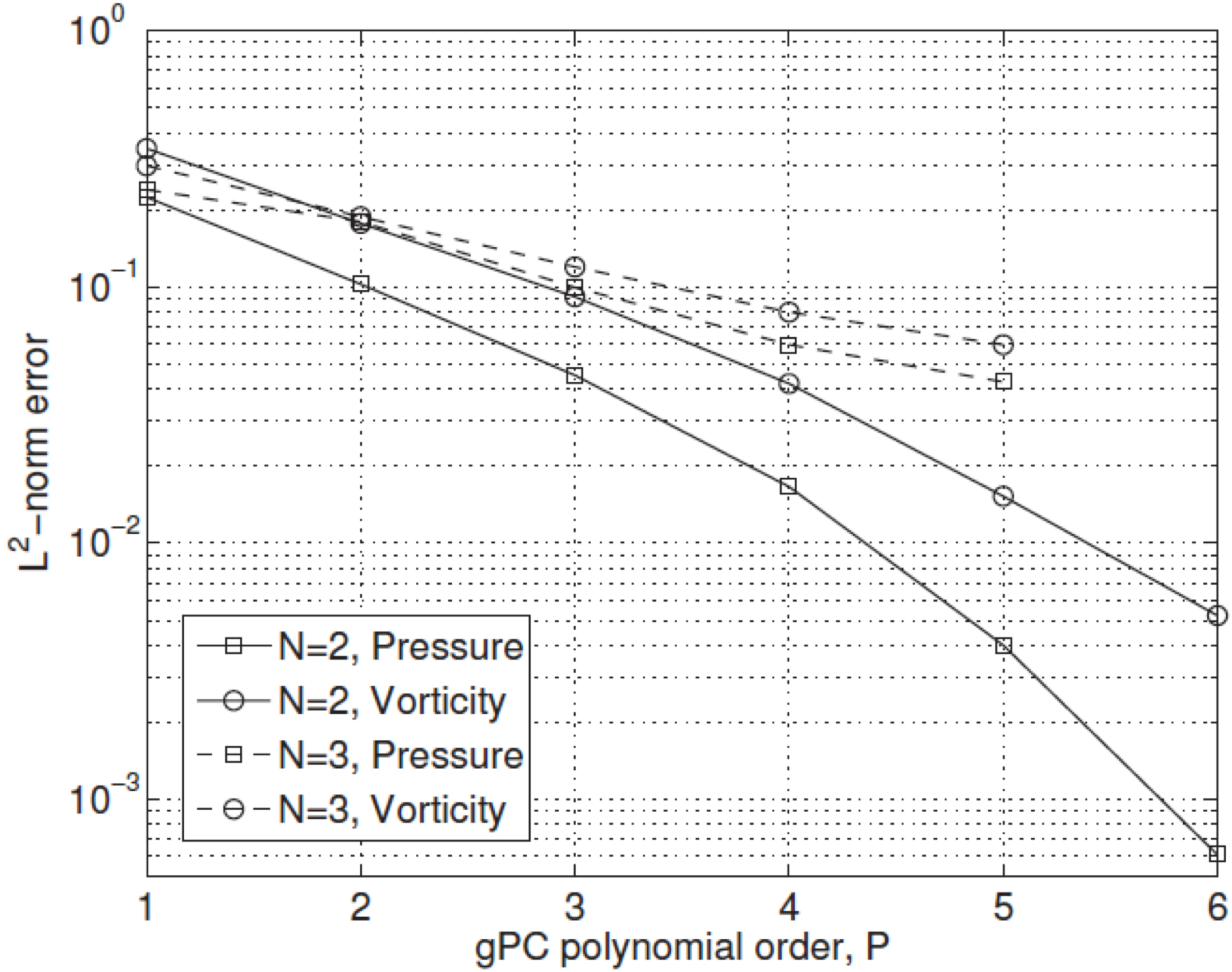

→ ***Pseudo-spectral convergence obtained***

PDF of vorticity thickness of time-averaged fl

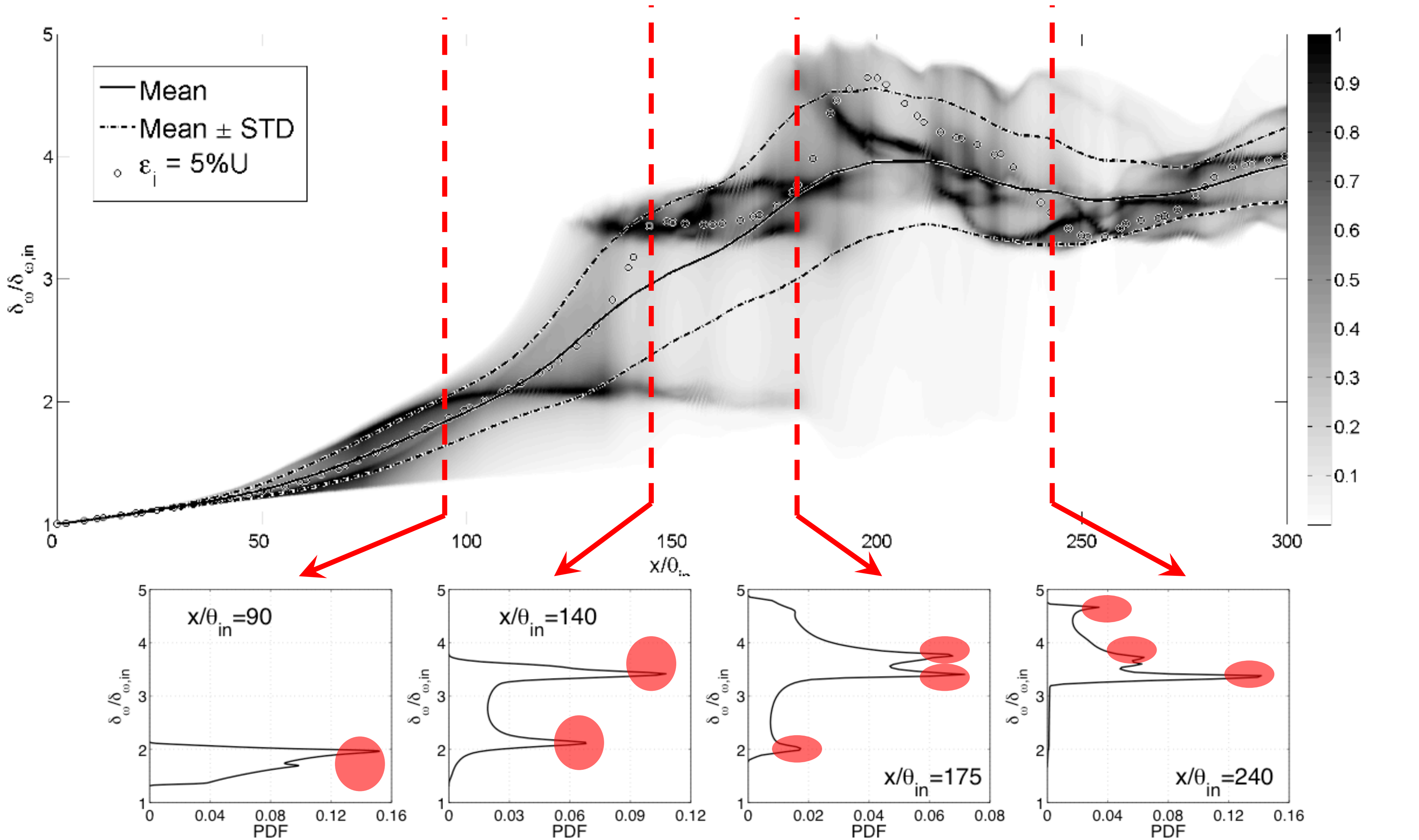

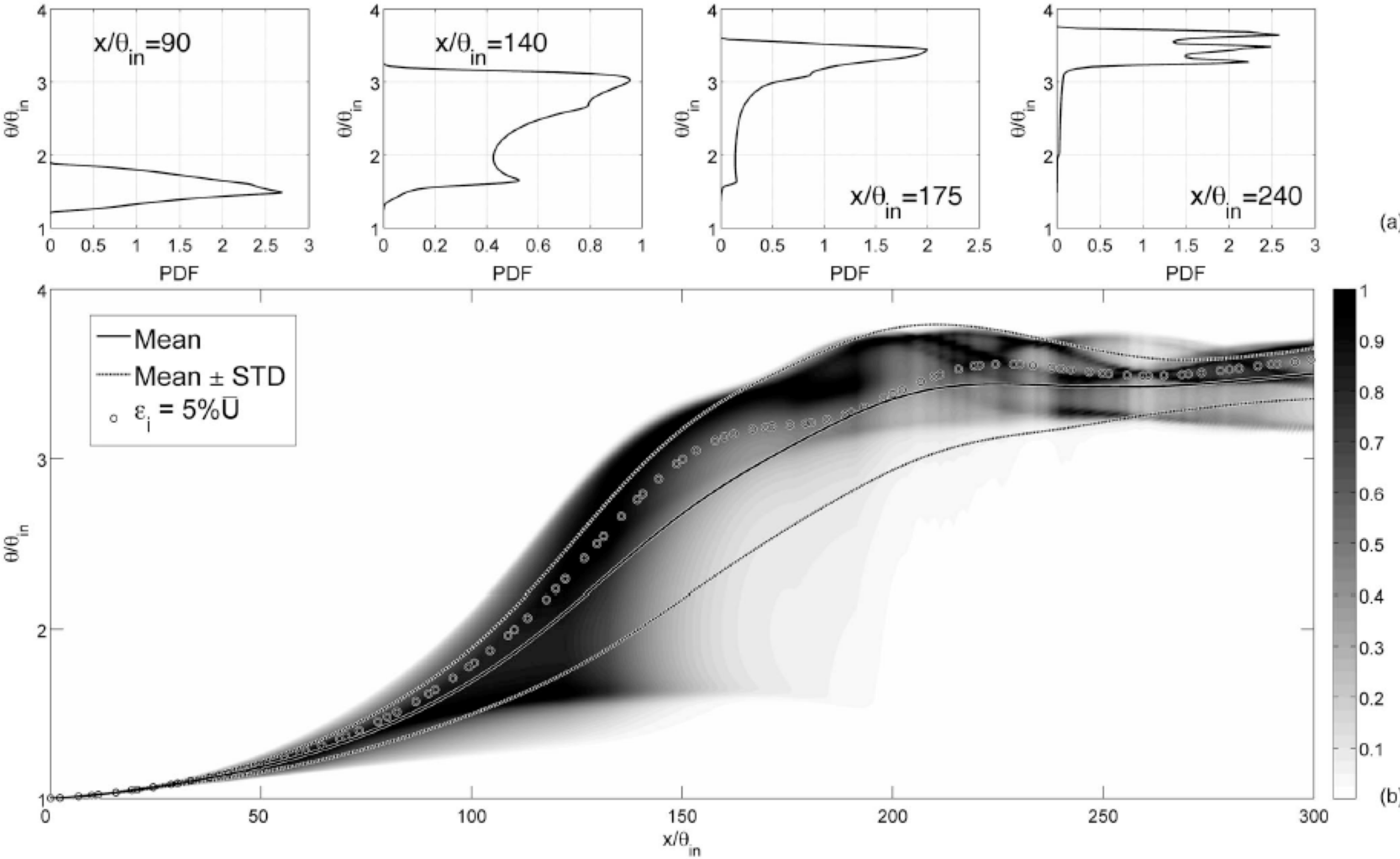

x/θin=90
x/θin=140
x/θin=175
x/θin=240
θ/θin
PDF
(a)
Mean
Mean ± STD
εi = 5%Ū
x/θin
(b)

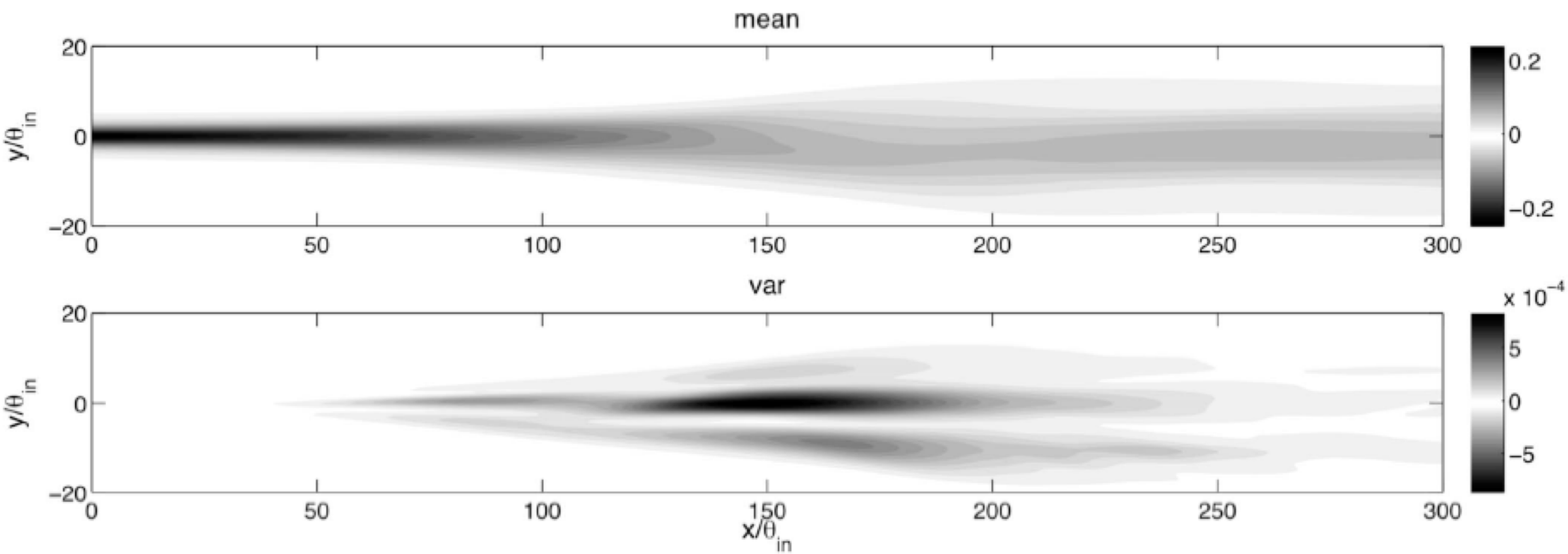

FIG. 6. Spatial distributions of the mean solution and variance of the time-averaged vorticity in the mixing layer with bimodal perturbation forcing.

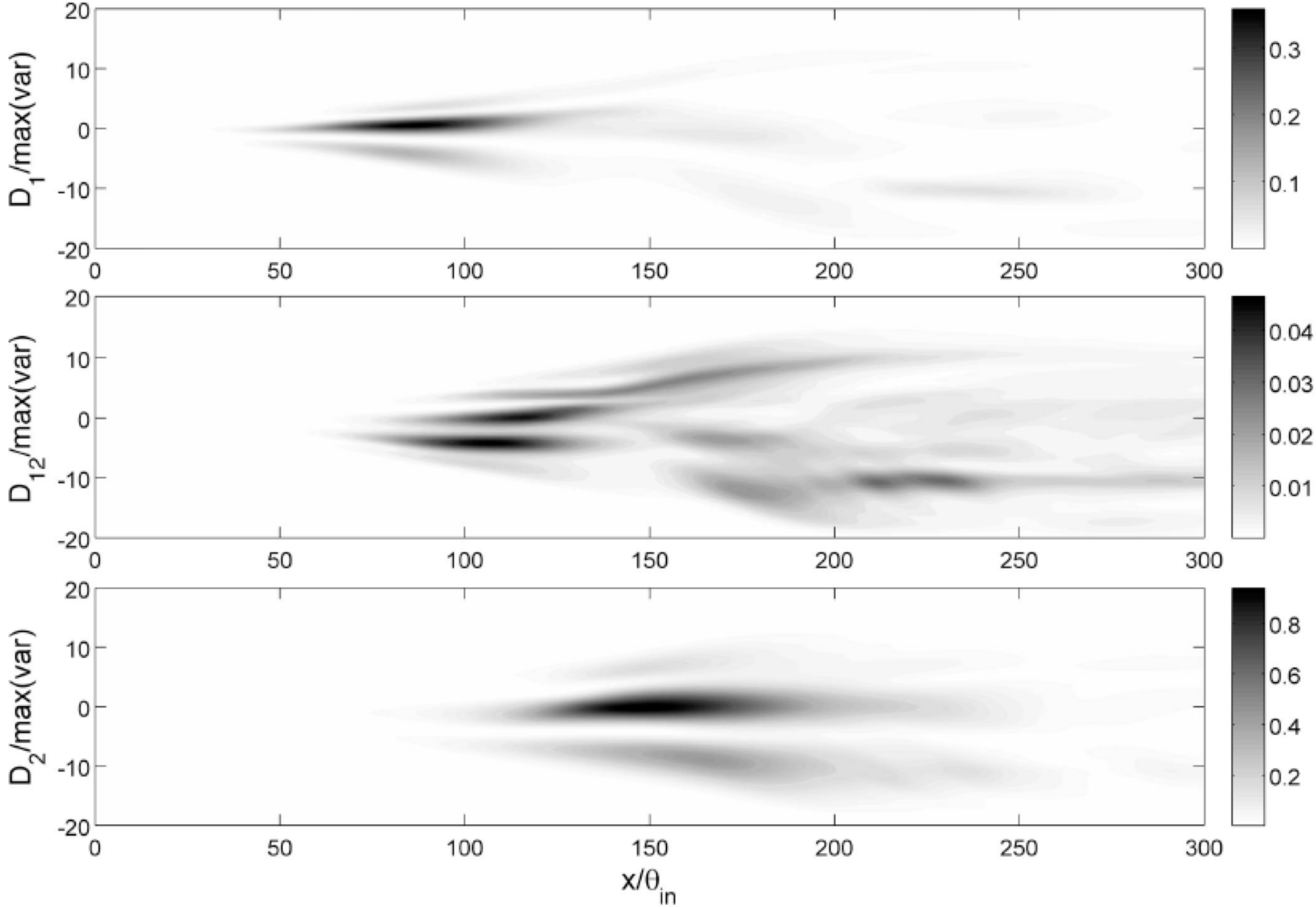

FIG. 10. Spatial distributions of the sensitivity indices (partial variances) of the time-averaged vorticity in the mixing layer with bimodal perturbation forcing.

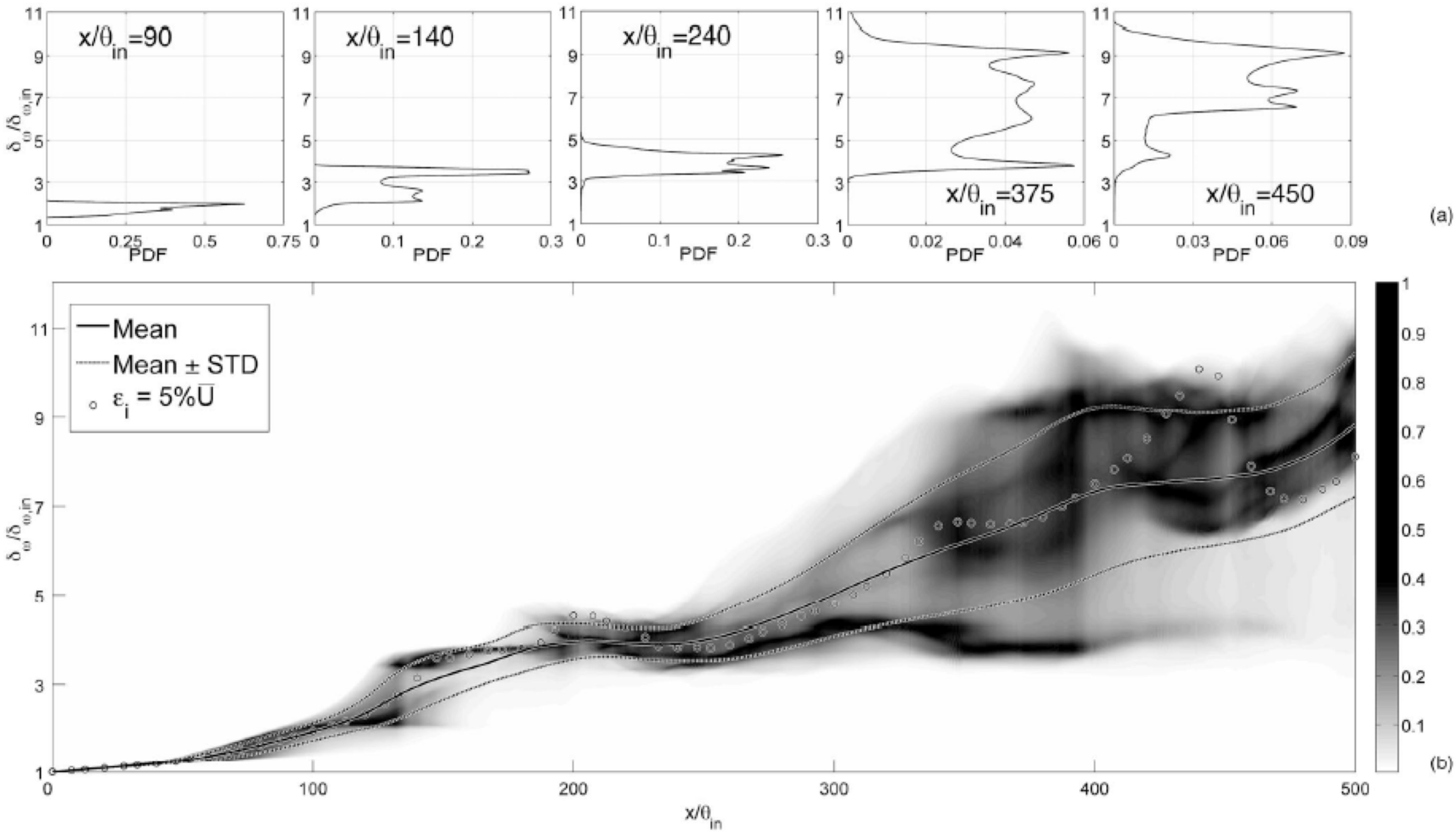

Trimodal case

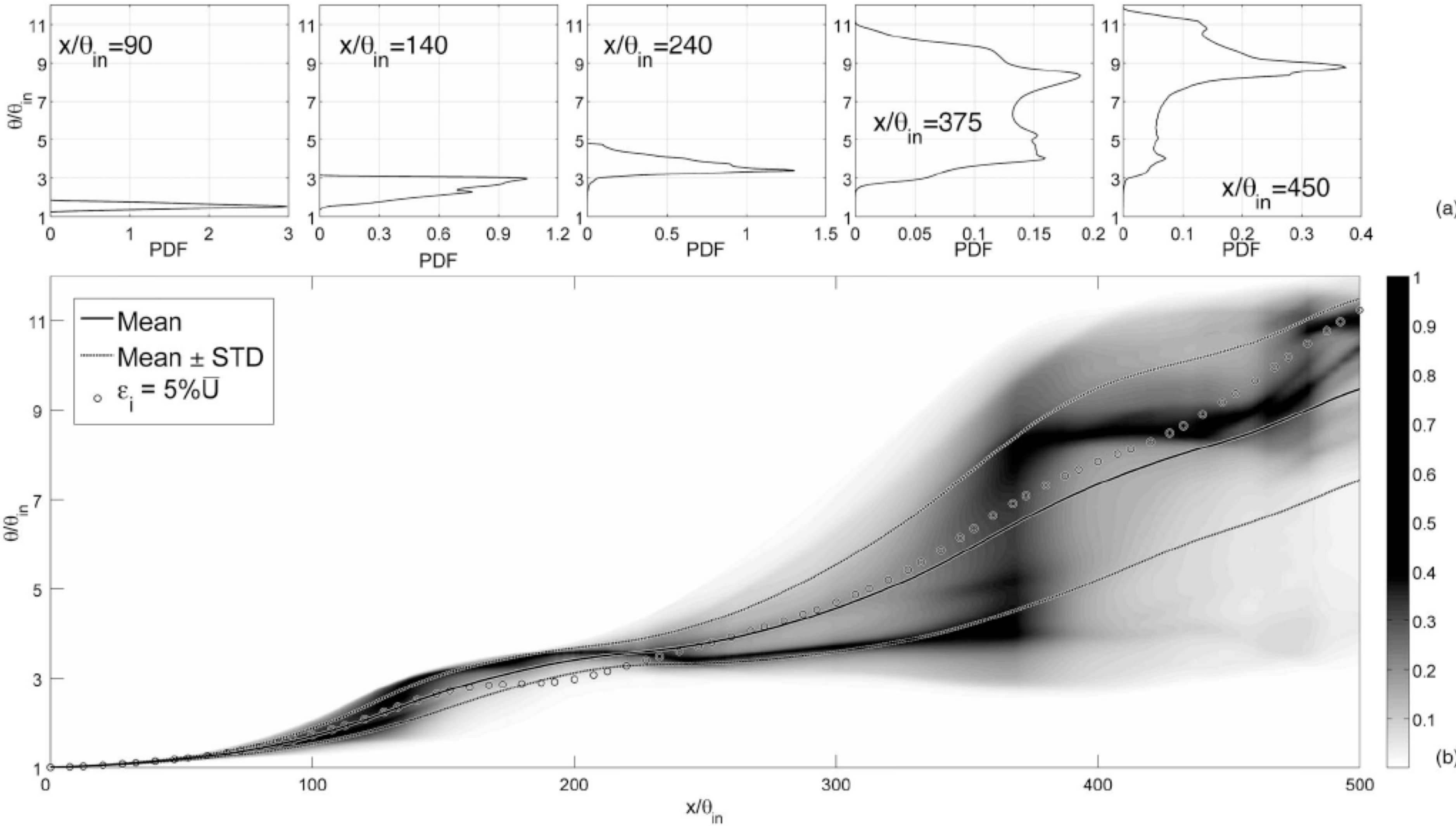

Trimodal case

gPC-UQ on RANS models

UNCERTAINTY IN THE COEFFICIENTS

RANS MODELS

k-ε

Launder-Sharma low-Re

$C_\mu = 0.09$

$C_{\varepsilon 1}=1.44$

$C_{\varepsilon 2}=1.92$

$\sigma_\varepsilon=1.30 \quad \sigma_\kappa=1$

k-ω

Menter - SST

$\beta_1=0.0750$

$\beta_2=0.0828$

$\gamma_1=0.55 \quad \gamma_2=0.44$

$\sigma_{\kappa 1}=0.85 \quad \sigma_{\kappa 2}=1$

$\sigma_{\omega 1}=0.5$

$\sigma_{\omega 2}=0.856$

$\beta^*=0.09$

MODEL PARAMETERS

DATA FROM LITERATURE USED IN INDUSTRIAL APPLICATIONS

gPC-UQ on RANS models

Considering THREE CANONICAL TURBULENT FLOWS

- **freely decaying homogeneous isotropic turbulence**
- **homogeneous shear flow in the asymptotic regime**
- **boundary layer in the logarithmic region.**

ANALYTICAL EXPRESSIONS

$$
\begin{aligned}
C_\mu &= \left(\frac{\mathcal{K}_{log}}{u_\tau^2}\right)^{-2} & C_\mu &= f\left(\frac{\mathcal{K}_{log}}{u_\tau^2}\right) \\
C_{\varepsilon_1} &= \frac{C_{\varepsilon_2}-1}{\frac{\mathcal{P}}{\varepsilon}} & C_{\varepsilon_1} &= f\left(n, \frac{\mathcal{P}}{\varepsilon}\right) \\
C_{\varepsilon_2} &= 1 - \frac{1}{n} & C_{\varepsilon_2} &= f(n) \\
\sigma_\varepsilon &= \frac{\kappa_{VK}^2}{\sqrt{C_\mu}\left(C_{\varepsilon_2}-C_{\varepsilon_1}\right)} & C_\mu &= f\left(n, \frac{\mathcal{P}}{\varepsilon}, \kappa_{VK}, \frac{\mathcal{K}_{log}}{u_\tau^2}\right) \\
\sigma_\mathcal{K} &= 1 & & -
\end{aligned}
$$

$$
\begin{aligned}
\beta^* &= \left(\frac{\mathcal{K}}{u_\tau^2}\right)^{-2} & \beta^* &= f\left(\frac{\mathcal{K}}{u_\tau^2}\right) \\
\beta_1 &= -\frac{\beta^*}{n} & \beta_1 &= f\left(n, \frac{\mathcal{K}_{log}}{u_\tau^2}\right) \\
\gamma_1 &= \frac{\beta_1}{\beta^* \frac{\mathcal{P}}{\varepsilon}} & \gamma_1 &= f\left(n, \frac{\mathcal{P}}{\varepsilon}, \frac{\mathcal{K}_{log}}{u_\tau^2}\right) \\
\sigma_{\omega_1} &= \frac{\sqrt{\beta^*}\left(\beta_1\beta^* - \gamma_1\right)}{\kappa_{VK}^2} & \sigma_{\omega_1} &= f\left(n, \frac{\mathcal{P}}{\varepsilon}, \kappa_{VK}, \frac{\mathcal{K}_{log}}{u_\tau^2}\right) \\
\sigma_{\mathcal{K}_1} &= \frac{\beta_1\sigma_{\omega_1}}{\beta^*} & \sigma_{\mathcal{K}_1} &= f\left(n, \frac{\mathcal{P}}{\varepsilon}, \kappa_{VK}, \frac{\mathcal{K}_{log}}{u_\tau^2}\right)
\end{aligned}
$$

MODEL COEFFICIENTS ➔ FLOW PROPERTIES

Aix*Marseille université

gPC-UQ on RANS models

LITERATURE SURVEY

n

$\frac{\mathbf{K_{log}}}{\mathbf{u_\tau^2}}$

$\boldsymbol{\varkappa_{vk}}$

$\frac{\mathbf{P}}{\boldsymbol{\varepsilon}}$

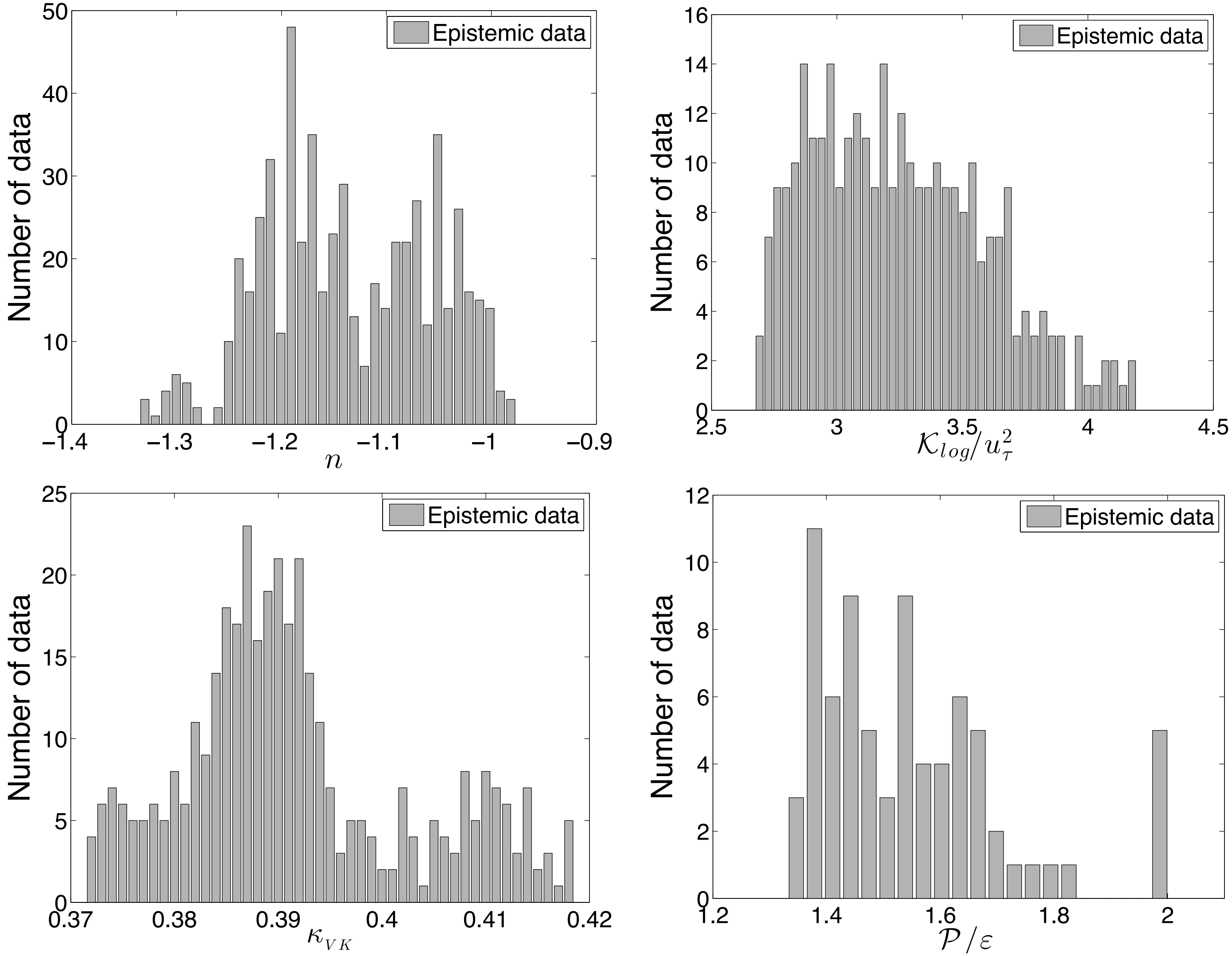

gPC-UQ on RANS models

CONTINUOUS PDF APPROXIMATION FOR THE EPISTEMIC INPUT PARAMETERS

n

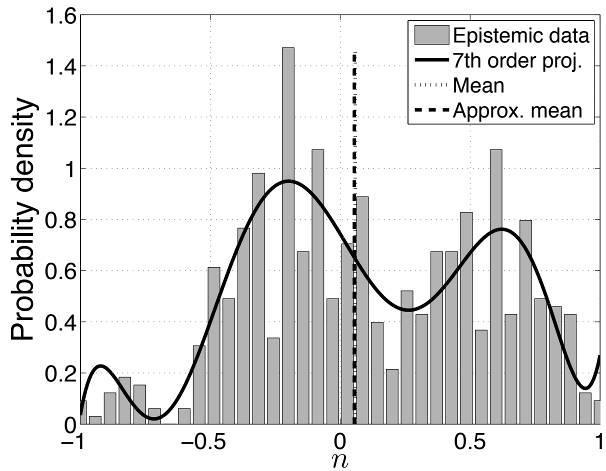

$\frac{K_{log}}{u_\tau^2}$

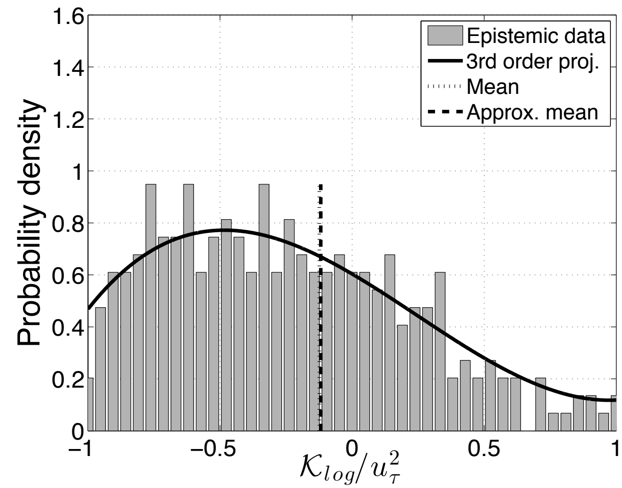

K_{vk}

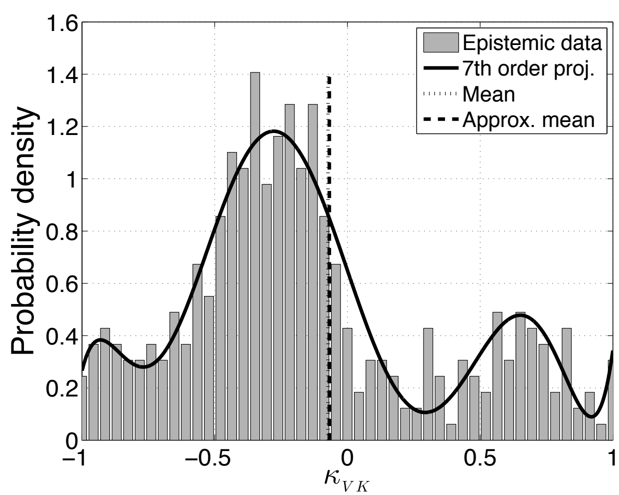

$\frac{P}{\varepsilon}$

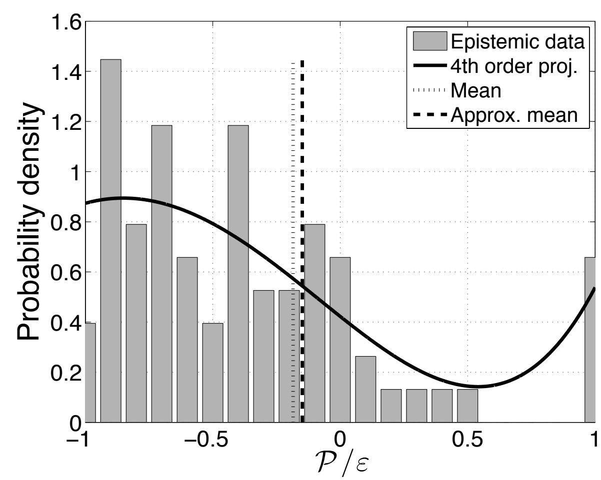

UNCERTAINTY PROPAGATION IN THE k-ε LS MODEL COEFFICIENTS

C_μ

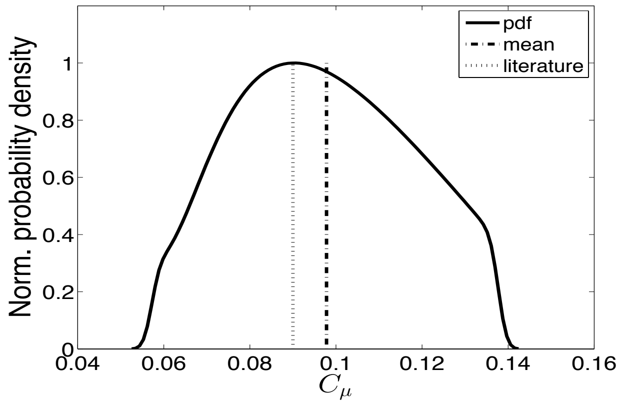

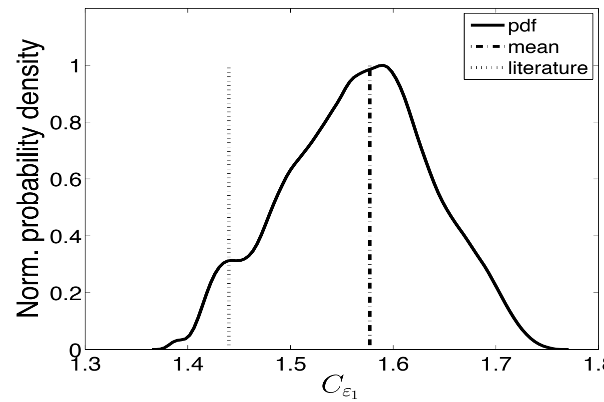

$C_{\varepsilon 1}$

$C_{\varepsilon 2}$

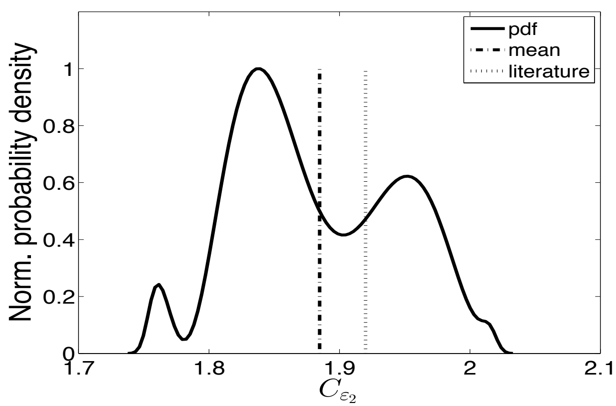

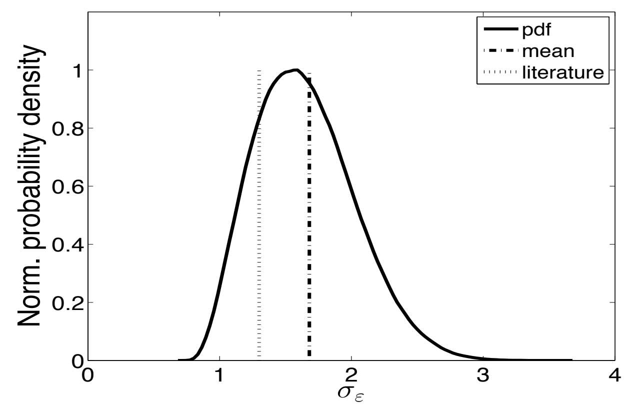

σ_ε

Mean value for $C_\mu \approx 0.09$

High sensitivity to P/ε

gPC-UQ on RANS models

UNCERTAINTY PROPAGATION IN THE k-ω SST MODEL COEFFICIENTS

γ_1 $\sigma_{\omega 1}$

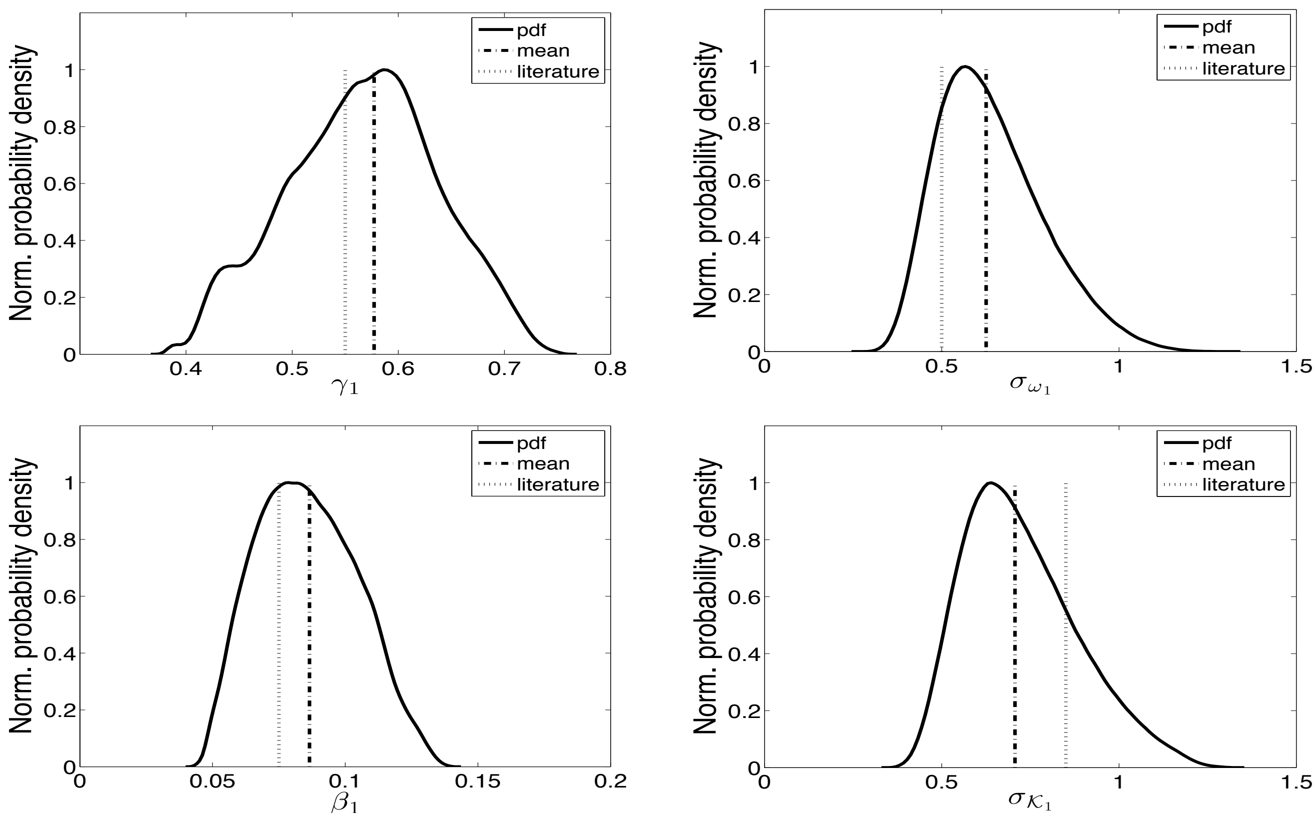

β_1 σ_{k1}

Mean values ≈ literature

High sensitivity to P/ε

Aix*Marseille université

gPC-UQ on RANS models

SOME RESULTS: FRICTION VELOCITY

k-ε LS | k-ω SST

Re_τ=950

Re_τ=2000

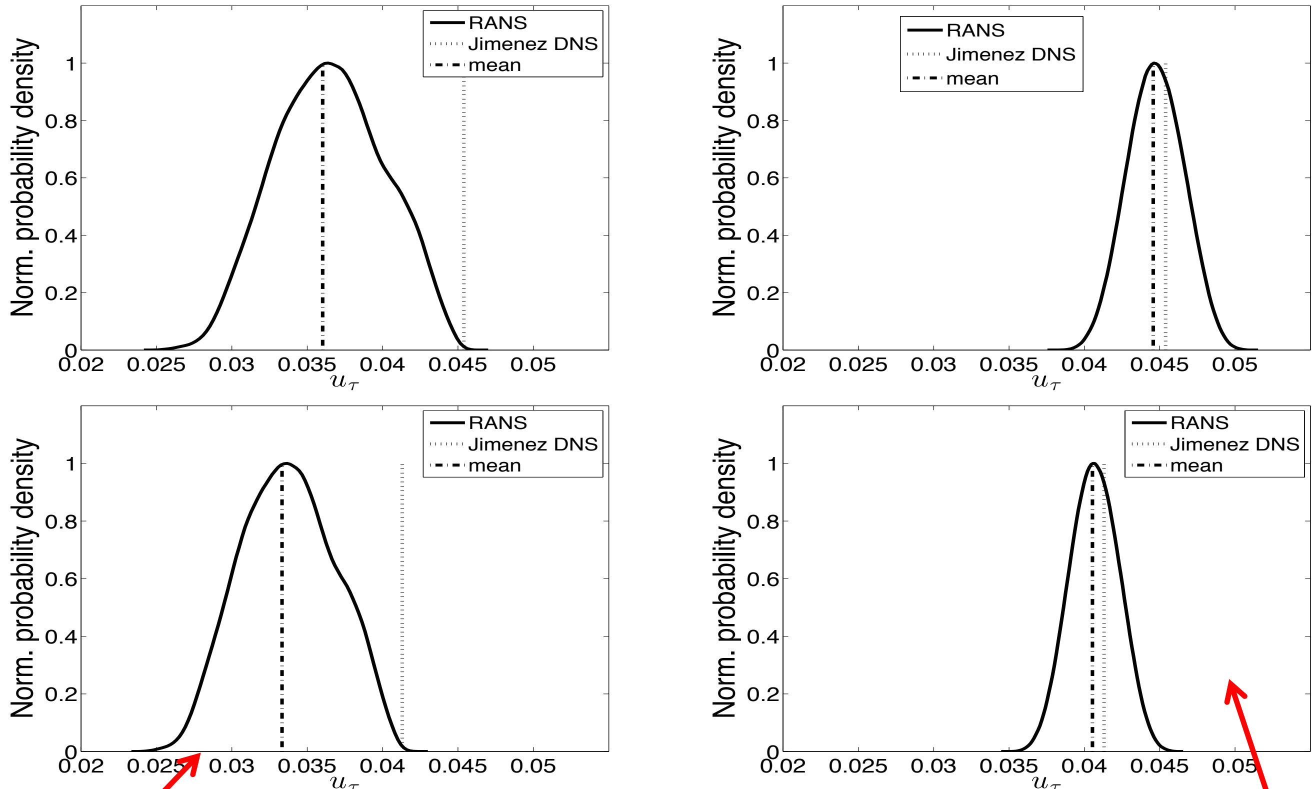

Underprediction and high variance

High sensitivity to P/ε

Less sensitive

SOME RESULTS: EDDY VISCOSITY PROFILE

k-ε

LS

Re_τ=2000

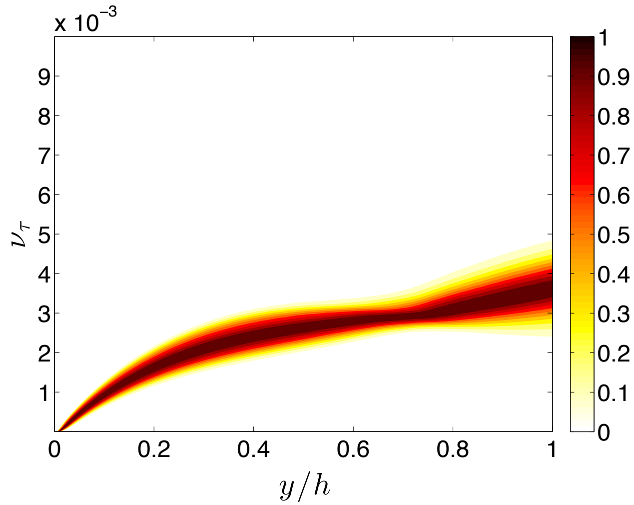

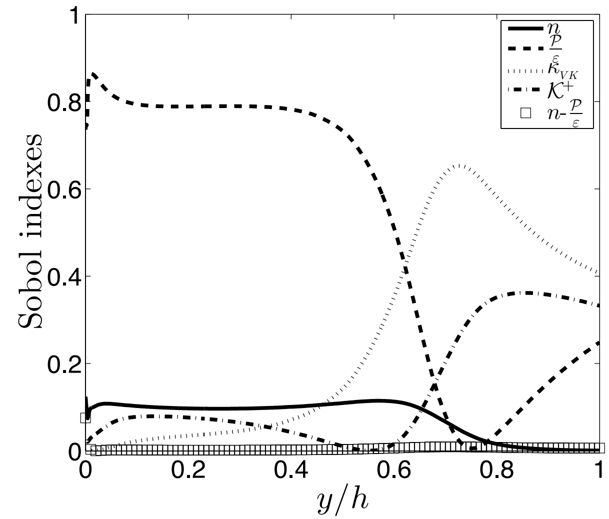

k-ω

SST

Re_τ=2000

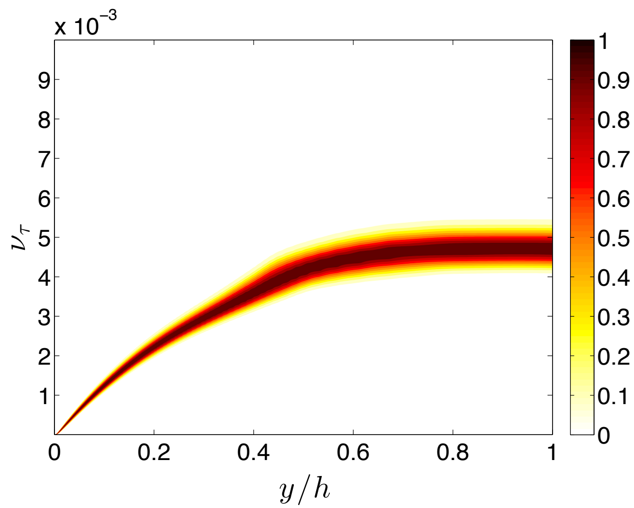

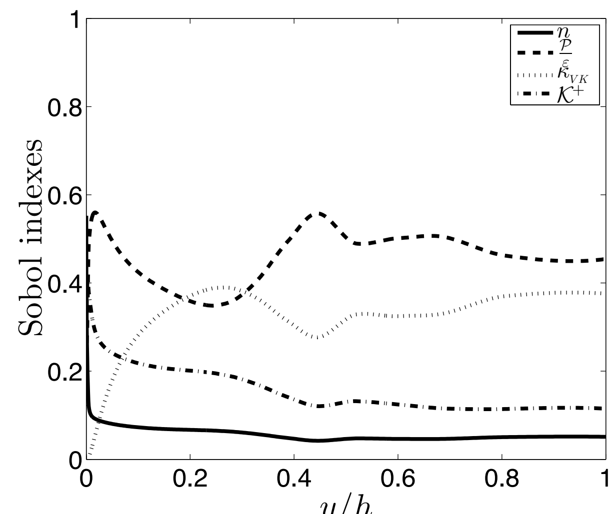

Aix*Marseille université

gPC-UQ on RANS models

SOME RESULTS: LOCAL L_2 ERROR ON THE VELOCITY

$$eU(y) = \sqrt{\frac{(U(y) - U_{DNS}(y))^2}{U^2_{DNS}(y)}}$$

k-ε

LS

Re_τ=2000

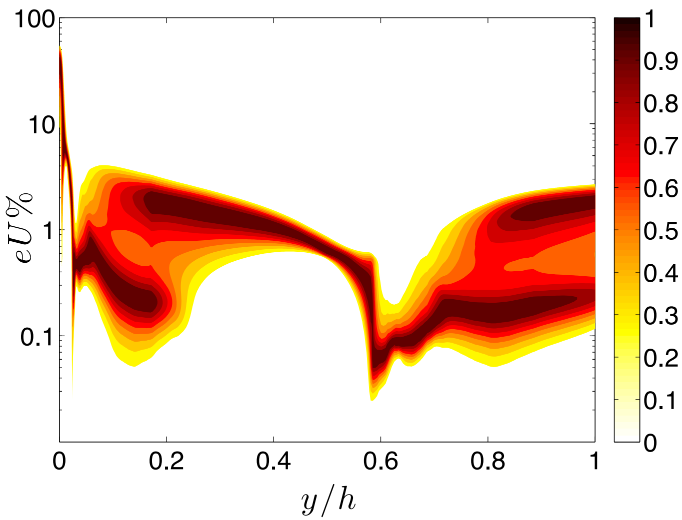

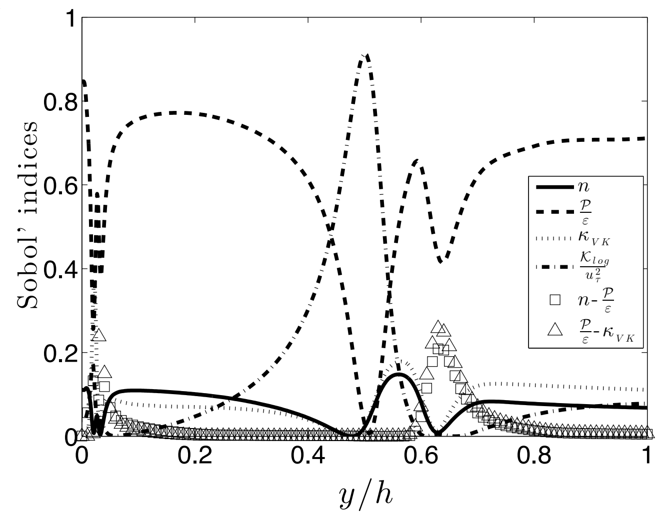

k-ω

SST

Re_τ=2000

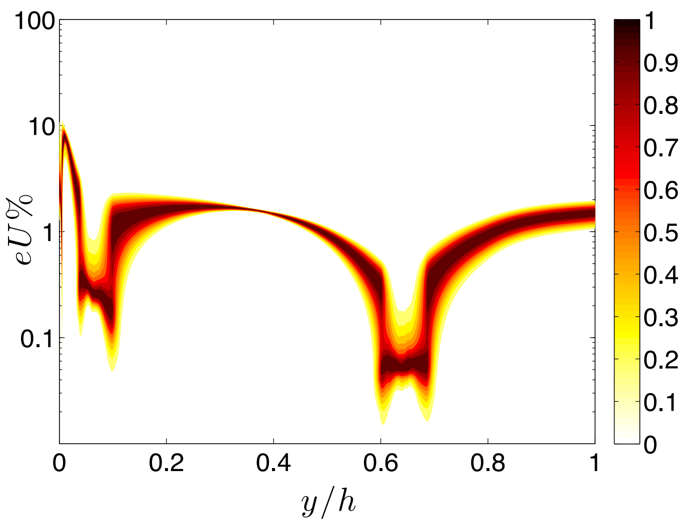

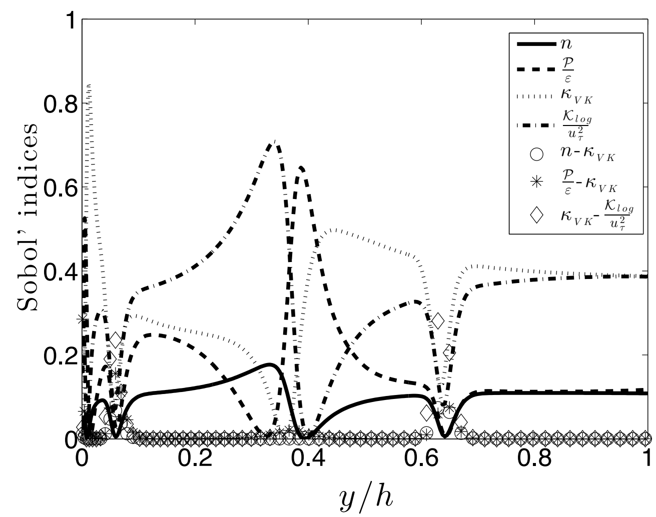

Thank you !